STUDY OF CREEP BEHAVIOUR OF UNTREATED AND ADDITIVE TREATED JUTE GEOTEXTILES

SHAFIQUL ISLAM

MASTER OF SCIENCE IN CIVIL ENGINEERING

(GEOTECHNICAL)

DEPARTMENT OF CIVIL ENGINEERING

BANGLADESH UNIVERSITY OF ENGINEERING AND TECHNOLOGY

MARCH, 2017

STUDY OF CREEP BEHAVIOUR OF UNTREATED AND ADDITIVE TREATED JUTE GEOTEXTILES

A Thesis submitted by

Shafiqul Islam

Student No. 0412042212P

A Thesis Submitted to the Department of Civil Engineering in Partial Fulfillment of the Requirement for the Degree of

Master of Science in Civil Engineering

Bangladesh University of Engineering and Technology

March, 2017

DEDICATED TO

My respected Supervisor
Dr. Mohammad Shariful Islam
And
My Family

The thesis titled "**Study of Creep Behaviour of Untreated and Additive Treated Jute Geotextiles**", submitted by Shafiqul Islam, Roll No. 0412042212P, Session April 2012 has been accepted as satisfactory in partial fulfillment of the requirement for the degree of Master of Science in Civil Engineering on 11th March, 2017.

BOARD OF EXAMINERS

Dr. Mohammad Shariful Islam **Professor** **Department of Civil Engineering** **BUET, Dhaka.**	**Chairman** **(Supervisor)**
Dr. K.A.M. Abdul Muqtadir **Professor and Head** **Department of Civil Engineering** **BUET, Dhaka.**	**Member** **(Ex-Officio)**
Dr. Abu Siddique **Professor** **Department of Civil Engineering** **BUET, Dhaka.**	**Member**
Lt Col Md. Masudur Rahman **Instructor Class-A** **Department of Civil Engineering** **Military Institute of Science and Technology (MIST)** **Mirpur, Dhaka.**	**Member** **(External)**

DECLARATION

It is hereby declared that this thesis and the studies embodied in it are the result of the investigation carried out by the author under the supervision of Dr. Mohammad Shariful Islam and the guidance of Dr. Abdul Jabbar Khan, Professor, Department of Civil Engineering, Bangladesh University of Engineering and Technology. Wherever contributions of others were involved, every effort has been made to indicate this clearly with due reference to the literature and acknowledgement of collaborative research and discussions. Neither thesis nor any part of it has been submitted to or is being submitted to for any other purposes (except for publication).

Shafiqul Islam

Shafiqul Islam

Bangladesh University of Engineering and Technology

March, 2017

ACKNOWLEDGEMENT

First of all gratefulness to Almighty ALLAH for the blessing that gave me the ability to complete this thesis work successfully.

I wish to express my deepest gratitude to my supervisors Dr. Mohammad Shariful Islam and my mentor Dr. Abdul Jabbar Khan, Professor, Department of Civil Engineering, Bangladesh University of Engineering and Technology, for their continuous supervision, guidance and valuable suggestions with consistent encouragement at all the stages of my work. It is their kindness to provide me the necessary references and knowledge to carry out the work smoothly. Their relentless expertise and keen interest in this topic was the sources of my inspiration for the work.

I am grateful to Dr. Abdul Muqtadir, Professor and Head, Department of Civil Engineering, BUET, for his support and guidance from the Department. I also want to express my gratitude to Dr. Abu Siddique, Professor of the Department of Civil Engineering, BUET, for his valuable information and suggestions that made this thesis work resourceful. Sincere thanks to Lt Col Md. Masudur Rahman, Instructor Class-A, Department of Civil Engineering, Military Institute of Science and Technology (MIST), for giving his valuable time and advice to make this thesis fruitful.

I am grateful to the technical staffs of the geotechnical laboratory of BUET for their continual assistance in laboratory works.

I am thankful to my parents for their continuous support and prayer. Last but not the least, I am grateful to my wife for her patience and moral supports during my study period.

ABSTRACT

Jute geotextiles (JGTs) are used in many civil engineering applications. JGTs are applied under various loading conditions for different time duration. Similar to geosynthetics, JGTs also show different load-strain-time responses under different loading regime at isothermal conditions. To determine the response of JGT at different loading and time, an approach called strain envelope, which is already being applied for geosynthetics, was considered. The study was carried out on selected JGT samples to evaluate the strain components (i.e., recoverable strain (ε_R) and locked strain (ε_L) through isochronous curve in order to develop strain envelop in isothermal conditions. To assess the strain components of selected JGTs, creep tests were conducted following ASTM specifications for geosynthetics. Four types of JGTs, untreated and additive treated with two different mass combinations(627gsm and 724gsm) which are commonly used in Bangladesh for different geotechnical purposes, were selected for this investigation,.

To determine loads for creep test, wide-width tensile strength test was performed for all type of samples. The test was conducted at three different strain rates: (10±3)%/min, (50±5)%/min and (100±10)%/min. Test results revealed that, unlike the synthetic geotextiles, strain rate is insignificant on the strength of JGTs in machine direction as well as in cross machine direction.

Isochronous curves were developed from creep test results. From isochronous curves of selected JGTs, the possible design life for a particular load or the load carrying capacity at the End of Design Life (EDL) can be predicted for a limit strain under isothermal conditions. Strain envelops of selected JGTs show that locked strain (ε_L) increases and the recoverable strain(ε_R) decreases with the increase in loading time. Results also indicate that when a particular strain is developed within a shorter duration, larger value of ε_R and smaller value of ε_L are found. On the other hand, when relatively longer duration is taken to generate the same amount of strain, comparatively smaller value of ε_R and larger value of ε_L can be seen.

It is expected that the findings and observations of the study will be useful for the application of JGTs in various civil engineering works, as well as for the standardization of JGTs.

TABLE OF CONTENT

Title		Page No
Decleration		i
Acknowledgements		ii
Abstract		iii
Contents		iv
Notations		vii
List of Tables		ix
List of Figures		x
CHAPTER ONE	**INTRODUCTION**	
	1.1 General	1
	1.2 Background of the Research Work	2
	1.3 Objectives of the Research Work	3
	1.4 Research Methodology/Experimental Design	3
	1.5 Outline of the Thesis	4
CHAPTER TWO	**LITERATURE REVIEW**	
	2.1 General	6
	2.2 Types of Geotextile	6
	2.2.1 Synthetic Geotextile	7
	2.2.2 Natural Fibered Geotextile	7
	2.2.2.1 Variety of JGT	7
	2.3 Treatment Process of JGTs	9
	2.4 Historical Development of Textile as Soil Reinforcement	10
	2.4.1 Development of Geosynthetics as Engineering Material	10
	2.4.2 Development of JGT as Engineering Material	11
	2.5 Properties of Geotextile	12
	2.6 Applications of JGT	12
	2.6.1 Use of JGTs in Road Construction	13
	2.6.2 Use of JGTs in Road and Hill Slope Protection	14
	2.6.3 Use of JGTs in River Bank Protection	15
	2.7 Past Research on JGTs	16

2.8 Potentiality of JGT in Bangladesh Context 19
2.9 Functional Mechanism of RSS 19
2.9.1 Reinforced Fill 19
2.9.2 Retained Fill 21
2.9.3 Facing Units 22
2.9.4 Connections 22
2.10 Mathematical Models to Represent Creep Responses of Geosynthetics 23
2.11 Design Approaches for RSS 23
2.11.1 Limit Equilibrium Approach (LEA) 24
2.11.1.1 AASHTO Standard Specifications for Highway Bridges (1997) 24
2.11.1.2 DIBt Method (1998) 25
2.11.1.3 HA 68/94 Method (1997) 26
2.11.2 Hybrid Approach 27
2.11.2.1 BS8006 (1995) Method 27
2.7.2.2 TBW Design Method (1998) 31
2.11.3 Limit State Approach (LSA) 34
2.11.3.1 Model for Internal ULS Mechanism 35
2.11.3.2 Model for Internal SLS Mechanism 35
2.12 Types of Action Consider in RSS 36
2.12.1 Single-Stage Actions (SSAs) 37
2.12.2 Multi Stage Actions (MSAs) 38
2.13 Strain Responses of Material Under SSA 39
2.13.1 Elastic Material 40
2.13.2 Plastic Material 41
2.13.3 Elasto - Plastic Material 43
2.13.4 Elasto-Visco-Plastic Material 45
2.14 Design Strength of Geotextiles for RSS 47
2.14.1 Reference Strength 47
2.14.1.1 Reference Strength for SSAs 47
2.14.1.2 Reference Strength for MSAs 48
2.14.2 Partial Factors and Design Strength 50

CHAPTER THREE TEST PROGRAM

3.1 General 51

3.2 Tests for Physical Properties of JGT 51

3.2.1 Mass per Unit Area 51

3.2.2 Nominal Thickness 52

3.3 Tests for Mechanical Properties of JGT 53

3.3.1 Constant Rate of Strain Test 54

3.3.2 Sustained Load Creep Test 57

3.4 Isochronous Load-Strain Curves 57

3.5 Development of ε_R - ε_L Plot and Strain Envelope for EVP Material 59

CHAPTER FOUR RESULTS AND DISCUSSIONS

4.1 General 61

4.2 Physical Properties of JGT 61

4.2.1 Mass per Unit Area 61

4.2.2 Nominal Thickness 62

4.3 Mechanical Properties of JGT 62

4.3.1 Wide-Width Tensile Strength 62

4.3.2 Sustained Load Creep Test 64

4.4 Extrapolation of Creep Test Data 65

4.5 Isochronous Curves of JGT 67

4.6 Development of ε_R - ε_L Plot and Strain Envelope for JGTs 70

CHAPTER FIVE CONCLUSIONS AND RECOMMENDATIONS

5.1 General 80

5.2 Conclusions 80

5.3 Recommendations for Future Study 81

REFERENCES 82

APPENDIX A 87

APPENDIX B 91

NOTATIONS

$\emptyset$	Friction Angle of Soil
ϕ'_{cv}	Constant Volume Angle of Friction
ϕ'_{p}	Peak Angle of Friction of Soil
σ_v	Vertical Stress on Reinforcing Element
γ	Calculated Factor of Safety
γ_m	Partial Factor Obtained from CRS Tests
γ_1	Density of the Reinforced Fill
ε_E	Elastic Strain
ε_R	Recoverable Strain
ε_L	Locked in Strain
ε_P	Plastic Strain
ε_T	Total Strain
ε_V	Viscous Strain
μ	Coefficient of Friction Between Soil and Reinforcements
C_i	Coefficients of Interaction
F_{perm}	Permissible Working Load
K_a	Active Pressure
P_u	Ultimate Tensile Strength
P_s	Sustained Load
$P_{short\text{-}term}$	Sort-Term Load
P_{Ref}	Reference Strength
T_{al}	Long Term Strength
T_b	Reinforcement Base Strength
T_{cr}	Tensile Creep Rupture Strength
T_{cs}	Tensile Load in the Reinforcement
T_d	Design Strength
q_r	Imposed Bearing Pressure
t_{CP}	Construction Period
t_{RL}	Reinforcement Loading Period
AASHTO	American Association of State Highway and Transportation Officials
ASTM	American Society for Testing and Materials
ASAE	American Society of Agricultural Engineers
AT	Additive Treated
BJMA	Bangladesh Jute Mills Association
BJMC	Bangladesh Jute Mills Corporation
BJRI	Bangladesh Jute Research Institute
BS	British Standard
BUET	Bangladesh University of Engineering and Technology
BWDB	Bangladesh Water Development Board

CBR	California Bearing Ratio
CPT	Calcutta Port Trust
CRE	Constant Rate of Extension
CRS	Constant Rate of Strain
DIN	German Institute for Standardization
EDL	End of Design Life
EVP	Elasto-Visco-Plastic
GRSS	Geosynthetic Reinforced Soil Structures
IJIRA	Indian Jute Industries Research Association
IJSG	International Jute Study Group
ISE	Isochronous Strain Energy
ISG	Improve Subgrade
ISO	International Standards Organization
JGT	Jute Geotextile
JDPC	Jute Diversification Promotion Centre
LEA	Limit Equilibrium Approach
LGED	Local Government Engineering Department
LSA	Limit State Approach
MD	Machine Direction
MSA	Multi Stage Action
NTP	Normal Temperature and Pressure
PVD	Prefabricated Vertical Drain
PWD	Public Work Department
RF	Reduction Factor
RHD	Roads and Highways Department
RSS	Reinforced Soil Structure
SLS	Serviceability Limit State
SRDI	Soil Resource Development Institute
SSA	Single Stage Action
ULS	Ultimate Limit State
US	Ultimate Strength
XMD	Cross Machine Direction

LIST OF TABLES

		Page No.
Table 2.1	Summary of the jute diversification and promotion project	18
Table 4.1	Average mass per unit area of untreated and additive treated JGTs	61
Table 4.2	Average thickness of untreated and additive treated JGTs	62
Table 4.3	Wide-width test results of untreated JGTs for different strain rate in machine direction and cross machine direction at constant temperature, 21°±2	63
Table 4.4	Wide-width test results of additive treated JGTs for different strain rate in machine direction and cross machine direction at constant temperature, 21°±2	63
Table 4.5	Summary of wide width test result of JGT untreated and additive treated JGTs at different strain rate in machine direction and cross machine direction	64

LIST OF FIGURES

		Page No.
Figure 2.1	Geotextile made from synthetic fiber: (a) woven fabrics, (b) non-woven fabrics and (c) knitted fabrics	7
Figure 2.2	Geotextile made from natural fiber: (a) jute geotextile and (b) coir geotextile	7
Figure 2.3	Types of JGT: (a) woven, (b) nonwoven and (c) open weave	8
Figure 2.4	Photographs of treated JGTs: (a) bitumen treated and (b) additive treated	9
Figure 2.5	Use of JGT to improve load bearing capacity of subgrade (Khan et al., 2014)	13
Figure 2.6	Application of JGTs to control hill slope erosion: (a) application of JGT and (b) stabilized slope with grown vegetation within one year (Islam et al., 2014)	14
Figure 2.7	Application of treated JGT to form natural filter cake to stabilize river bank	15
Figure 2.8	Reinforce stabilization of soil: (a) concrete wall to retain soil and (b) soil retention by geotextile reinforcement	20
Figure 2.9	Reinforced embankment slope	20
Figure 2.10	Different sections of reinforced soil structures: (a) retained fill, (b) and (c) without retained fill (Pradhan, 1996)	21
Figure 2.11	Assessment of SLS base strength TCS (BS8006, 1995)	31
Figure 2.12	Typical distribution of active earth pressure in a retaining wall	33
Figure 2.13	Distribution of force due to active earth pressure for wedge check	33
Figure 2.14	Strain distribution in individual reinforcement due to active earth pressure	33
Figure 2.15	Examples of SSA: (a) sustained loading, (b) cyclic loading and (c) impact or short term loading (Mahaseth, 2002)	37
Figure 2.16	Examples of MSA: (a) stepped loading, (b) P_s plus cyclic loading and (c) sustained plus $P_{short\text{-}term}$ (Mahaseth, 2002)	39
Figure 2.17	Strain response of elastic material under SSA: (a) sustained loading, (b) cyclic loading and (c) impact or short term loading (Mahaseth, 2002)	41

Figure 2.18	Strain response of plastic material under SSA: (a) sustained loading, (b) cyclic loading and (c) impact or short term loading (Mahaseth, 2002)	42
Figure 2.19	Strain response of elasto-plastic materials to SSA: (a) sustained loading, (b) cyclic loading and (c) impact or short term loading (Mahaseth, 2002)	44
Figure 2.20	Strain response of EVP materials to SSA: (a) sustained loading, (b) cyclic loading and (c) impact or short term loading (Mahaseth, 2002)	46
Figure 3.1	Constant rate of strain test setup for geotextile	55
Figure 3.2	Constant rate of strain test of JGT: (a) Wolpert machine and (b) tested sample	55
Figure 3.3	Creep test setup: (a) sample under loading and (b) setup to count deformation	56
Figure 3.4	Creep test setup, series of loading verses time (Mahaseth, 2002)	58
Figure 3.5	Deriving Isochronous load-strain curves for EVP geosynthetics: (a) total strain-time plot and (b) isochronous load-strain curves (Mahaseth, 2002)	58
Figure 3.6	Combinations of strain components for different sustained loadings to EVP material (Mahaseth, 2002)	59
Figure 3.7	Total strain, ε_T and its components with respect to time for EVP material (Mahaseth, 2002)	59
Figure 3.8	Plot of ε_R - ε_L to develop strain envelope for EVP material (Mahaseth, 2002)	60
Figure 4.1	Total strain vs log time (hr) for untreated 627gsm in machine direction	64
Figure 4.2	Strain vs. time curves and best fitted curves for the strain vs. time relationships of untreated 627gsm in machine direction	65
Figure 4.3	Trend line coefficients: (a) coefficient A obtained from linear fit curve and (b) coefficient B obtained from linear fit curve	66
Figure 4.4	Extrapolation of coefficients: (a) coefficient A of linear fit curve and (b) coefficient B of linear fit curve	66
Figure 4.5	Extrapolated total strain vs log time (hr) for untreated 627gsm in machine direction	67
Figure 4.6	Isochronous curves derived from creep test result: (a) untreated 627gsm and (b) untreated 724gsm	68

Figure 4.7	Isochronous curves derived from creep test result: (a) additive treated 627gsm and (b) additive treated 724gsm	69
Figure 4.8	Load vs recoverable strain for untreated 627gsm in machine direction: (a) tested sample response and (b) extension of test result	71
Figure 4.9	Load vs locked strain for untreated 627gsm in machine direction	71
Figure 4.10	(a) Load vs. total strain graph and (b) load vs. recoverable strain graph for untreated 627gsm in machine direction at 0.1hr for different limiting strains	72
Figure 4.11	(a) Load vs. total strain graph and (b) load vs. recoverable strain graph for untreated 627gsm in machine direction at 1 hr for different limiting strains	72
Figure 4.12	(a) Load vs. total strain graph and (b) load vs. recoverable strain graph for untreated 627gsm in machine direction at 10 hr for different limiting strains	73
Figure 4.13	(a) Load vs. total strain graph and (b) load vs. recoverable strain graph for untreated 627gsm in machine direction at 100 hr for different limiting strains	73
Figure 4.14	(a) Load vs. total strain graph and (b) load vs. recoverable strain graph for untreated 627gsm in machine direction at 1000 hr for different limiting strains	74
Figure 4.15	(a) Load vs. total strain graph and (b) load vs. recoverable strain graph for untreated 627gsm in machine direction at 10000 hr for different limiting strains	74
Figure 4.16	(a) Load vs. total strain graph and (b) load vs. recoverable strain graph for untreated 627gsm in machine direction at 100000 hr for different limiting strains	75
Figure 4.17	2% limit strain and it's component vs log time obtained from creep test of untreated 627gsm in machine direction	75
Figure 4.18	5% limit strain and it's component vs log time obtained from creep test of untreated 627gsm in machine direction	76
Figure 4.19	10% limit strain and it's component vs log time obtained from creep test of untreated 627gsm in machine direction	76
Figure 4.20	Strain envelopes at different limit strain in machine direction for: a) untreated 627gsm, b) untreated 724gsm	78
Figure 4.21	Strain envelopes at different limit strain in machine direction for: a) additive treated 627gsm and b) additive treated 724gsm	79

CHAPTER ONE

INTRODUCTION

1.1 General

Use of geotextile for embankment stabilization, reinforcement of soil, grade separation of road layers and many other civil engineering applications is a common practice for many years. Present knowledge and understanding about the behavior of materials, many kinds of soil retaining systems have been established. Soil can be retained by external retaining structures like, retaining walls, shore and sheet pile or internally stabilization by in situ reinforcement through nailing of reinforcement like, metal strip, geotextile etc. In an internally stabilized system, the reinforcing elements, such as metallic strips or polymeric geotextiles or geogrids are placed in horizontal layers. As a result of this placement, the lateral pressure arising from each section is counterbalanced by local reinforcing elements. Use of nets, mats, or other types of structural/mechanical reinforcement, protect embankment or hill slopes against surficial erosion and shallow mass movement by improving their establishment and performance. Geotextiles and geogrids have been successfully used as road subgrade reinforcement in order to increase the load carrying capacity of the reinforced soil subgrade system and thereby to reduce the total thickness of the pavement. Design methods and charts for this purpose have been proposed by many researchers (Koerner, 1998). The economy accrued from the Reinforced Soil Structures (RSSs) may vary in the range of 20 – 80%, depending on the heights of these applications compared to conventional solutions (Jones et al., 1996). The method of reinforcing subgrades with geotextiles is found to be more effective on weaker subgrades. Geotextile can deform enough to mobilize its full tensile strength and thereby increase the load carrying capacity of the reinforced subgrade to its full extent (Khan et al., 2009). The load transfer mechanism in RSS is mainly due to the development of shear forces at the soil-reinforcement interface. Geosynthetics show different responses under varied time and load conditions. To choose the appropriate input design parameters for geosynthetics, the analysis method based on creep test under different loading is found effective due to the duration of the test.

1.2 Background of the Research Work

Elias et al. (1998) suggested that geosynthetic should be designed considering its creep behavior. Current design codes for geosynthetics are not based on the difference in the response of geosynthetics, under different types of loading over time. In this context, McGown et al. (2004) suggested to use the Isochronous Strain Energy (ISE) approach which is developed by Khan (1999), for the characterization of the load–strain–time–temperature behavior of geosynthetic reinforcements. But due to the complexity of ISE approach a simpler approach called strain envelop concept, which already being accepted for geosynthetics. This strain envelop concept is applicable for Jute Geotextiles (JGTs) also. This behavior of JGTs is needed to evaluate.

In absence of any recognized testing standard for JGTs, the American Society for Testing and Materials (ASTM), British Standard (BS), German institute for standardization (DIN) and International Standards Organization (ISO) methods of testing synthetic geotextiles are most commonly adopted for JGTs to determine its properties (Khan, 2008). The strain rate suggested by ASTM 4595, for synthetic geotextiles is based on the fact that synthetic geotextiles are Elasto-Visco-Plastic (EVP) in nature and hence strain rate sensitive. However, JGTs are elasto-pastic material (Mohy, 2005). So the strain rate suggested in ASTM for tensile strength test of geosynthetics, may not be identically applicable for JGTs.

The selection of JGT for a particular geotechnical engineering application depends on adequate and suitable fabric properties, as well as specific functional characteristics in respect of end-use requirements. As jute is a biodegradable material, some treatment techniques like, bitumen treated, additive (liquid latex) treated can enhance the design life of JGT from 5 years to up to 20 years (Abdullah, 1999). With this background in mind, four types of JGTs viz. Untreated (UT) and Additive Treated (AT) of two different masses 627gsm and 724gsm, were selected for this research work, which are commonly used in Bangladesh for different geotechnical purposes. The longevity of additive treated JGT is almost 18 month with the contact of water, where as untreated JGTs degrades within 6 month. For this research work the UT samples were supplied by Bangladesh Jute Mills Corporation (BJMC) and the AT samples were collected from Bangladesh Jute Research Institute (BJRI) through Jute Diversification and Promotion Centre (JDPC).

1.3 Objectives of the Research Work

The main objectives of the research are as follows:

1) To determine the strain response (ε_R; ε_L and strain components for particular limiting strain) of selected JGTs by developing isochronous load-strain curves through creep test data in isothermal condition.
2) To develop strain envelops of selected JGTs for different limiting strains.
3) To perform wide width tensile strength test at different strain rate to identify the effect of strain rate on the strength of JGTs.

1.4 Research Methodology/Experimental Design

The research was conducted as per the following steps:

1) Four types of JGTs, untreated and additive treated of two different masses 627gsm and 724gsm were selected for this investigation, which are commonly used in Bangladesh for different geotechnical purposes.
2) Physical properties i.e., mass per unit area and thickness of JGT samples was determined as per ASTM D5261-10 and ASTM D5199-01, respectively.
3) The JGT samples for wide width tensile strength test were prepared accordance with ASTM D4595-11. Nine specimens of each type JGT, viz. UT and AT in two different mass 627gsm and 724gsm in both direction MD and XMD, were prepared for testing. A set of three sample of each type JGT were tested at three different strain rate (10±3)%/min, (50±5)%/min and (100±10)%/min, to evaluate the strain rate sensitivity of JGTs.
4) Unconfined creep test on UT and AT JGT samples were performed as per ASTM D5262-07 test method. The samples were prepared according the specified test method. The loads for creep test were chosen based on the percentage of geotextiles's wide width tensile strength. Creep tests were conducted using 10% (P_{10}), 20% (P_{20}), 30% (P_{30}) and 40% (P_{40}) of ultimate tensile strength (P_u) of a particular sample. Samples were loaded for 1000 hours and readings were taken at 0.01, 0.1, 0.25, 0.5, 1, 2, 5, 10, 30,100, 200, 500 and 1000 hour. After 1000 hours, the loads were removed and the elastic strain was also being measured.

5) A series of isochronous (load-strain) curves have been prepared from creep test result for the specified loads, as well as for higher loads by extrapolation of test results. The test results are then used to evaluate and develop elastic strain, visco-plastic strain and strain envelops for different limiting strain.

1.5 Outline of the Thesis

The complete thesis is divided into number of chapters. The sequential chapters will make it easier to understand the chronological developments of the research work, which were conducted to achieve the objectives mentioned earlier. The contents of each chapter are presented below:

Chapter one describes the background, objectives and the methodology of the research work. Finally the formation of the thesis is presented in this chapter.

Chapter two initially discusses the types and applications of geotextile, specially the JGTs. In the perspective of Bangladesh the academic researches and outcomes of the field trials on JGTs are reviewed in this chapter. The significant features and different components of RSSs are presented in Chapter Two. The mathematical models to simulate the behavior of geosynthetics and recent design approaches for RSSs are described in this chapter. The types of loading condition, which are considered for RSSs, as well as the strain responses of geotextile under Single Stage Action (SSA) are incorporated in this chapter. The potentiality of JGTs in the context of Bangladesh is also presented in chapter two.

In chapter three the standard test procedures of physical and mechanical (strength) properties of RSSs are discussed, which are applicable for JGTs also. In addition different types of loading actions are discussed with examples and the isothermal strain responses of various materials, ranging from perfectly elastic to EVP under these actions are presented here. Different strain components of these materials are identified, for various combinations of time and limiting strain. Further, the understandings of strain envelop for EVP materials under SSA are also presented on the basis of Boltzmann's superposition principle.

The test results of physical and mechanical (strength) properties of JGTs are presented in chapter four. The assessment of strain rate sensitivity of JGTs is discussed here. In this chapter, different strain components of tested JGTs under SSA and their various combinations of time and limiting strain are developed on the basis of Boltzmann's

superposition principle. Further, the formation of strain envelops for different limiting strains of the selected JGTs are described in this chapter.

Chapter Five comprise the conclusions obtained from the understanding of test results. Recommendations for future studies have also been listed in this chapter on the basis of present study.

CHAPTER TWO

LITERATURE REVIEW

2.1 General

The creep responses of reinforcement fabrics are needed to measure/assume, because in service life the material will be subjected to a complex pattern of loading and unloading cycles. It is not feasible to obtain experimental data to cover all possible loading situations and for each individual case, the determination of input parameters which are required for design. JGT established itself as an important engineering (especially geotechnical) materials by its diverse and effective uses. The development of JGTs as engineering materials and its various applications are described in this chapter. The potentiality of JGTs in the context of Bangladesh is also presented in this chapter. The response and properties of RSSs are needed to predict at operational conditions. The significant features of different components of RSSs are presented in this chapter. The mathematical model to simulate the behaviour of geotextiles (geosynthetics or JGTs) and recent design approaches available for RSSs is described in this chapter. The types of loading condition are considered for RSSs, as well as the strain responses of geotextile under Single Stage Action (SSA) are incorporated in this chapter.

2.2 Types of Geotextile

According to ASTM geotextile is permeable fabric (they use the word synthetic fabric because till a few years ago almost all type of geotextiles were made by synthetic fabrics) used with foundation, soil, rock, earth, or any other geotechnical engineering-related material as an integral(essential) part of human-made project, structure, or system. According to ASAE (American Society of Agricultural Engineers) geotextile is a fabric placed on or between the soil and earth retaining structure to enhance water movement in soil and retard soil movement, work as soil reinforcement and separation. Geotextiles can be classified based on the type of fiber it is made, which are sythetic geotextile and natural fibered geotextile.

2.2.1 Synthetic Geotextile

Synthetic geotextiles are made by synthetic fiber like polyester, polyamide, polypropylene, polyethylene and further prepared in three different categories – woven fabrics, non-woven fabrics and knitted fabrics, Fig. 2.1.

(a) (b) (c)

Fig. 2.1: Geotextile made from synthetic fiber: (a) woven fabrics, (b) non-woven fabrics and (c) knitted fabrics

2.2.2 Natural Fibered Geotextile

Geotextiles are can also made from naturally grown fiber, such as jute fiber and coir as shown in Fig. 2.2.

(a) (b)

Fig. 2.2: Geotextile made from natural fiber: (a) jute geotextile and (b) coir geotextile

2.2.2.1 Variety of JGT

JGT can be classified into three distinct types considering the distinct fabric characteristics and form, which are woven, nonwoven and open weave commonly known as soil saver.

i) Woven JGT: These types of JGTs are manufactured by adopting techniques which are similar to weaving usual clothing textiles. This type has the characteristic appearance of two sets of parallel threads or yarns. The yarn running along the length is called warp and the one perpendicular is called weft. Woven JGTs has established its effectiveness in performing functions of separation, filtration, drainage and initial reinforcement.

ii) Nonwoven JGT: Non woven geo-synthetics can be manufactured from either short staple fibre or continuous filament yarn. The fibers can be bonded together by adopting thermal, chemical or mechanical techniques or a combination of techniques. Non-woven geotextiles are manufactured through a process of mechanical interlocking or chemical or thermal bonding of fibres/filaments.

iii) Open Weave JGT: Open weave JGT is a woven fabric which is manufactured by interlacement of thick warp and weft jute roves (yarns) set at right angle to each other through conventional jute loom with pore size of about 20mm **x** 25mm, (Ghosh et al., 2014). This type of JGT used to control surface soil erosion, slope protection and in treated condition for embankment stabilization.

(a)

(b)

(c)

Fig. 2.3: Types of JGT: (a) woven, (b) nonwoven and (c) open weave

In the perspective of Bangladesh, the advantages of JGTs are as follows,

1) Production cost is very low compare to other natural and synthetic geotextile.
2) Installation process of JGT is easy, even unskilled/semi-skilled person can do the job.
3) Eco-friendly due to its biodegradability within one year in untreated condition.
4) Longevity can be achieved up to 4/5 years by some simple treatment techniques, which allow it to use for medium to long term applications.
5) As the total production process (raw materials to finishing face) is done in Bangladesh, it improves the local economy.

2.3 Treatment Process of JGTs

JGT is environmental friendly, biodegradable, hydrophobic, anionic and locally available materials. It is also a renewable source of energy as natural biomass. Normally Jute fibre is swelled and degraded within six months with the contact of water in untreated condition. So some treatment technique is necessary to enhance its design life up to 5–20 years for medium term to long term applications.

(a) (b)

Fig. 2.4: Photographs of treated JGTs: (a) bitumen treated and (b) additive treated

i) **Treatment with Bitumen Emulsion of Specific Density:** Carbon black was prepared with required quantity of volatile oil and then bitumen emulsion was added with paste and stirred. After mixing homogenously, the emulsion was laminated on the modified hessian cloth by brass manually and dried in sunlight or open area at Normal Temperature and Pressure (NTP).

ii) Treatment with Silicate of Specific Viscosity: Silicate solution was prepared by adding hot water and stirred according to need and then used on the modified bitumen treated samples manually and dried at NTP.

iii) Treatment with Ca-base Grease Composite: Ca-base grease was added with required amount of carbon black and prepared a paste by adding volatile oil. The composite paste was then rubbed haphazardly by hand on the modified hessian cloth and completed the rubbing by brass. After rubbing a small amount of carbon black was sprayed over the located area or full sample and then again rubbed by brass.

iv) Rot-Proofing Treatment: Sodium Carbonate and Sulfate of Copper is mixed with water and sprayed manually over jute fabrics. The treated fabrics were dried in sun light at NTP (Pradhan, 2008).

2.4 Historical Development of Textile as Soil Reinforcement

Historically, RSSs were constructed using organic materials as reinforcements, like timber, straw or reeds. Later, as early as the 19th century, Pasley (1822) recognized the potentiality of more advanced forms of reinforcement. His use of canvas as a reinforcing membrane may arguably be considered as the first application of geotextile reinforcement, (Jones et al., 1996). Due to the biodegradability of this material, Pasley's structures were expected not to be very durable in the long term.

2.4.1 Development of Geosynthetics as Engineering Material

The use of non-metallic materials (geosynthetics) as permanent reinforcement could be seriously contemplated only after the development of synthetic polymer based materials. Synthetic fabrics were known prior to 1940, but it was not until late 1960s and early 1970s that the advances in synthetic fabrics and geosynthetics produced materials meant that their longevity could be assured (Jones et al., 1996).

Netherland was the first country to take the initiative and used man-made geotextiles in 1953 for a massive delta project. The project was carried to save the delta from ravages of floods generated from the North Sea. Other developed countries such as the USA followed suit and started using man-made geotextiles for prevention of soil erosion. By the late 1960s man-made geotextiles became globally popular. It has to be admitted that the effectiveness of man-made geotextiles was established after years of rigorous research,

studies and field trials backed by intensive marketing by the producers before the users felt confident to use the new product. The growth of man-made geotextiles over the last three decades has been remarkable. From 10.2 million sq. meters in 1970 the consumption soared to 2475 million sq. meters in 2006-07- the growth rate being 10% to 15% since 2000-01. The market for geotextiles is still confined to the USA, Canada, developed countries in Western Europe, Japan and Australia. These countries account for nearly 33% of the global consumption (jutegeotech.com).

2.4.2 Development of JGT as Engineering Material

The research and development effort with jute fiber started first in Indian Jute Industries Research Association (IJIRA), Kolkata. The effort lacked the desired focus in the initial stages. Nevertheless it was possible to convince some of the end-using organizations such as Calcutta Port Trust (CPT) to undertake field trials in the late 1980s. Concurrently some of the overseas technical institutions such as Singapore National University (SNU), Bangladesh University of Engineering and Technology (BUET) also initiated research and development exercises with JGTs.

One of the major reasons of the insignificant consumption of natural geotextiles could be the lack of systematic and thorough study on performance of JGT and its effects on soil of varying characteristics under different nature, magnitude and frequency of imposed loads. The studies conducted so far in the field of natural geotextiles in general have not been as intensive as is desired. Things however have started changing in so far as jute is concerned.

Interestingly jute hessian was applied in a road at Dundee, Scotland in 1920, in Strand Road at Kolkata by Bengal PWD in 1934 and in Mynamar during the 2nd world war with reported success. The concept of geotextiles was not known at that time. There was a long period of lull after these applications. JGT was first consciously used for slope stabilization at Sahasradhara, Uttarakhand by CSWCRTI (Central Soil & Water Conservation Research & Training Institute) in1987, for control of riverbank erosion at NayacharIsland in the Hugli estuary by Calcutta Port Trust in 1989, for restoration of a severely damaged road at Kankinada, Andhra Pradesh by CRRI (Central Rice Research Institute) in 1996 and for control of railway track settlement at Madhusudanpur in Howrah-Burdwan Chord line in 2001(jutegeotech.com).

Laboratory studies on the physical and engineering properties of different varieties of geotextiles as well as some field studies have been carried out by BUET, Local Government Engineering Department (LGED), Roads and Highways Department (RHD), Bangladesh Water Development Board (BWDB) and Soil Resource Development Institute (SRDI) in recent years. Bangladesh Jute Research Institute (BJRI) has developed some treatment techniques for JGTs which may enhance their non-biodegradability (Abdullah, 1999). Development of such durable JGT materials is likely to allow them to be used in short-term to medium-term soil reinforcement applications (Khan, 2008).

2.5 Properties of Geotextile

There are three main properties which are required and specified for a geotextile are its mechanical responses (tensile strength, bursting strength, flexibility, tearing strength and frictional resistance), filtration ability (porosity, permeability, permittivity, transitivity, turbidity/soil retention, filtration length etc.) and chemical resistance with physical properties (specific gravity, mass per unit area and thickness).These are the properties that produce the required working effect. They are all developed from the combination of the physical form of the fibers, their textile construction and the chemical characteristics. For example, the mechanical response of a geotextile will depend upon the orientation and regularity of the fibers as well as the type of fiber from which it is made. Also, the chemical resistance of a geotextile will depend upon the size of the individual component fibers in the fabric, as well as their chemical composition.

2.6 Applications of JGT

Bangladesh is the second highest jute producer, almost 42% (1,452,044 m/t) of world growth, (top 5 of Anything.com) and jute itself eco-friendly in nature. JGT have emerged as potential candidate to replace the geosynthetics in various civil engineering applications (Khan et al., 2014). The properties of jute such as flexibility and strong coherence with soil attribute to its better performance in soil matrix. BJRI has developed several treatment techniques for JGTs which may enhance their non-biodegradability (Abdullah, 1999). Development of such durable JGT materials is likely to allow them to be used in short-term to medium-term soil reinforcement applications i.e., rural roads, construction of access roads, hill and road slope protection, river bank and flood embankments stabilization etc. (Khan, 2008).

2.6.1 Use of JGTs in Road Construction

It is hypothesized that three mechanisms are involved with increase of load carrying capacity of subgrades due to use of JGT following the process described herein. First, the JGT layer as long as it does not decompose acts as an initial reinforcement through membrane action. JGT takes some extra load via its in-plane tensile resistance. Second, the first layer of ISG (Improve Subgrade), made of sand, absorbs a lot of moisture from the subgrade. This absorbed moisture in the ISG layer is then absorbed by the JGT layer. It may be noted that JGTs have moisture absorption capacity of 3-4 times their dry weight, i.e. one square meter of 627 gsm JGT is capable of absorbing about 2.0 litre of water. This absorption of moisture from subgrade increases the dry density and hence the shear strength of the subgrade material increases. This phenomenon occurs as long as the JGT is not fully decomposed. By the time JGT is decomposed, the third mechanism also takes place. The subgrade soil becomes more competent through the consolidation process due to the surcharge load of sub-base and base layer and also partly due to the traffic movement on the black top. This third mechanism, would have occurred anyway even without JGT application. But the process is enhanced due to the absorption characteristics of JGT. The test results reveal that the load carrying capacity of the road sections increases from 1.5 to 7.0 times due to use of JGT over a range of time interval (Khan et al., 2014).

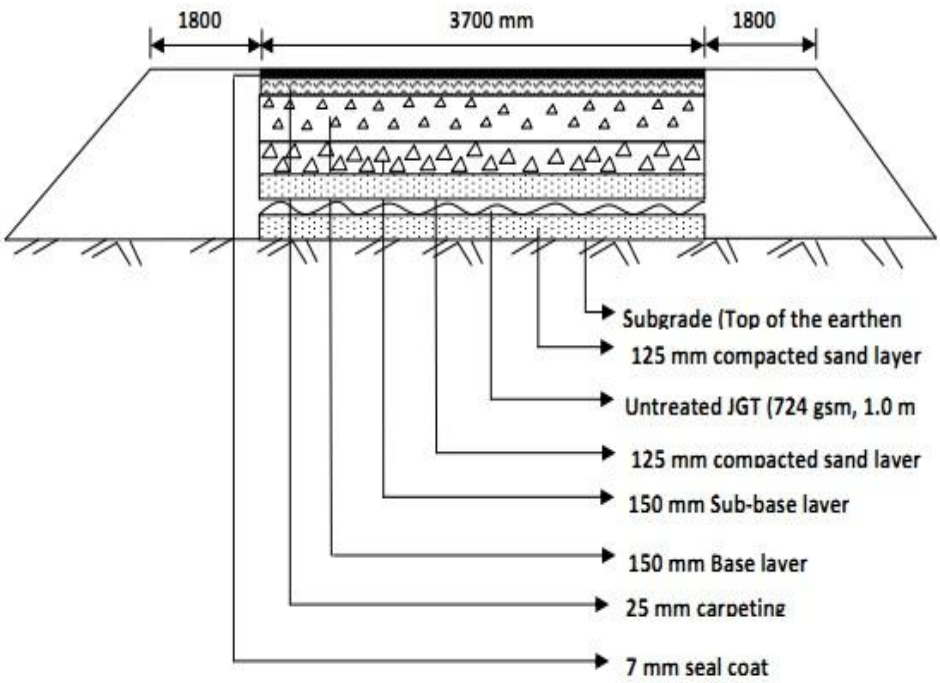

Fig. 2.5: Use of JGT to improve load bearing capacity of subgrade (Khan et al., 2014)

2.6.2 Use of JGTs in Road and Hill Slope Protection

Open weaved JGTs known as soil saver with vegetation usually used slope protection work. Open-weave products can store runoff water behind their thick weft fibres, which act as 'mini-dam', so reducing runoff volume. The JGTs are fixit by tamping of live, rootable vegetative cuttings or 'U' shaped fixing pins into the ground. Then long rooted selected type grasses are planted. Usually JGTs can absorb water equivalent to 300% to 400% of its dry weight. This high water-holding capacity will allow the fibres to absorb incoming rainfall before it contributes to or generates surface runoff. By intercepting and absorbing rainfall, the weight of geojute will increase over time, giving excellent contact with the soil beneath. This will retard flow on the soil/geotextile interface, limiting erosion and undercutting beneath the geotextile failure (Rahman, 2009). Soil saver breaks the runoff velocity by about 35%-40% and thus reduces significant amount of soil loss (JMDC, 2008).

(a) (b)

Fig. 2.6: Application of JGTs to control hill slope erosion: (a) application of JGT and (b) stabilized slope with grown vegetation within one year (Islam et al., 2014)

As the water holding capacity of JGTs are so high, in dry season it helps to retain the soil moisture. Hence, it helps the planted vegetation like vetiver to grow even in the dry season. On the other hand, in rainy season it protects soil erosion. So geo-jute is helping the vegetation to grow in all the seasons. Geo-jute is a biodegradable material which becomes composed fertilizer within 12 month in untreated condition. Hence high strength long rooted vetiver grass will take place the function of geo-jute by this time. Its roots grew more than 25 cm within three months and its leaves grew more than 30 cm in a month. Vetiver grass can grow in sandy silt. It has high tolerance to weather variation.

Moreover, it is not a grazing type grass. So, it is sustainable vegetation. Its root has high tensile strength which grabs the soil firmly. Hence the laid geo-jute over the exposed surface helps to control soil erosion primarily and as the geo-jute degrades with time, vegetations like vetiver grasses grew up and took over the function of geo-jute (Islam, 2013).

2.6.3 Use of JGTs in River Bank Protection

One of the reasons of erosion of river banks may be attributed to seepage of water flow in sudden draw down situation. Such flow of water causes soil to be washed away resulting in river bank erosion (Khan et al., 2014).

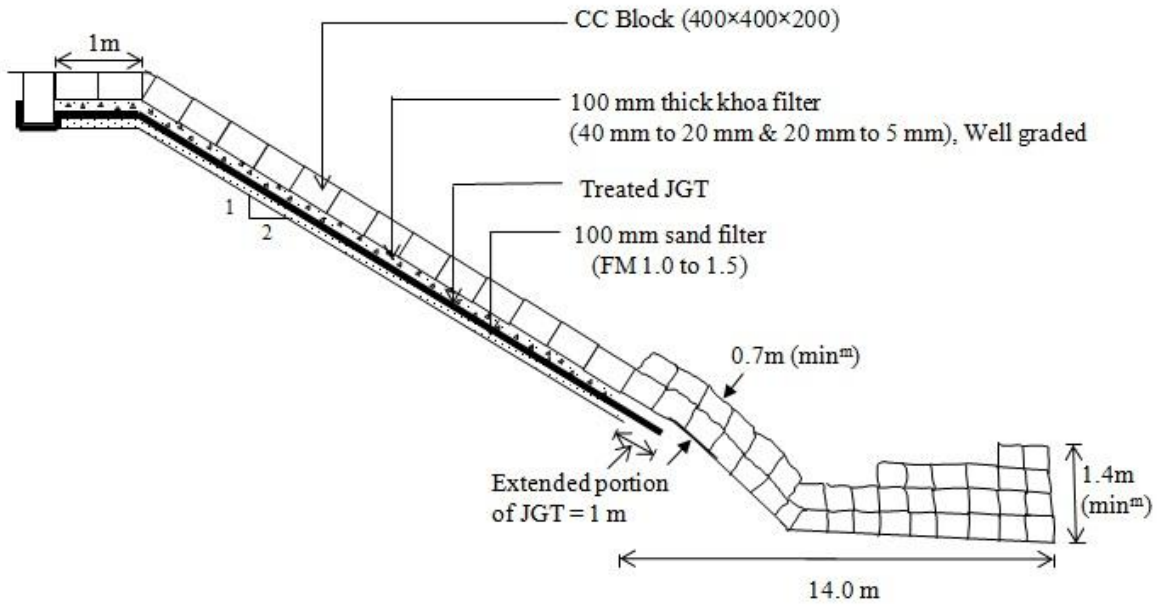

Fig. 2.7: Application of treated JGT to form natural filter cake to stabilize river bank

JGT being permeable material, allows the retained water within soil to across its plane and also to disperse water along its plane. The cross permeability depends on several factors, especially pore size of JGT called porometry. The porometry of JGT is also the determinant in retention of soil-particles on which it is laid. JGT provides a technically superior solution to conventional granular graded filters used for control of erosion of river banks. JGT can be manufactured with pore sizes commensurate with the median grain size of the base-soil to ensure their retention. At the same time, water is allowed to pass across and along JGT in the required measure without causing development of any differential overpressure. JGT, first retain the coarser particles of the soil and the coarse particles

block smaller ones in the soil which in turn prevents migration of even smaller grains. This phenomenon is known as filter cake formation. This is an indication of formation of natural filter within the soil and its optimum consolidation. Soil properly overlain by JGT is seen to develop filter cake happen within a period of 6/7 months from the date of application according to laboratory tests carried out in research institutes. Development of filter cake is a sure indication that the base-soil attained natural stability. Once the soil attains natural stability, function of any separating fabric (manmade or natural) becomes redundant (Kabir, 2015).

2.7 Past Research on JGTs

Jute fiber and products from jute fiber of Bangladesh have a long golden history but the use of jute fiber as engineering materials came in to consideration in late 90s. In Bangladesh, BUET did some research and field trials along with LGED, RHD, BWDB and SRDI. In the last 15 years. Some researches have been carried on JGT under the supervision of BUET. In the year 2005 Mohy showed that JGT can be used efficiently as separator between two dissimilar materials and to reinforce weak soils for short term to medium term applications. His study also showed that, permittivity and apparent opening size of tested geojute allow these to be used in filtration function behind flexible wall systems, which allow the backfill soil to be retained in its position. Although, the geojute materials were found to be suitable for pressure drainage applications. He estimated that if synthetic geotextiles are replaced with geojute in civil engineering applications, significant economic benefit can be obtained.

Islam (2008) did research to investigate soil – jute geotextile interaction by means of pullout tests. He used two types of untreated jute geotextiles (Wool Pack and DW Jute Bag) and dredged fill sand samples for the pullout test. The sand samples were collected from the stack yard of Kaliakoir by pass construction project, Joydevpur-Tangail road, Gazipur, Bangladesh. The results of this study indicate that the dredged fill sand soils can be successfully reinforced with jute geotextile reinforcements and the coefficients of interaction (C_i) are equal to 0.9 - 0.95 for all tests indicating good bonding between the tested soil and jute geotextiles. In the same year Wahidul Islam did study to investigate the feasibility of using Prefabricated Vertical Drain (PVD) made of jute fiber in accelerating the consolidation process of soft soil under surcharge. The performance of jute PVD was

found as similar to synthetic PVD where as synthetic PVD is two times costly than jute PVD.

Rahman (2009) did study on jute geotextiles for two different applications related to road construction. In one application, open mesh type untreated geojute was used to stabilize the road slopes from raindrop erosion until the vegetations were established. Both laboratory testing and field trial was undertaken for this purpose. All the test data and observations suggest that the geojute and vegetation system reduces the surface runoff by 85% and reduces the eroded soil particles by 93% in comparison to an exposed slope. The system was also found eco-compatible and cost-competitive. In another application, woven type treated DW Twill was used for the purpose of subgrade soil reinforcement of a flexible pavement. A systematic laboratory investigation and field trial was carried out. The test results showed that the CBR (California Bearing Ratio) value increases by 1.5 times with the application of jute geotextiles in subgrade soil. This finding has been used in design and construction of a segment of road following the guideline practiced in Bangladesh. The study also reveals that higher cost competitiveness of jute geotextiles reinforced subgrade may be obtained for CBR values less or equal to 2.0.

Islam (2013) did research on JGT and his research was on the use of vegetation and geo-jute for slope protection. The main objective of his research was to search most suitable vegetation and to investigate its application for slope protection. Use of vetiver grass and geo-jute in stabilizing road embankment and slope against rain-cut erosion was investigated. Field trials were made in embankment and pond slope. Three sites were selected in three different geographic regions in Bangladesh. He found that vetiver plantation increases the stability of the slope by 50% and the cost of slope protection by vetiver grass and geo-jute is significantly lower than the cost of other available slope protection measures. So from his study, it can be said that vetiver grass plantation with geo-jute is a cost effective and sustainable green solution for the protection of slope against rain-cut erosion in Bangladesh.

Kabir (2015) did research to investigate the effectiveness of JGT as filter material for river bank protection. Two types of JGTs were selected for the study. To investigate the effectiveness of JGT in river bank protection, both field trial and laboratory simulation were performed. For field trial, a site was selected where river bank protection work was going on. Soil samples were collected from the river bank and grain size analysis was performed on those samples in order to investigate formation of filter cake underneath the

JGT. For laboratory simulation, a model was arranged in geotechnical laboratory of BUET. Soil collected from the river bank was used in the model and untreated JGT was used as a filter material. From field trial it was found that, when JGT was used as filter material in river bank protection, natural soil filter cake was formed partially. Since the river bank remained in good shape for more than two years, it can be said that the partially formed filter cake was stable. From laboratory simulation, it was found that filter cake forms partially after a certain period of time. Both the field trial results and laboratory simulation results indicate that the JGT may be considered as an alternative to synthetic geotextiles as filter material for protection of bank slopes of mild to moderate rivers.

From the year 2010 to 2014 a lot of field trials have been undertaken in the areas of river bank protection, rural road construction and hill slope management both in Bangladesh and in India under the auspices of a research and development project funded by Common Fund for Commodities (CFC), Government of India (GoI) and Government of Bangladesh (GoB).

Table 2.1: Summary of the jute diversification and promotion project

Project Area	Rural Road Construction: 5 Sites (1km each) River Bank Protection: 3 Sites (500 m each) Hill slope Stabilization: 2 Sites (300 m each)
Types of JGT Developed by this Project	Open Weave (Hill Slope Stabilization) Woven (River Bank Protection and Rural Road Construction Non-woven (Filtration and Drainage)
Specifications of JGT	Rural Road Construction- 627,724 and 760gsm (Woven) River Bank Protection- 627gsm (woven) Hill Slope Stabilization- 500, 600 700gsm (Open Weave)
Outcome of the Project	Rural Road Construction - Provide reinforcement and improve the quality of rural roads - Increase life span of the road Soil Erosion Control - Reduce rain drop impact and run off velocities - Improve soil fertility Reduce landslides and stabilize the slope

Jute Diversification Promotion Centre (JDPC), of Ministry of Textiles & Jute of GoB has been functioning as the collaborating institution to coordinate the activities in Bangladesh part. International Jute Study Group (IJSG) acted as a supervisory body of this jute diversification project. BJRI, SRDI, RHD, BWDB, LGED, Special Works Organization (SWO) of Bangladesh Army, Bangladesh Jute Mills Corporation (BJMC) and Janata Jute

Mills contributed as facilitating agencies (FAs) of the project. As implemented and monitored by the researchers of Bangladesh University of Engineering & Technology (BUET) and FAs, the outcome performance of the trial sites were found highly satisfactory (Khan, 2016).

2.8 Potentiality of JGT in Bangladesh Context

It is appreciated that LGED has a program of constructing about 4000 km rural roads each year. This single application area may consume about 25million square metre of JGT every year. The BWDB, on average completes about 120 km of river bank protection works. This application area is likely to consume 4 million square metre of JGT every year. For hill slope erosion control and road side slope erosion control there is an additional local demand of 100 million square metre of soil saver type of JGT. Considering per square metre rate of 50-60 BDT, mandatory use of JGT in the three identified application areas is likely to create a local market of 7000 million BDT (approx. 85 million USD). It may be noted that this will enhance the present earning situation of jute sector at least by 25 percent. It has been confirmed by the jute manufacturers and Bangladesh Jute Mills Association (BJMA) that any amount of JGT may be produced and supplied should there be demand for this material (Khan, 2016).

2.9 Functional Mechanism of RSS

The load transfer mechanism in RSS is mainly due to the development of shear forces at the soil-reinforcement interface. Horizontal layers of compacted soil and reinforcement are typical ingredients employed in the construction of RSSs. Some kinds of facings are essential in order to prevent localized surface erosion along the exposed side of the reinforced soil mass, Fig. 2.8. In RSS, the strength of the structure is mainly attributed to the strength of reinforcements by adding tensile strength to the soil mass and by increasing soil strength as a result of increased soil confinement (Jewell, 1980). Ultimately it enables the construction of stable soil structures at angles steeper than the angle of repose of the soil, Fig. 2.9. A number of components like reinforced fill; retained fill; sub-soil; reinforcements; facing units and connections are composed in a Reinforced soil structures.

2.9.1 Reinforced Fill

The load transfer mechanism in RSS is mainly due to the development of shear forces at the soil-reinforcement interface. This major requirement of frictional forces has resulted in

the use of cohesionless or slightly cohesive soil backfills with high friction angles (Yogarajah, 1993).

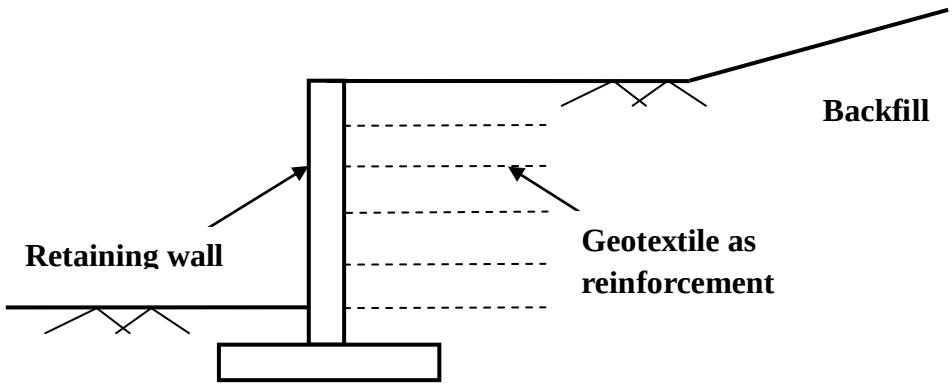

(a)

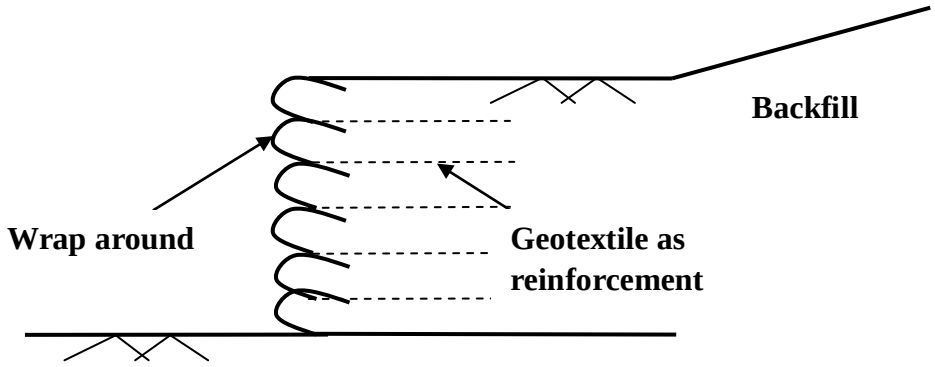

(b)

Fig. 2.8: Reinforce stabilization of soil: (a) concrete wall to retain soil and (b) soil retention by geotextile reinforcement

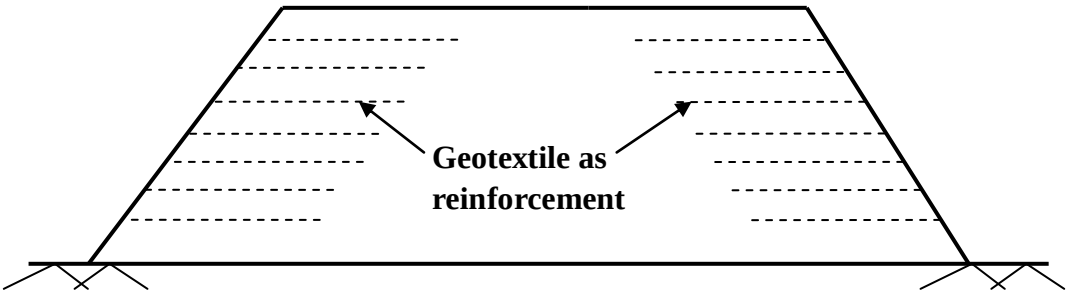

Fig. 2.9: Reinforced embankment slope

Most codes of practice and most design methods suggest granular soils with little or no cohesion to be used, for example, BE3/78 (1987), Geospec 2 (1989), BS8006 (1995), American Association of State Highway and Transportation Officials (AASHTO, 1997), Deutsches Institut Für Bautechnik **(**DIBt, 1998) and Tensar Tie-Back Wedge (TBW)

Method (1998). Generally, it has been suggested that the granular materials should not contain more than 15% finer than 0.08mm, (Lee, 1978). Nevertheless, these days cohesive RSS are also being constructed in some countries on an increasing scale especially in Japan (Kasahara et al., 1992).

2.9.2 Retained Fill

Most of the time, retained fill (fill behind the reinforced soil section) may be present in RSSs, Fig.2.10 (a). However, at times when structures are built to reinstate existing slopes or to widen an existing road, they may not contain the retained fill, Fig.2.10 (b) and (c), but the in-situ soil behind the reinforced fill.

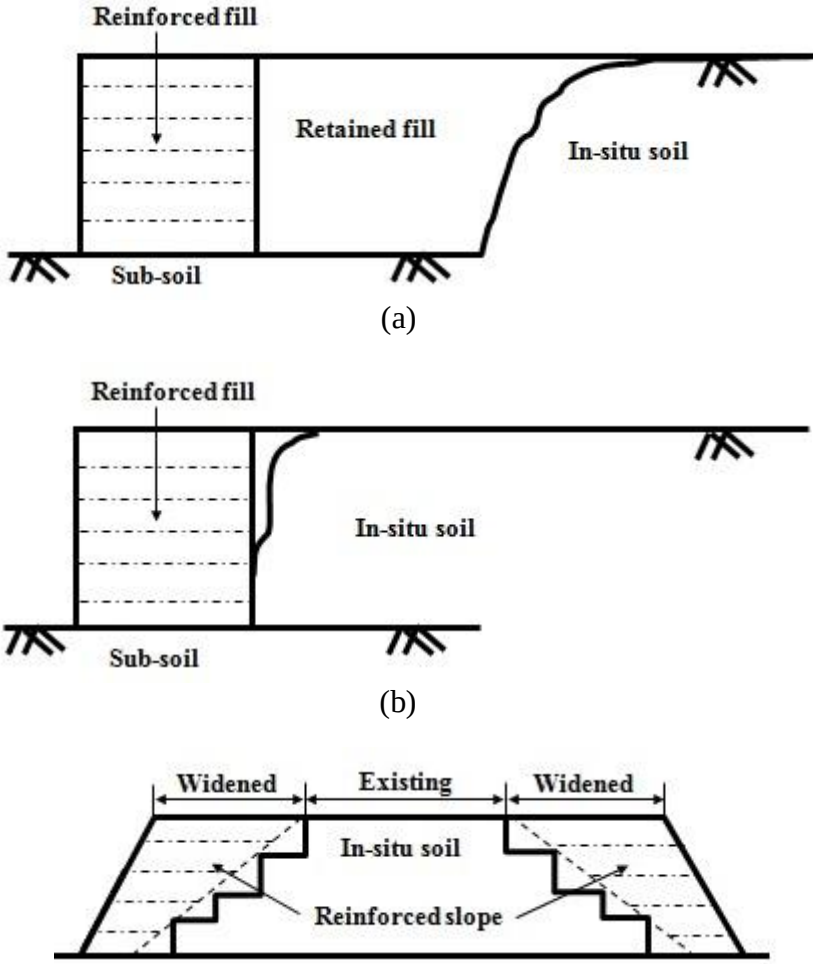

Fig. 2.10: Different sections of reinforced soil structures: (a) retained fill, (b) and (c) without retained fill (Pradhan, 1996)

Otherwise, the retained fill will be the same soil as that of the reinforced fill. Good quality retained fills should be used and their properties appropriately determined, since the

properties of the retained fill may govern the external stability of the reinforced soil structures.

2.9.3 Facing Units

RSSs like walls and steep slopes are generally provided with some kinds of facing to prevent localized surface erosion and progressive failure, although structurally being insignificant. Various kinds of facings have been developed over the years to suit the structures and the site condition. Of these, the most common are concrete panels, (incremental, full height and segmental) and “wrap around” facings where the facing is provided by wrapping the reinforcement around the outside of the compacted soil layer, Fig. 2.8. Facings may be selected to be relatively rigid or flexible and lightweight. The latter is employed to resist low pressures only (Jones, 1993 and Tatsuoka, 1993). Commonly, they share a relatively low cost per unit area of exposed surface (Jones et al., 1988).

2.9.4 Connections

For RSSs with facings, connections between the reinforcement and the facings are vital in that they should be able to transmit the stress from the ends of reinforcement to the facing. In addition, the tensile load-deformation behaviour and flexural properties of the connections are equally important. The different possible connections i.e. vertically sliding connections, loose fitting connections, rigid connections which are tightened up during or after placement of the fill (McGown et al., 1993).

Andrawes and Yogarajah (1994) have reported from large scale model tests carried out on 2m high reinforced soil walls with different connection types that when the reinforcing elements were locked-on to facing units (with no horizontal or vertical movement allowe(d), the maximum tensile strain occurred close to the facing and thereafter was essentially linear away from the facing. On the contrary, the maximum tensile strain occurred away from the facing for loose fitting connections. For the latter case, larger shear resistance was mobilized in the soil and this resulted in reduced lateral earth pressures on the facing units.

2.10 Mathematical Models to Represent Creep Responses of Geosynthetics

Several attempts have been made in the past to simulate the behaviour of geosynthetics with an aim to,

1) Facilitate analysis of the behaviour of geosynthetics products.
2) Assist with extrapolation and interpolation of experimental data.
3) Reduce the need for extensive, time consuming creep tests.

In this regard, various mathematical models, varying from simple to complex, have been developed and been successful in characterizing the problems associated with the mechanical behaviour of geotextile as soil reinforcement. The most successful of the mathematical models are based on spring and dashpot elements to represent the elastic and viscous responses of geosynthetics respectively. Most well known models are, Maxwell model, Kelvin or Voigt model, Maxwell and Kelvin model, Zener (standard linear soli(d) model, Esteve's method and Boltzmann superposition principle.

The creep behaviour of geosynthetics to date has assumed that the level of the applied stress is constant, while in service the material may be subjected to a complex pattern of loading and unloading cycles. It may not be feasible to obtain experimental data to cover all possible loading situations for determining the input parameters for design.

For tackling the problem of the sort above, the simplest theoretical model has been presented by Boltzmann to predict the strain response to a complex stress history. This is referred to as the Boltzmann superposition principle. This model propose that for a linear visco-elastic material, the strain response to a complex loading history is merely the algebraic sum of the strains due to each step in loading. The implication of the idea in this principle is that the behaviour of a geosynthetic is a function of its entire loading history. This principle of Boltzmann is explained in detail in the section 2.13 with the aid of Fig.s for the loading history and its strain response against time.

2.11 Design Approaches for RSS

The current design approaches to external stability have been founded on classical methods for gravity retaining walls with the appendices of internal stability calculations to take the effect of reinforcements into account. Majority of the design methods for RSS is based on Limit Equilibrium Approach (LEA). Though limit state principles are included in

some design codes and methods, which are termed as hybrid approach as they are based partly on LEA and partly on Limit State Approach (LSA).

2.11.1 Limit Equilibrium Approach (LEA)

The method of analysis is based on the assumption that all the constituting elements simultaneously reach their limiting stress conditions. This method calls for the following stability analyses to be carried out to ensure the safety of the structures, external stability and internal stability.

The reinforced soil zone is assumed to act as a monolithic structure. The analyses of external stability for the RSSs are similar to that of the conventional retaining walls and involve the analysis of:

1) Sliding of the structure at the base
2) Overturning of the structure
3) Bearing failure of the subsoil, and
4) Overall stability of the structure

The internal stability analysis, which is different from that of a customary retaining wall, consists of the following:

a) Tension failure of the reinforcing elements
b) Wedge/pull-out failure of the reinforcing elements

No direct or explicit analysis for deformation of the soil boundary is considered in this approach. It is assumed that once the external and internal stability criteria are satisfied, the deformation criteria will also be satisfied. Many design methods have evolved on the basis of the LEA. Examples of these are the AASHTO (1997), the DIBt (1998) and the HA 68/94 (1997) methods.

2.11.1.1 AASHTO Standard Specifications for Highway Bridges (1997)

This method suggests the procedure for designing walls and steep slopes. The soil property used in the analysis is the peak angle of friction (ϕ'_p) and the long term strength (T_{al}) of the reinforcing element for SSAs and MSAs such as sustained loading plus traffic loading is calculated by:

$$T_{al} = \frac{T_{ult}}{RF} \tag{2.1}$$

where,

RF = Reduction factor

= RF_{CR} x RF_{ID} x RF_D

T_{ult} = Short term CRS rupture strength of the reinforcing element per meter width

RF_{CR} = Reduction factor for long term rupture strength

RF_{ID} = Reduction factor for damage from placing and compaction

RF_D = Reduction factor to prevent rupture of the reinforcement due to chemical and biological degradation

The RF_{CR} is determined by comparing the CRS rupture strength (at 10% per minute strain rate) to the long-term rupture strength of a geosynthetic at a specific time and temperature. The RF_{CR} thus depends on the type, design lifetime and operational temperature of the reinforcement. The RF_{ID} and RF_D are determined by comparing the CRS rupture strengths of a geosynthetic 'before' and 'after' construction damage and environmental degradation respectively.

2.11.1.2 DIBt Method (1998)

This design method is based on the DIBt No. Z20. 1-102 and is meant for designing walls and steep slopes. Stability analyses have to conform to different DIN Codes, e.g. the sliding check has to conform to DIN 1054 and the bearing check to DIN 4017.The soil property used in the analysis is the constant volume angle of friction (ϕ'_{cv}) and the permissible working load (F_{perm}) of the reinforcing element for SSAs and MSAs such as sustained loading plus traffic loading is calculated by:

$$F_{perm} = \frac{F_B}{A_1 A_2 \gamma} \tag{2.2}$$

where,

F_B = Short term CRS rupture strength of the reinforcing element per meter width

A_1= Reduction factor for long term strength, (2.40 to 2.75)

A_2= Reduction factor for damage from placing and compaction, (1.05 to 1.5)

γ = calculated Factor of Safety, (1.75)

The reduction factor A_1 is determined by comparing the CRS rupture strength (at 33% per minute strain rate) to the long-term rupture strength of a geosynthetic at a specific time and temperature. The reduction factor A_1 thus depends on the type, design lifetime and operational temperature of the reinforcement. The reduction factor A_2 is determined by comparing the CRS rupture strengths of a geosynthetic 'before' and 'after' construction damage. The values of A_2 thus depend on the type of the soil and the type of geosynthetic.

For design against sustained loading plus traffic loading, the live load surcharges are treated as uniformly distributed surcharge loads that are effective over the whole design life. Two loading cases are considered: permanent traffic loads (load case 1), where the overall factor of safety (FOS) is given as $\gamma_1 = 2.0$, and for temporary traffic loads (load case 2), where overall (FOS) is given by $\gamma_2 = 1.5$.For design against sustained loading plus short-term earthquake loading, F_{perm} is increased by considering $A_1 = 1$ and $\gamma = 1.31$.

2.11.1.3 HA 68/94 Method (1997)

The British HA design method is based on the department of transport advice note HA 68/94. It provides a single unified limit equilibrium design approach for all types of reinforced highway earthworks with slope angle ranging from 10° to 70° to the horizontal. The design presumes that the foundation is competent.

The philosophy of the design method lies in using the soil strength parameters that represent the minimum conceivable values so that no further overall factor of safety needs to be applied to the design. The design suggests the use of the constant volume angle of friction (ϕ'_{cv}) and the design strength ($T_{(d)}$ of the reinforcing elements for SSA is determined from:

$$T_d = \frac{f_k}{\gamma_m} \tag{2.3}$$

where,

f_k=Characteristic long term strength (at 10% limiting strain) of there inforcing element per meter width

γ_m=Partial factor obtained from CRS tests

No specific design strength ($T_{(d)}$ is suggested for sustained loading plus traffic loading or sustained loading plus earthquake loading within this method. A two- part wedge method is the basis for analysis. The reinforcement length at the base of the structure is determined using a trial and error method to obtain the wedge that gives the disturbing force equal to zero. This is termed as the T_{ob} mechanism. The length at the top of the structure is based on the so-called T_{max} mechanism. This process involves a trial and error method used to find the wedge that gives the maximum disturbing force, which is known as the T_{max} mechanism. Different wedges are analyzed at different depths, to ensure that the disturbing force does not exceed the resisting force from the reinforcing elements. In this method, individual reinforcing elements are not checked against rupture failure, neither any factor of safety is applied.

2.11.2 Hybrid Approach

Few design codes and methods like BS8006 (1995) and the TBW method (1998) have used hybrid approach for the design of RSSs. The main features of these methods are dealt in the following sections.

2.11.2.1 BS8006 (1995) Method

BS8006 has adopted a limit state design approach whereby individual partial factors applied to the various forces acting on the structure and the soil/reinforcement properties. Their purpose is to apply appropriate PFs where they are required, i.e. the greatest partial factors to the greatest uncertainty.

The peak effective shear strength parameters are recommended for the soils for both Ultimate Limit State (ULS) and Serviceability Limit State (SLS) analyses, i.e. ϕ'_p, c'_p. For walls, steep slopes and embankments the design strength ($T_{(d)}$ of the reinforcement for SSAs and MSAs (sustained loading plus traffic loading) is taken as

$$T_d = \frac{T_b}{f_m} \tag{2.4}$$

where,

T_b= Unfactored reinforcement base strength

f_m=Partial factor

Reinforcement base strength ($T_{(b)}$ should be as:

1) For the ULS the base strength is the tensile creep rupture strength (T_{cr}) at the appropriate times and design temperature.
2) For the SLS the base strength is the tensile load in the reinforcement (T_{cs}) which induces the prescribed post construction limit state strain (0.5% for abutments and 1.0% for retaining walls).

For design against sustained plus traffic loading, the traffic loads are calculated as the wheel load divided by the contact area and considered as a uniform surcharge load over the whole design lifetime. For design against sustained plus earthquake loading, no T_d is suggested within this code.

The partial factor (f_m) has two components:

$$f_m = f_{m1} \text{ x } f_{m2} \tag{2.5}$$

where,

f_{m1} = Partial Factor related to the intrinsic properties of the material

f_{m2} = Partial Factor concerned with the effects of construction and environmental effects

Partial Factor f_{m1} is further divided into several components as:

$$f_{m1} = f_{m11} \text{ x } f_{m12} \tag{2.6}$$

$$f_{m1} = (f_{m111} \text{ x } f_{m112}) \text{ x } (f_{m121} \text{ x } f_{m122}) \tag{2.7}$$

where,

f_{m11} = Partial Factor related to the consistency of the manufacturer

f_{m12} = Partial Factor related to the extrapolation of test data dealing with Base Strength

f_{m111} = Partial Factor related to whether or not a standard for specification, manufacture and control testing of the reinforcement exist

f_{m112} = Partial Factor for whether or not standards for the dimensions and tolerances exist

f_{m121} = Partial Factor for the assessment of available data

f_{m122} = Partial Factor for extrapolation of the statistical envelope over the expected service life of the reinforcement

Partial Factor f_{m2} is also divided into several components as:

$$f_{m2} = f_{m21} \text{ x } f_{m22} \tag{2.8}$$

$f_{m2} = (f_{m211} \text{ x } f_{m212}) \text{ x } f_{m22}$ (2.9)

where,

f_{m21} = Partial Factor which deals with the installation damage of the reinforcements

f_{m22} = Partial Factor which deals with the environmental effects of the reinforcements

f_{m211}=Partial Factor related to short term effects of damage prior to and during installation

f_{m212} = Partial Factor for the long term effects of the short term damage

All the Partial Factors are certified and specified by the British Board of Agreement (BBA) for applications within UK.

i) ULS Analysis: Four types of checks are performed within the analysis, which are as follows,

(a) Sliding Analysis: The factor of safety against sliding failure (f_s) is given by the equation:

$$f_s R_h \leq R_v \frac{\tan \phi'_p}{f_{ms}} + \frac{c'_p L}{f_{ms}} \tag{2.10}$$

where,

f_s =Factor of Safety against base sliding (1.20)

R_v= Vertical factored resultant force

R_h= Horizontal factored disturbing force

ϕ'_p= Peak angle of friction

c'_p = Effective cohesion of soil

L= Effective base width for sliding

f_{ms}=Partial Factor for material (1 for $\tan\phi'_p$ and 1.6 for c'_p)

(b) Bearing Failure: The imposed bearing pressure (q_r) must be compared to the factored ultimate bearing capacity as follows:

$$q_r < \frac{q_{ult}}{f_b} + \gamma D_m \tag{2.11}$$

where,

f_b=Factor of Safety for bearing capacity (1.35)

q_{ult}= Ultimate bearing capacity of the foundation

D_m= Embedment depth

(c) Reinforcement Rupture: Each layer of reinforcement requires checking against rupture. The maximum tensile force in the ith layer T_i is then calculated by:

$$T_i = K_a \sigma_v S_v \tag{2.12}$$

where,

K_a= Coefficient of active earth pressure within the reinforced zone

σ_v= Vertical stress on reinforcing element

S_v= Vertical spacing of reinforcing element

In order to ensure stability with regard to rupture failure, the following relationship must be satisfied:

$$\frac{T_d}{f_n} \geq T_i \tag{2.13}$$

where,

T_d=Design Strength of the reinforcement

f_n=Partial Factor for economic ramifications of failure

(d) Pullout Failure: The resistance provided by each individual reinforcing element must be taken to be the lesser of (i) pullout resistance, or (ii) the design strength. The total resistance from all reinforcing elements is checked by:

$$\sum_{i=1}^{n} \frac{T_d}{f_n} \, or \, \frac{2L_{ei}}{f_p f_n}\left[\mu\left(f_f \gamma_1 h_i + f_f w_s\right) + \frac{c'_r}{f_{ms}}\right] \geq T \tag{2.14}$$

where,

L_{ei}= Anchorage length beyond failure plane

f_p= Partial Factor against pullout [=1.30]

μ= Coefficient of friction between soil and the reinforcements

f_f= Partial Factor for surcharge load

γ_1 = Density of the reinforced fill

h_i=Depth of reinforcement of ith layer

w_s = Surcharge load

c'_r= Adhesion between the fill and reinforcement

f_{ms} =Partial Factor for c'_r

T = Total tensile force to be resisted by reinforcing elements

ii) SLS Analysis: For a polymeric reinforcement where short term axial tensile stiffness decreases with time through the agency of creep, the strain occurring between the end of construction and the end of selected design life can be estimated from isochronous load strain curves for these two times. Fig. 2.11 demonstrates this procedure, where T_{cs} is the capacity of the reinforcement at a prescribed limiting value of post construction strain.

2.11.2.2 TBW Design Method (1998)

Due to the relatively large strains occurring within RSSs, critical state or constant volume shear strength properties are used for the soils i.e. ϕ'_{cv}, c'_{cv}, in this method. The T_d of the reinforcement for SSAs is given by:

$$T_d = \frac{T_c}{f_{m1} x f_{m21} x f_{m22} x f_{m3}} \tag{2.15}$$

where,

T_c= Extrapolated creep strength (at 10% limiting strain) of the reinforcement at specified design life time and operational temperature

f_{m1}= Partial Factor to allow for material manufacturing variations and confidence in the extrapolated strength

f_{m21}= Partial Factor for the effects of construction activities

f_{m22}= Partial Factor for the effects of environmental degradation

f_{m3}=Overall Factor of Safety (1.35)

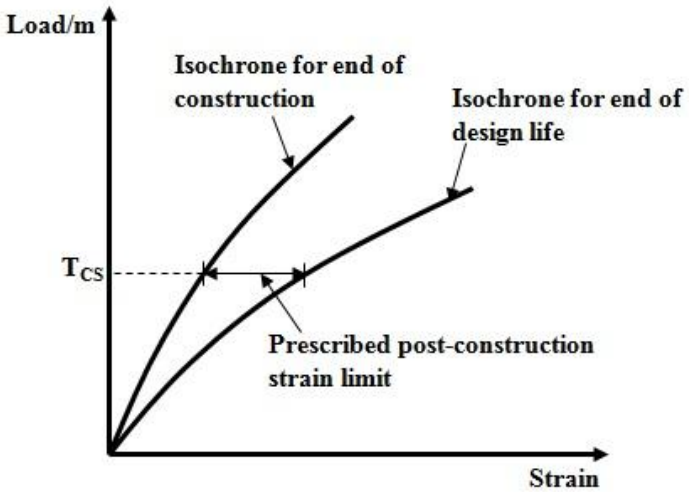

Fig. 2.11: Assessment of SLS base strength TCS (BS8006, 1995)

For the design against MSAs, no T_d is suggested thereby. The partial factor f_{m1} and the overall factor of safety f_{m3} are specified by the manufacturers. Partial factors f_{m21} and f_{m22} are obtained by comparing the short term CRS rupture strengths 'before' and 'after' an event in the case of construction damage or environmental degradation.

i) ULS Analysis: The procedure for ULS analyses adopted in this method conforms to BS8006 (1995) except that no partial factors is applied to the soil properties. Further this method differs in that a factor of safety of 2.0 is applied to sliding, bearing and pullout failure but no factor of safety is applied against rupture failure.

ii) SLS Analysis: Two types of checks are performed for SLS conditions that are as follows:

(a) Check for Active Earth Pressure: This check is to scrutinize the post-construction strain occurring in the reinforcements due to overburden pressure. The assumption is that wedges emanating from the toe at angles greater than (45°- $\phi_p'/2$) mobilize full active pressure given by K_a, while wedges at angles less than ϕ_p'mobilize zero active pressure i.e. K is zero. The active pressures acting on wedges at angles between ϕ_p' and (45°- $\phi_p'/2$) are obtained by linear interpolation, Fig. 2.12.The force mobilized in the ith reinforcement T_i is given by K_a x σ'_{vi}, at any point. For normal walls, the force required to mobilize 1% post-construction strain (T_{1pcs}) (usually around two-third of the creep limited strength) is determined for each reinforcement type from isochronous curves. The actual post-construction strain ($\varepsilon_{p(c)}$ in an individual reinforcement is then approximated by the equation:

$$\varepsilon_{pc} = \frac{T_i}{T_{1pcs}} \tag{2.16}$$

Likewise approach is adopted for bridge abutments, but here the serviceability limit is reduced to 0.5% post-construction strain.

(b) The Wedge Check: To perform the check, out of balance force for a series of wedges is first determined and then the out of balance force for each wedge is distributed amongst the reinforcements cut by the wedge in proportion to their strength Fig. 2.13. Groups of wedges at 2° intervals are analyzed at the base of the wall and at levels of one tenth of the height of the face. The strain in each wedge for the individual reinforcement is then determined in accordance with Eq. 2.16 and a strain distribution curve is obtained, Fig.

2.14. The area under the curve divided by the reinforcement length is defined the average post-construction strain for each grid.

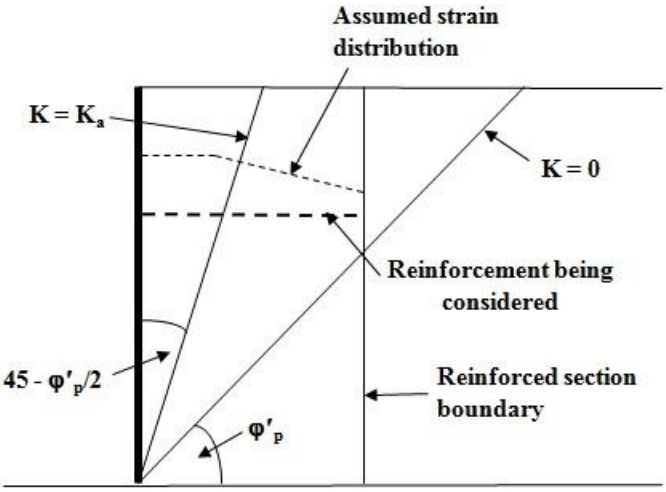

Fig. 2.12: Typical distribution of active earth pressure in a retaining wall

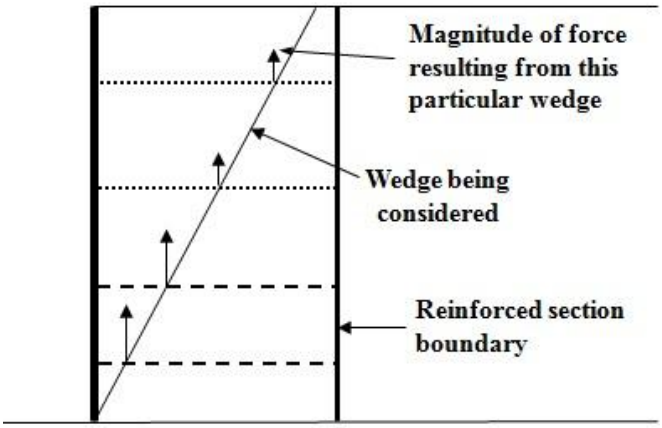

Fig. 2.13: Distribution of force due to active earth pressure for wedge check

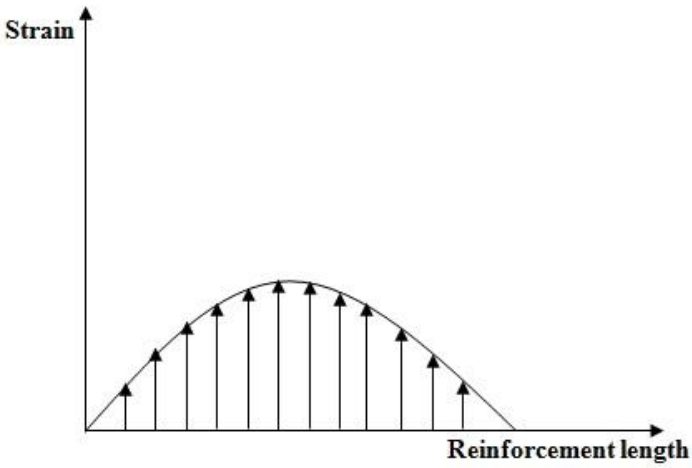

Fig. 2.14: Strain distribution in individual reinforcement due to active earth pressure

2.11.3 Limit State Approach (LSA)

The soil as well as the geosynthetics, both influence the behaviour of RSSs, and the equilibrium is too complex to be reflected by a single 'lumped' factor or global factor of safety. Rather the procedure should be to select representative design values for the parameters influencing stability and then to perform calculations to show that possible undesirable design situations do not occur. This is considered in the limit state approach (Jewell, 1996).

The LSA differs from others in that no global factors of safety are used in this approach, rather PFs are applied to the calculations where uncertainties lie. The aim of using PFs is to distribute margins of safety to the places in the calculation where there are uncertainties. Further, PFs have the advantage that "margins of safety" can be shared appropriately amongst the main parameters employed in the design. For example, a structure may be subjected to two actions, one adverse and another favorable, so that the nominal value of each cancels the other. Thus the resistance required for the structure would be very small or zero, on the basis of the nominal action. But in reality if one of the actions is different from the expected value, the required resistance might be tremendously high. This possible situation can be arrested using PFs, while could be missed in the global factor of safety approach (McGown et al., 1998). Essentially, there are two main areas of concern for design in limit state approach. Firstly, the risk of collapse must be shown to be acceptably small by means of ULS calculations. Secondly, the risk of excessive deformations interfering with the functioning of the structure must also be shown to be acceptably small by means of SLS calculations.

The LSA of design is set out in International and European Standards (ISO 2394 and CEB Bulletin III) and is becoming widely accepted in geotechnical engineering. The draft Eurocode 7 (1995) for geotechnical engineering is based on the limit state approach. The LSA to the design of RSSs should be based on internal force equilibrium and internal strain compatibility as set out by Jewell (1984 and 1988). Valid mechanisms for ULS and SLS analyses need to be identified first and then the appropriate parameters of the materials can be identified on the basis of these mechanisms. The mechanisms regarding the external stability and operational performance of RSSs are considered to be the same as that for conventional soil structures. Only the differences between conventional soil structures and RSSs are the mechanisms regarding the internal stability and operational performance.

2.11.3.1 Model for Internal ULS Mechanism

Creep test data for geosynthetics are most appropriate to the design of RSSs under SSAs. To simulate the creep test conditions and to facilitate the direct application of the test data to the design of a prototype structure, a constant out of balance force must be applied to the reinforcements from the end of construction to EDL. A situation of this sort can be achieved only when the tensile strain in the soil is large enough to mobilize the large strain ϕ'_{cv} at the end of construction. Thereafter, until the end of design life, the soil may strain further whereas the mobilized shear strength of the soil will remain constant, i.e. the ϕ'_{cv} will continue to be mobilized. For the above condition, a model limit state mechanism for RSSs can be identified. In this model it is assumed that a constant load is applied to the reinforcements from the time of switch-on of gravity (t_{SOG}) to EDL.

Practically, all the loads are not applied instantaneously, although it is generally assumed that they are applied simultaneously at some point during the construction period, (t_{CP}). Sometimes, the overall construction period may be much longer than the reinforcement loading period, (t_{RL}), depending on the construction procedures adopted. For example, a wall may be fully propped until the fill is placed to full height, during which time the reinforcements will not be loaded, but will be loaded only when the props are removed. This necessitates for the great care to be taken while selecting the t_{RL}. When the loads are "switched-on", say at two-thirds of t_{RL}, they will develop a strain in the soil, (ε_{SOG}), sufficient to mobilize the large strain ϕ'_{cv} of the soil. If such a situation is achieved, there would be no change in the out of balance force from the time of switch-on of gravity to the end of the design life and the geosynthetic reinforcements will always carry the same load. Creep test data thus directly apply and the model limit state mechanism applies.

2.11.3.2 Model for Internal SLS Mechanism

As stated above, in practice all loads are not applied instantaneously. Similar to the ULS condition, it can be assumed that all the serviceability limit loads are applied at say two-thirds of t_{RL}, although this depends on the construction procedures. Normally, these loads mobilize an angle of friction (ϕ'_{mRL}) in the soil less than the peak angle of friction (ϕ'_p). With time, the soil and the reinforcement strain and at the end of design life, the mobilized angle of friction (ϕ'_{mEDL}) is likely to remain less than the ϕ'_p but higher than the mobilized angle of friction at the end of construction loading. As the mobilized shear strength of the

soil increases with time, the force required to be carried by the reinforcements will gradually become less, which means that the applied force on the reinforcements will change with time. If the change is significant, then an iterative approach to the determination of the deformations in the soil and the reinforcements must be undertaken.

2.12 Types of Action Consider in RSS

Actions for RSS should include all loads, forces and displacements related to any specific limit state condition. In addition, the duration of actions needs to be considered, including changes in actions resulting from changes in the properties of materials with time. There are various kinds of actions that may be likely to be imposed on the structures during their operational tenure, identified and classified in many ways by various codes. Various types of actions are identified in Eurocode 1 (1996) for structural engineering. Actions have also been suggested in Eurocode 7 (1995) for geotechnical engineering such as:

Direct Actions can be classified in the following manner:

i) Permanent actions e.g. self-weight of structures, fittings, fixed equipment, road surfacing etc.

ii) Variable actions e.g. imposed loads, wind loads or snow loads.

iii) Accidental actions e.g. explosions or impacts from vehicles.

Dynamic actions, which cause significant acceleration of the structure or structural member. Dynamic effects may be taken into account either by increasing the magnitude of the static actions or by the introduction of an equivalent static action.

Indirect actions can be classified as:

a) Permanent actions e.g. settlement of support.

b) Variable actions e.g. temperature effect.

In simple term, the actions occurring in practice may be broadly grouped into two categories;

1) SSAs (e.g. sustained, cyclic, impact etc.)

2) MSAs (e.g. stepped, sustained plus cyclic, sustained plus short-term etc.)

These actions are illustrated with suitable diagrams in the following sections.

2.12.1 Single-Stage Actions (SSAs)

The actions when applied alone are termed as SSAs. It could be sustained loading for long period, cyclic or short-term loading in nature. The sustained loading may represent the dead weight (self weight) of the structure or surcharge loading on it which could be constant or variable over the design life. The cyclic loading may represent the traffic loads that are transient in nature in a regular interval although the design life of the RSS. Similarly, an impact load due to an explosion or an earthquake force may be considered as the short-term loading because of the possibility and duration of the event.

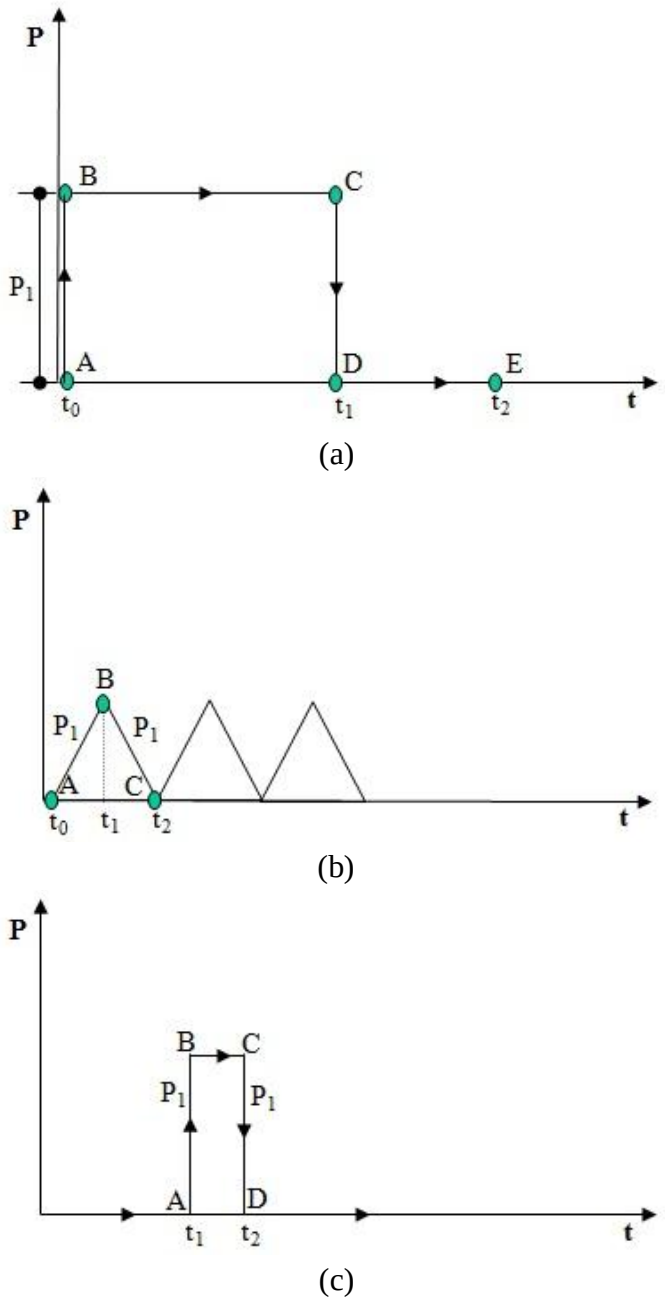

Fig. 2.15: Examples of SSA: (a) sustained loading, (b) cyclic loading and (c) impact or short term loading (Mahaseth, 2002)

Fig. 2.15 illustrates the nature of different SSAs, i.e. sustained, cyclic and impact, respectively. Fig. 2.15(a) is an example of sustained loading where a load P_1 is applied at t_0, sustained until t_1 and removed thereafter. Fig. 2.15(b) is an example of cyclic loading where the load P_1 is applied gradually from t_0 to t_1 and released in the same fashion from t_1 to t_2 forming the loading and unloading phases in each cycle. The action may repeat for a number of cycles. Similarly, Fig. 2.15(c) is an example of an impact loading where a load P_1 is applied from t_1 to t_2 for a short duration and released completely on one or more occasions during the life time of the structure.

2.12.2 Multi Stage Actions (MSAs)

The actions imposed on the RSSs are not wholly static, intermittent or dynamic although the design life of the structure. In most of the applications there will be a combination of different types of the SSAs, which are termed as MSAs.

Examples of MSAs are stepped loading representing dead weight plus different surcharge loading at different period of design life, sustained plus cyclic loading representing dead weight plus variable traffic load, and sustained plus short-term loading representing dead weight plus impact load due to an explosion or earthquake for short duration.

Fig. 2.16(a), (b) and (c) demonstrate these MSAs respectively. Fig. 2.16 (a) is an example of stepped loading where a load P_1 is applied at t_0 and sustained until $t_{1,}$ to which an additional load P_2 is added and sustained until t_2. In the same manner, another load P_3 is added to them at t_2 and sustained.

Fig. 2.16(b) is an example of sustained plus cyclic loading representing dead load plus traffic load. A sustained load P_s is applied at $t_{0,}$ to which a gradually increasing transient load P_t is added from time t_1 to t_2 and released in the similar fashion from t_1 to t_2, thus forming a complete cycle. Similarly another cycle is completed followed by the consecutive cycle, thus forming a chain of loading and unloading cycles.

Fig. 2.16(c) is another example of sustained plus short-term loading. A sustained load (P_s) is applied at t_0 and a sort-term load ($P_{short\text{-}term}$) is imposed from t_1 to t_2 and released.

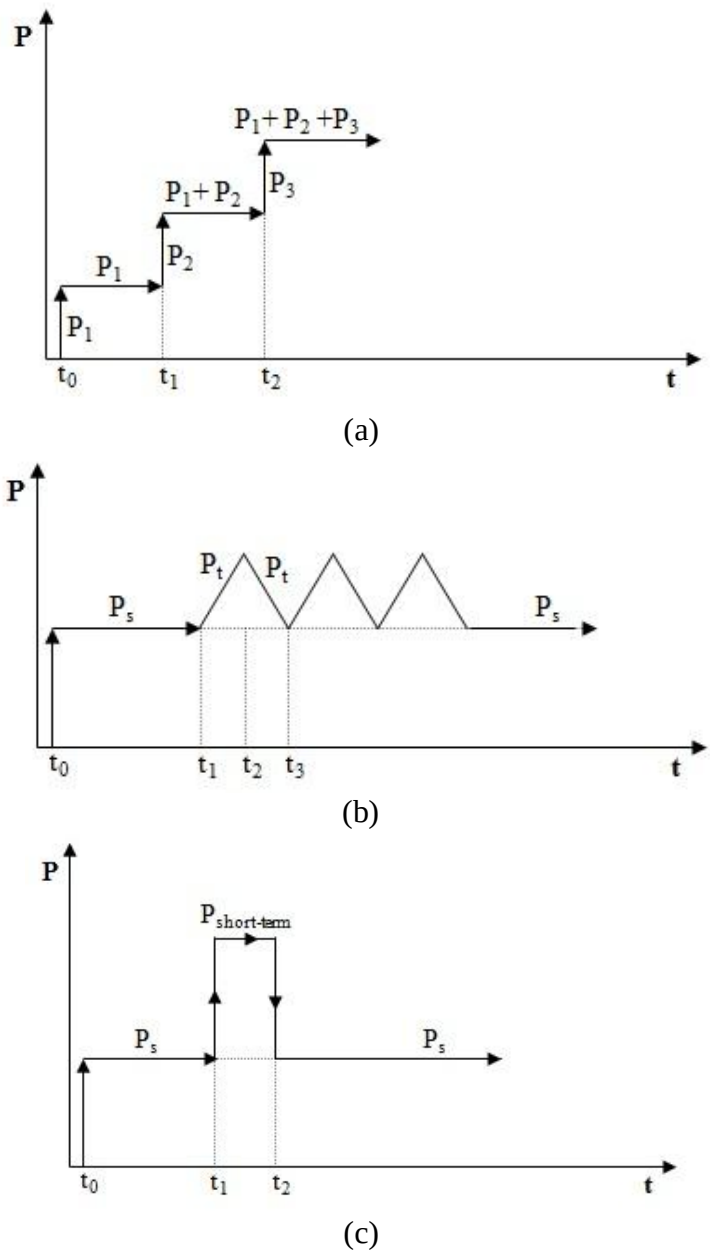

Fig. 2.16: Examples of MSA: (a) stepped loading, (b) P_s plus cyclic loading and (c) sustained plus $P_{short\text{-}term}$ (Mahaseth, 2002)

2.13 Strain Responses of Material Under SSA

The materials in engineering application may be chiefly categorised into elastic, plastic and viscous on the basis of their responsive behaviour to different loading regimes, i.e. the manner in which they react to the act of loading on them over the design life of the materials. However many materials, owing to their complex intrinsic structure, may exhibit more than one of the above properties, and hence may be characterizes elastic, plastic and elasto - plastic and EVP materials accordingly. The behaviour of these

materials upon subjection to loading may be best illustrated with the aid of Figures as in the following sections.

2.13.1 Elastic Material

Elasticity is the ability of a body to resist a distorting influence or deforming force and to return to its original size and shape when that influence or force is removed. Solid objects will deform when adequate forces are applied on them. If the material is elastic, the object will return to its initial shape and size when these forces are removed. The physical reasons for elastic behaviour can be quite different for different materials. For polymers, elasticity is caused by the stretching of polymer chains when forces are applied. Perfect elasticity is an approximation of the real world. Most materials which possess elasticity in practice remain purely elastic only up to very small deformations.

Fig. 2.17 (a), (b) and (c) illustrate the strain response of a elastic material under SSA, viz. sustain, cyclic and short term loading, respectively. These are the qualitative plots of total strain verses time. In Fig. 2.17(a), at time t_0, the material has no strain at point A, but attains an instantaneous elastic strain (ε_E), with the application of the sustained load P_1 corresponding to point B, Fig. 2.17(a), which is sustained as long as the load is continued till time t_1, point C. Immediately after withdrawal of the load P_1 at t_1, the ε_E retards back to zero, point D. That is the whole of the ε_E strain is recovered leaving no residual /locked in strain, since the material is elastic.

Fig. 2.17(b) is a ε_T –t plot of a elastic material under the cyclic loading shown in Fig. 2.17(b). The elastic strain increases gradually from zero at t_0, point A to ε_E t_1, point B as the load P_1 increases from zero to peak during the loading phase. This elastic strain ε_E reduces to zero following the reduction in the load P_1 at t_2, point C. The whole of the elastic strain ε_E is recovered leaving no locked in strain ε_L.

In the same manner, in the Fig. 2.17(c), the elastic strain increases from zero, point A to ε_E, point B at t_1 with the application of the $P_{short\text{-}term}$ as in the Fig. 2.17(c). This strain is sustained from B to C corresponding to the load $P_{short\text{-}term}$ and retards back to zero at t_2, point D leaving no locked in strain ε_L, i.e. the whole of the elastic strain ε_E is recovered. Thus in the case of a elastic materials the relation between different strain can be express as,

$\varepsilon_T = \varepsilon_E = \varepsilon_R$

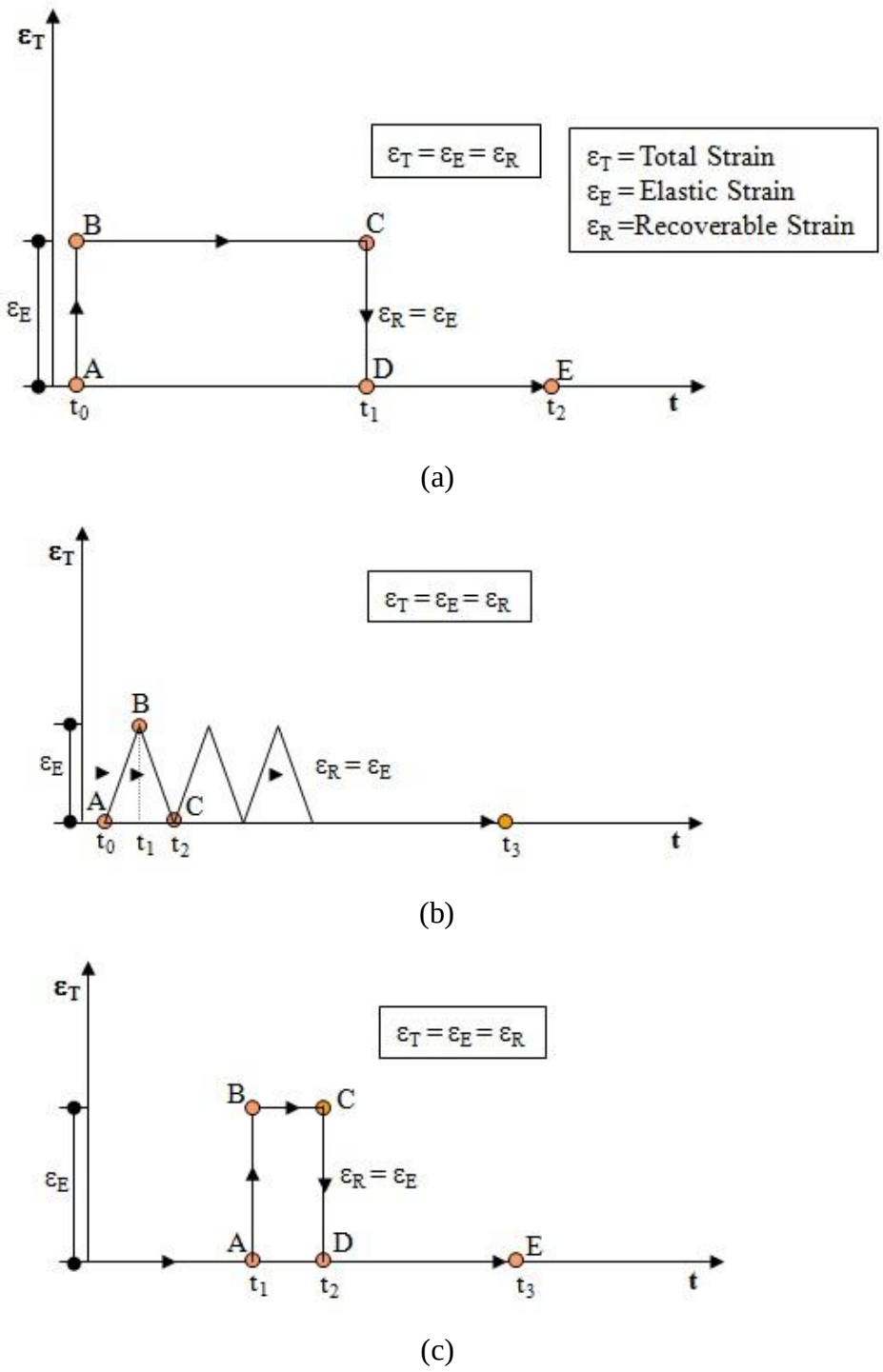

Fig. 2.17: Strain response of elastic material under SSA: (a) sustained loading, (b) cyclic loading and (c) impact or short term loading (Mahaseth, 2002)

2.13.2 Plastic Material

Plasticity describes the deformation of a material undergoing non-reversible changes of shape in response to applied forces. In engineering, the transition from elastic behaviour to plastic behaviour is called yield. For many ductile metals, once the load exceeds a

threshold – the yield strength – the extension increases more rapidly than in the elastic region; now when the load is removed, some degree of extension will remain. Generally, plastic deformation is also dependent on the deformation speed, i.e. higher stresses usually have to be applied to increase the rate of deformation. Such materials are said to deform visco-plastically.

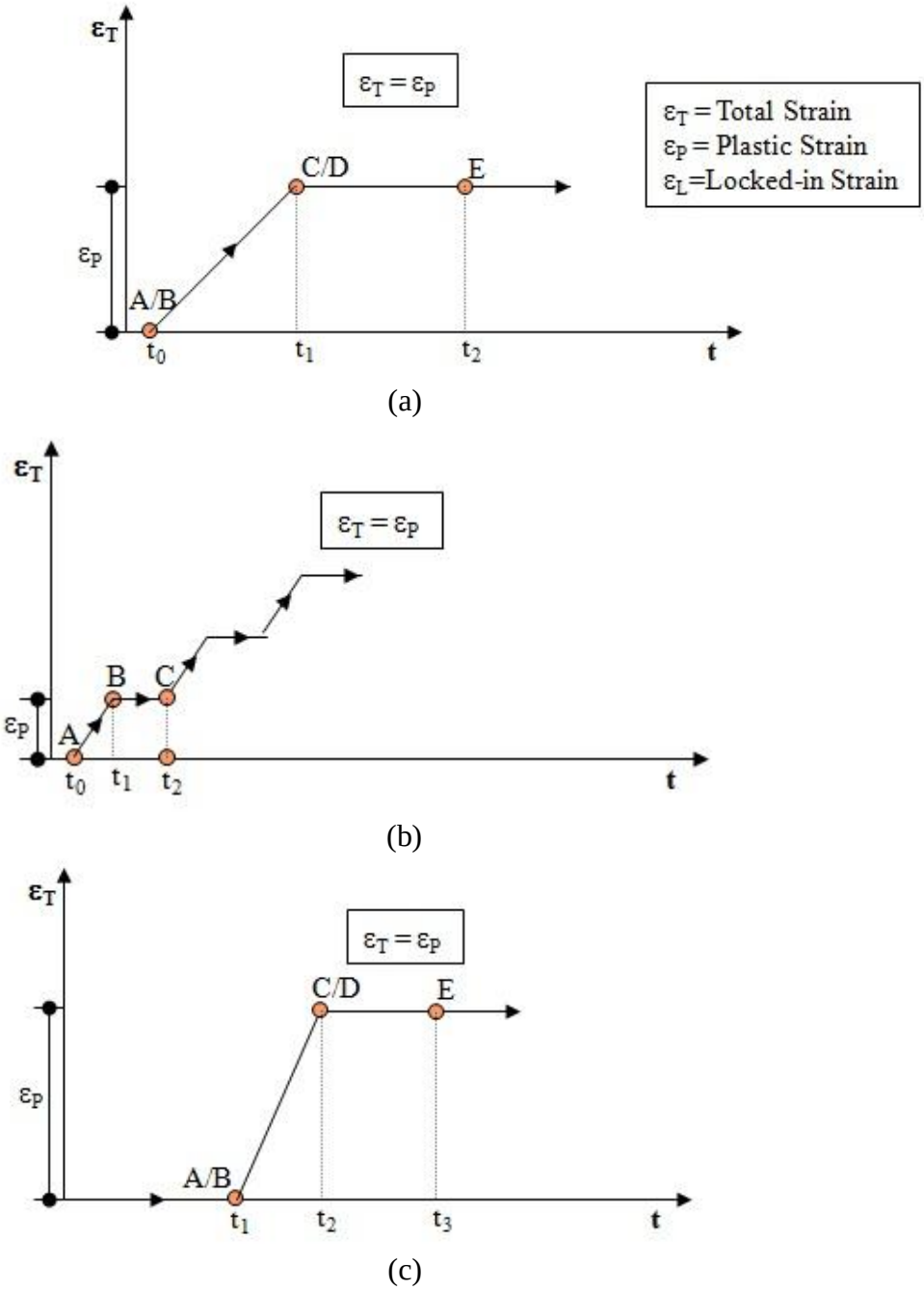

Fig. 2.18: Strain response of plastic material under SSA: (a) sustained loading, (b) cyclic loading and (c) impact or short term loading (Mahaseth, 2002)

Fig. 2.18 (a), (b) and (c) are the qualitative plots of strain verses time showing the responsive behaviour of a plastic material corresponding to the loading sequences. In the case of sustained load in Fig. 2.18(a), at time $t_{0,}$ there is no strain with zero load at point A/B. With application of the load P_1, the plastic strain ε_P increases gradually (linearly) until point C/D as long as the load is sustained giving $\varepsilon_T = \varepsilon_P$ ($t = t_1$). Even after the load is withdrawn at time t_1, the strain is not recovered at all and the material inherits a residual/locked in strain ε_L, which continues to be left over at any time t_2, point E. Similarly, in the case of cyclic loading as in Fig. 2.18(b), the strain increases from zero to ε_P following the increasing load P_t from zero to peak, from t_0 to t_1, point A to B, gradually during the loading phase. After reaching the peak, the strain ε_P continues to persist even after the load P_t is released to zero gradually from t_1 to t_2, point B to C, during the unloading phase. That is, no strain is recovered and all of the ε_P is left as locked in ε_L. Hence, in the beginning of the next cycle the material has already acquired the locked in strain ε_L, point C. Fig. 2.18(c) is the case of short-term loading where the strain increases from zero to $\varepsilon_{P,}$ time t_0 to t_1, point A/B to C/D, as the short-term load. $P_{short\text{-}term}$ is sustained. At time $t_{1,}$ although, the load $P_{short\text{-}term}$ is released to zero, the strain ε_P does not recover at all and the whole of the ε_P is left as the locked in strain $\varepsilon_{L.}$ At any time t_2, the locked in strain is equal to ε_P. Thus, for the perfectly plastic materials, the relation between total strain, plastic strain and locked strain can be express as,

$$\varepsilon_T = \varepsilon_P = \varepsilon_L$$

2.13.3 Elasto - Plastic Material

This type of material exhibits both elastic and plastic properties when it stress between its elastic limit and breaking strength. It may be seen from the Fig.2.19, which an elasto-plastic material behaves partly like elastic and partly like a plastic material subjected to different SSAs, sustained, cyclic and short-term loading respectively.

For sustained loading, Fig. 2.19(a), at time t_0 (point A), with no strain with zero load, it acquires an instantaneous ε_E (point B) upon application of the load $P_{1,}$ followed by a linear increase in plastic strain $\varepsilon_{P\ (t\ =\ t1)}$ until the load is removed (point C) at time t_1. After removal of the load P_1, there is an elastic recovery ($\varepsilon_R = \varepsilon_E$), leaving the plastic strain $\varepsilon_{P\ (t\ =\ t1)}$ as a locked in strain $\varepsilon_{L,}$ that continues to persist corresponding to any time t_2 (point E).

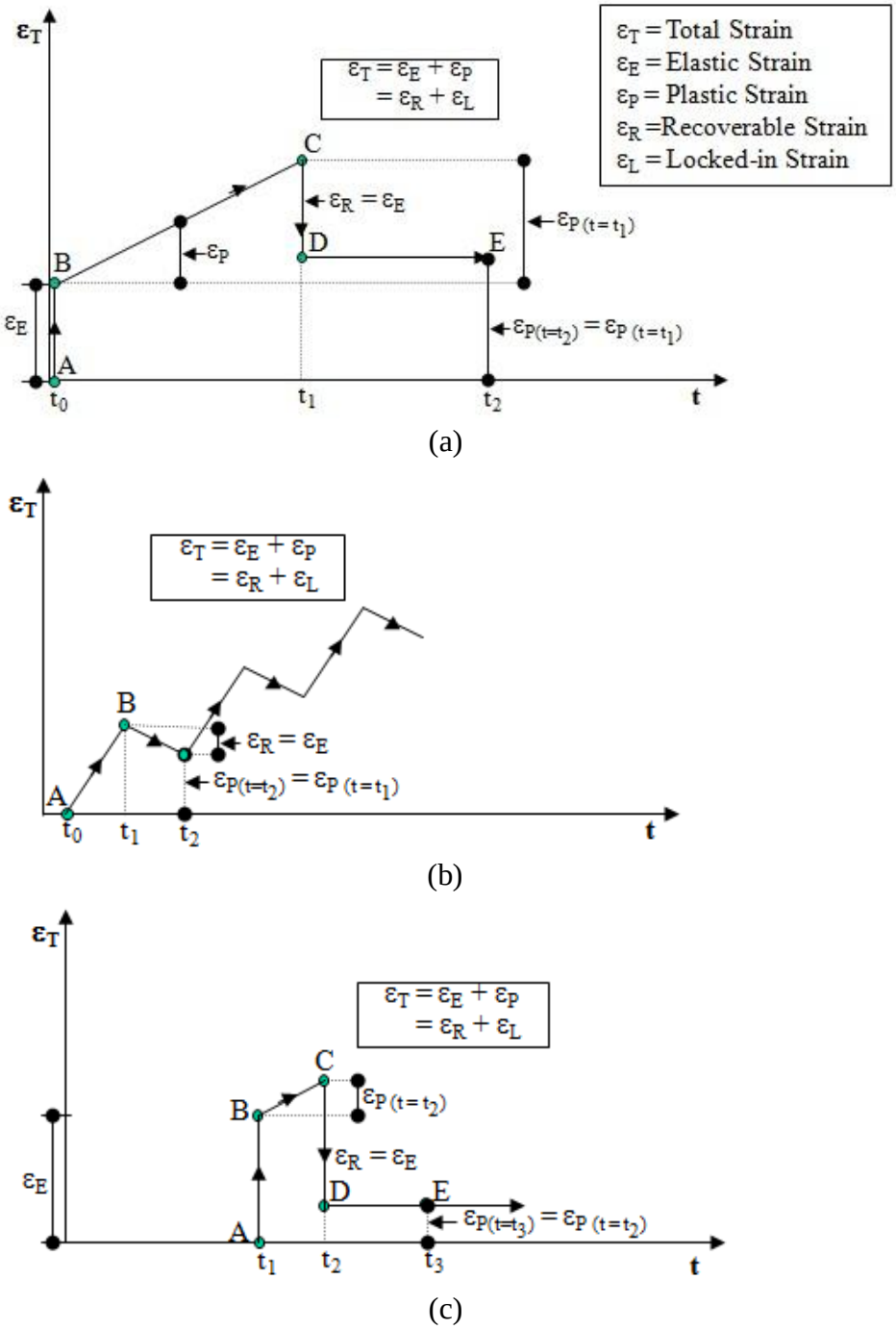

Fig. 2.19: Strain response of elasto-plastic materials to SSA: (a) sustained loading, (b) cyclic loading and (c) impact or short term loading (Mahaseth, 2002)

In the case of cyclic loading, Fig. 2.19(b), as the load P_1 increases from zero to peak, t_0 to t_1, the strain also increases from zero to $\varepsilon_{T\ (t\ =\ t1)}$, t_0 to t_1, point A to B during the loading phase. During the unloading phase, as the load P_1 is released gradually, t_1 to t_2, point B to C, the elastic strain ε_E is recovered gradually and fully at t_2, point C, leaving whole of the plastic strain ε_P as the locked in strain ε_L. That is, in the beginning of the next cycle, the

material will already have a locked in strain $\varepsilon_L = \varepsilon_{P\ (t\ =\ t2)}$, that will be followed by the similar pattern of strain as in the first cycle.

Similarly, under the short-term loading as in Fig. 2.19(c), at time t_0 (point A), from no strain with zero load, the material acquires an instantaneous elastic strain ε_E, point B, as the load P_1 is imposed. This elastic strain ε_E is followed by the gradual acquisition of plastic strain ε_P, t_1 to t_2, until sustenance of the load P_1, point C, which is reduced entirely to the plastic strain ε_P, t_2, point D. To say, the entire elastic strain ε_E is recovered back , while the plastic strain ε_P is left as the locked in strain ε_L, so that at any time t_3, the locked in strain $\varepsilon_L = \varepsilon_{P\ (t\ =\ t2)}$. Hence the strain response of elasto-plastic materials can be express as,

$$\varepsilon_T = \varepsilon_E + \varepsilon_P$$
$$= \varepsilon_R + \varepsilon_L$$

2.13.4 Elasto-Visco-Plastic Material

An EVP material exhibits the characteristics of an elastic in part, a viscous in part and of a plastic material in part, as can be seen from the Fig. 2.20 (a), (b) and (c), which are the strain responses of this material to the different SSA sustained, cyclic and short-term, respectively.

Fig. 2.20(a) is the strain response for the sustained loading where, at time t_0 (point A), the material has no strain with zero loads. With application of the sustained load P_1, at time t_0, it acquires ε_E, point B, followed by an attainment of plastic as well as viscous strain ($\varepsilon_P + \varepsilon_V$) gradually, with continuation of the load P_1 until time t_1, point C. Following the removal of the load P_1, the elastic strain ε_E is recovered completely leaving ($\varepsilon_P + \varepsilon_V$) as locked in strain $\varepsilon_{L\ (t=t1)}$, point D. With lapse of time, also the viscous part ε_V of the $\varepsilon_{L\ (t=\ t1)}$ is recovered gradually at t_2. Eventually, at any time t_3, the whole of ε_V is recovered leaving ε_P only as the locked in strain $\varepsilon_{L\ (t=\ t2)}$, point E.

Fig. 2.20(b), which is the strain response of the cyclic loading. At time t_0 (point A), the material has no strain with zero load. The strain increases gradually to $\varepsilon_{T\ (t=\ t1)}$, from t_0 to t_1, point A to B, as the load P_1 reaches to the peak gradually, during the loading phase. During the unloading phase, as the load P_1 is phased out gradually, there is elastic plus viscous recovery ($\varepsilon_E + \varepsilon_V$), from t_1 to t_2, point B to C, leaving the plastic strain $\varepsilon_{P\ (t=\ t1)}$, as

the locked in strain $\varepsilon_{L\ (t=\ t2)}$. This locked in strain will be accumulated at the commencement of the next cycle of loading.

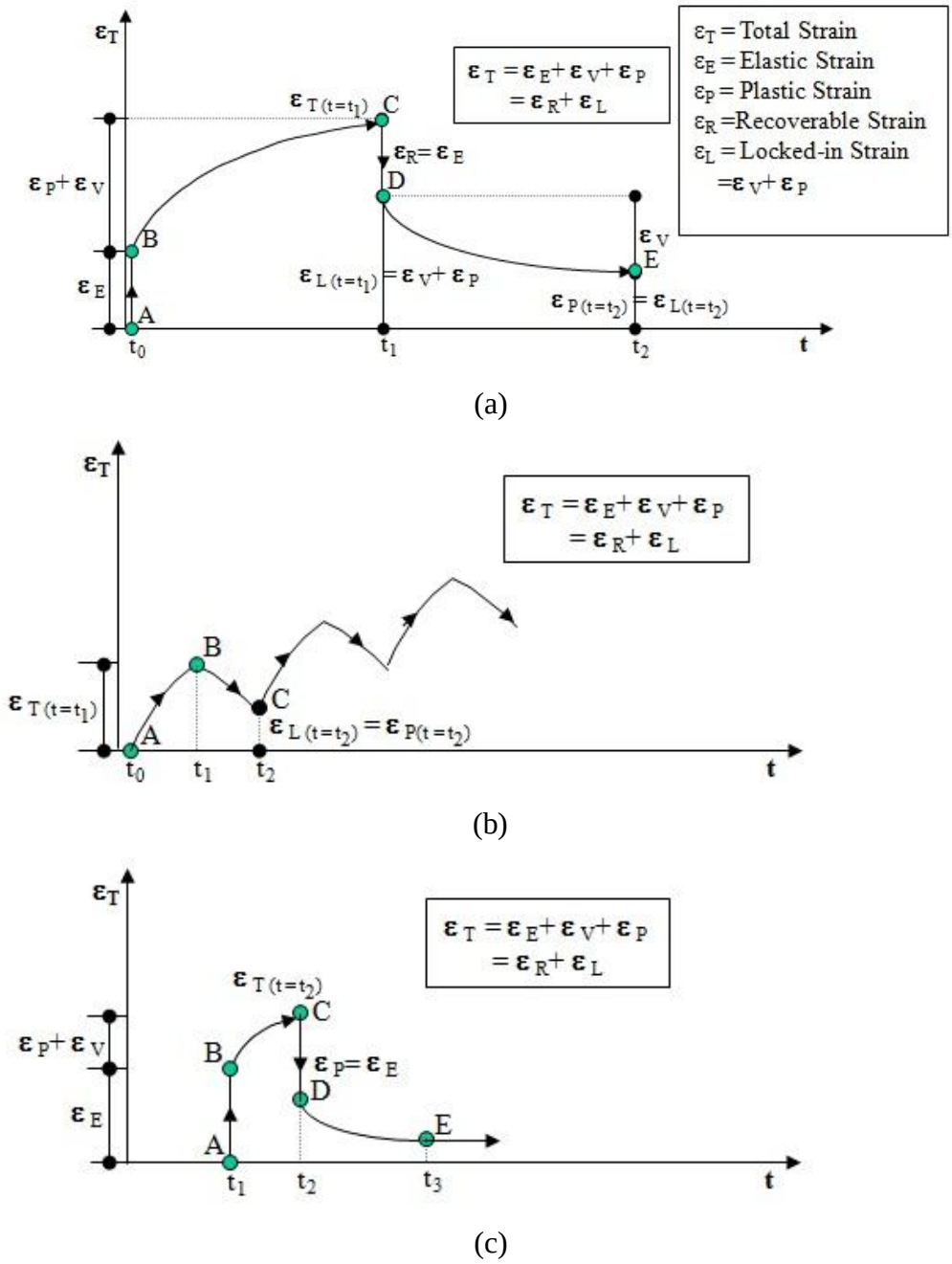

Fig. 2.20: Strain response of EVP materials to SSA: (a) sustained loading, (b) cyclic loading and (c) impact or short term loading (Mahaseth, 2002)

Similarly, Fig. 2.20(c) illustrates the strain response of the short-term loading. At $t_{0,}$ there is no strain with no load, point A, but attains an elastic strain ε_E immediately with the application of the short-term load. This elastic strain is followed by the development of

viscous and plastic strains as long as the load is maintained, t_1 to t_2, B to C. When this load is released at t_2, the elastic strain ε_E is fully recovered instantaneously and the viscous part ε_V in due time. Ultimately at any time t_3, the plastic strain is left over as the locked in strain ε_P. So total strain of elasto-visco-plastic material can be state as,

$$\varepsilon_T = \varepsilon_E + \varepsilon_V + \varepsilon_P$$
$$= \varepsilon_R + \varepsilon_L$$

2.14 Design Strength of Geotextiles for RSS

In the design of RSSs, two types of strength have been considered so far, viz. reference strength (P_{Ref}) and design strength ($T_{(d)}$. Various testing techniques have been developed to obtain P_{Ref}. Customarily, T_d for geosynthetics are determined by applying partial factors to the P_{Ref}. However, the partial factors need to be modified for their appropriate application (Khan, 1999).

2.14.1 Reference Strength

The P_{Ref} is obtained from different testing techniques, most often by constant rate of strain (CRS) and Creep tests. Various design codes and methods define P_{Ref} in different ways for SSAs and MSAs.

2.14.1.1 Reference Strength for SSAs

The maximum load at rupture of the 'Ex-works' materials under CRS tensile testing is chosen to be the basis of defining the P_{Ref} of geosynthetics by DIBt (1998) and AASHTO (1997). To avoid long-term creep rupture, the P_{Ref} is then obtained by dividing the CRS rupture strength by a RF, Fig. 2.21(a). The DIBt and the AASHTO design methods specify 33% per minute and 10% per minute strain rates respectively, for the CRS tests. Kabir (1984) and Yeo (1985) have shown that the CRS test can give different strengths at different test strain rates and temperatures.

Therefore, even for a particular type of geosynthetic the same reduction factor may not be applicable to all CRS data in order to obtain the long term creep rupture strength, i.e. the reduction factor is dependent on the strain rate used in the CRS test. Troost and Ploeg (1990), BS8006 (1995) and Jewell (1996) have defined the P_{Ref} as the load to cause creep rupture of 'ex-works' specimens at the end of design life (t_{dl}), Fig. 2.21 (b). However,

many geosynthetics exhibit a wide range of scatter of creep rupture strains for different sustained load levels, Fig. 2.20(c). Hence, the P_{Ref} defined on the basis of load at creep rupture for a specific design life time (t_{dl}), can be very difficult to select with any certainty related to the strain level developed at creep rupture (McGown et al., 1998).

Some design methods define the P_{Ref} as the load obtained from the isochronous load-strain curves, corresponding to a performance limit strain (ε_P), for example the TBW Method (1998) and the HA 68/94 Design Method (1997). This value is always less than the strength at creep rupture, Fig. 2.21(d). Adoption of the ε_P to define the P_{Ref} for ULS design can be seen to be the quite conservative choice of strength value (Khan, 1999).

This way, the Reference Strengths for SSAs are defined in two different ways, i.e. on the basis of long term creep rupture strength, and on the basis of long term creep at a limiting strain.

2.14.1.2 Reference Strength for MSAs

MSA is sustained loading plus traffic loading that may be applied to the reinforced roads. Although the traffic loads are transient in nature, in most of the design codes, they are calculated as the wheel load divided by the contact area; viz. BS5400 Part2 (1978), and considered as a uniform surcharge load over the whole design life time, Geoguide1 (1989), BS8006 (1995) and AASHTO (1997). This implies that these codes permit the reference strengths for SSAs to be used in designs for sustained loading plus traffic loading. The external and internal stability analyses for the sustained loading plus traffic loading are carried out for the critical loading combination as outlined in the respective codes.

The consideration of wheel contact pressure as a sustained load over the whole design lifetime of the structure does not consider the transient nature of the load which may be economical considering the EVP behavior of geosynthetics.

Further illustration of MSA is sustained loading plus short-term seismic loading. The development of designs for RSSs involving earthquake forces is presently empirical. Fukuda et al. (1994) reported that until 1993, the RSSs were designed for earthquake on the basis of the procedure for design under ordinary static conditions, as given by Jewell et al. (1984). In this procedure the long term creep rupture strength of geosynthetics was used as P_{Ref}. The structures, so designed, were found to maintain stability during the Loma

Prieta Earthquake in 1989 having a magnitude of 7.1 (Collin et al., 1992), and Kushiro Offshore Earthquake in 1993 having a magnitude of 7.8 (Fukuda et al., 1994).

During the Kobe (Hyogo-ken Nanbu), 1995 earthquake with magnitude of 7.2, a great number of RC columns and piers collapsed by shear failure in a brittle manner, in contrast to a number of geogrid soil retaining walls that performed very well. In particular, the geogrid reinforced soil retaining walls with full height rigid facings at Tanata did not collapse despite the site were located in one of the most severely shaken area (Tatsuoka et al., 1995). Similarly, the performance of seven geosynthetic-reinforced slopes and walls shaken in the Northridge, California earthquake of January 17, 1994, was adequate, particularly compared to the performance of other immediate neighboring structures (White and Holtz, 1997).

These data indicate that the geosynthetics were actually capable of taking higher loads applied rapidly, than the long-term creep strength used that time. After the adequate performance of RSSs in Loma Prieta Earthquake (1989) and Kushiro Offshore Earthquake (1993), it was suggested by Fukuda et al. (1994), AASHTO (1994) and Jones (1996) that the design strength of geosynthetic for sustained loading condition should be increased by 1.5 times when designing for sustained loading plus short term earthquake loading. In the recent codes/methods, as more confidence is gained from the performances of RSSs during recent earthquakes, factored short term CRS strengths of geosynthetics are suggested for use in designs against sustained loading plus short term earthquake loading, AASHTO (1997), NCMA (1997) and DIBt (1998).

However, it should be noted that the considerations of higher strengths of geosynthetics, from 1994 to 1998, were all empirical (Khan, 1999).The test results from the multi stage combined sustained-short term loadings revealed that after the subsidence of the short term load, the strain level in the geosynthetics is likely to be similar to that due to the sustained load alone in course of time, as if there were no occurrence of any earthquake ever (Khan, 1999). This further indicates that the geosyntheics are in fact capable of taking larger short-term load.

In this regard, it has been also reported by Kupec (2000) about the ability of the geosynthetics to take larger short-term load. The combined sustained-short term loading test results from the series used by him showed that even a load of 80% (1.8 times) the sustained load altered the material only temporarily and that with time this alteration

decreases. In the design codes/methods higher strengths of geosynthetics have been suggested, presumably, on the basis that the earthquake loading would be very transitory, but they do not pronounce any valid technical justification. It is unlikely that the same amount of high strength of geosynthetics may be available over the whole design lifetime of the structure, irrespective of the time of occurrence of an earthquake. If so, current practice of designing RSSs against earthquake might be unsafe.

2.14.2 Partial Factors and Design Strength

The strengths of the geosynthetics for ULS and SLS analyses require to be modified by applying PFs. Four PFs of major concern have been identified for geosynthetics, Voskamp and Risseeuw (1987), Jewell and Greenwood (1988), Greenwood and Jewell (1989) and Troost and Ploeg (1990) as the followings:

1) The Damage Factor; to allow for mechanical damage during construction.
2) The Environmental Factor; to allow for the chemical environment and microbiological exposure in the ground.
3) The Material Factor; to allow for the uncertainty inherent in the extrapolation of test data, and
4) The Overall Factor; to allow for the properties of materials not meeting the manufacturer's specification.

Conventionally, the design strengths for the geosynthetics are determined by applying PFs to the reference strengths. BS 8006 (1995), AASHTO (1997), DIBt (1998) and TBW (1998) suggest that the PFs should be determined by comparing the material strengths of geosynthetics "before" and "after' an event, as obtained from CRS tests. However, it should be noted that no PFs are given for the combined effects of MSAs.

CHAPTER THREE

TEST PROGRAM

3.1 General

Due to the complex behaviour of geosynthetics under different loading, it is difficult for designers to choose appropriate values as design inputs while designing RSSs with geosynthetics. In order to choose the appropriate input design parameters for geosynthetics such as, reference strength, design strength, PFs etc, it is important to understand the mechanical behaviour of geosynthetics under different loading regimes. The load carrying capacity at different time interval and limiting strain is also need to be recognized.

In this respect, ISE approach that is developed by Khan (1999), articulate the isothermal properties of geosynthetics under different loading regimes. But the approach is much complicated for practical purposes. For this reason, to ease this complexity for the practising engineers, a simpler approach called strain envelope concept has been admired.

Standard test procedure for physical and mechanical (strength) properties of Geosynthetic Reinforced Soil Structures (GRSSs) are discussed in this chapter, which will be applicable for JGTs also. Different strain components of JGTs are identified, for various combinations of time and limiting strain. Further, the understandings of strain envelop for EVP materials under SSA are also presented on the basis of Boltzmann's superposition principle.

3.2 Tests for Physical Properties of JGT

Physical properties of a geotextile used to control the quality of many geotextiles and geomembranes. It is more of a descriptive property than design-oriented property. In certain industrial applications, the thickness may be rigidly controlled within specified limits.

3.2.1 Mass per Unit Area

Mass per unit area is the proper term by which the weight of geotextile is meant. For geotextiles, mass per unit area is specified in grams per square meter and rounded to the

nearest 0.1 value. The mass per unit area of a geotextile is determined by weighing test specimens of known dimensions, which are collected from various locations over the full width of the laboratory sample. The calculated values are then averaged to obtain the mean mass per unit area of the laboratory sample.

As per ASTM D5261-10 a minimum five test specimens are cut such that they are representative of the entire roll width and with a combined minimum total area of 100,000 mm^2. Each test specimen should be equal to an area not less than 10,000 mm^2. Length and width is measured under zero geotextile tension. Since fabric cost is directly related to mass per unit area, it is an important property. Calculation of the mass per unit area of each of the specimen to be done as follows:

$$m = Ms \times 1{,}000{,}000/A \tag{3.1}$$

where,

m = Mass per unit area rounded to the nearest 0.1 gram/m^2
M = Mass of the specimen, gram and
A = Area of the specimen, mm^2

After calculating individual mass per unit area, the averages of all five specimens are to be found. In this research work mass per unit area of selected UT and AT, JGT samples were tested.

3.2.2 Nominal Thickness

Thickness is one of the basic physical properties of a geotextile. Thickness values are required in calculation of some parameters of geotextile and geomembrane such as, permeability coefficients, tensile stress (index) etc. The thickness of a geotextile is the distance between the upper and lower surface when measured under a specific pressure. The thickness of geotextiles and geomembranes may vary considerably depending on the magnitude and the duration of pressure applied. Thickness decreases when applied pressure is increased. To minimize variation, specific sample size and applied pressure are indicated in ASTM D 5199-01, to ensure that all results are comparable. As per this test method, the thickness testing instrument should have the thickness gage having a base (or anvil) and a free moving presser foot plate, whose planar faces are parallel to each other. A gage with a 2500 mm^2 presser foot and a base extend at least 10 mm in all direction

from the edge, should be used for thickness measurements of geotextiles. This instrument must be capable of measuring a maximum thickness of 10 mm to an accuracy of ± 0.02 mm. The gages should be constructed to permit gradual application of pressure of 2 ± 0.02 kPa on geotextiles.

Test specimens are collected from laboratory sample in a randomly distributed pattern across the width. No specimen taken at a distance of 100 mm from the roll edge. From each unit in the laboratory sample, test specimens are cut such that the edge of the specimens should extend beyond the edge of the presser foot by 10 mm in all directions. Normally 10 (ten) specimens are taken for each test.

An important consideration is to check whether the strain gauges have truly come into equilibrium under each load increment. The placement of a weight would introduce compression of the fabric. Thus, it is important to read the gauges as quickly as possible once the presser plate come to equilibrium at the standardized time duration. The thickness of jute fabric continues to decrease under pressure for considerable time because of compressibility (Kabir, 2015). For thickness tests, the suggested time interval by ASTM is only 5 sec. The average thickness, T_{avg} was calculated from the total thickness, T_{total} , and the number of layers tested, N by

$$T_{avg} = T_{total} / N \tag{3.2}$$

where,

T_{avg} = Average thickness
T_{total} = Total thickness
N = Number of layers tested

The total thickness of jute under uniform applied load in field condition can be estimated by multiplying the number of sheets used and the average single layer thickness at that particular load. In this research work thickness of UT and AT, JGT samples were measured.

3.3 Tests for Mechanical Properties of JGT

There are varieties of test methodologies developed to determine the strength of geosynthetics. Depending upon the time and the purpose, an appropriate test method needs to be selected. The tests are known as CRS test, creep test, stress relaxation test and cyclic

tests. These tests are conducted at different specimen shapes and sizes, loading methodologies, rates of load application and test temperature for measuring mechanical behaviour of geosynthetics (Kabir, 1984).

Test specimens must be in sufficient size and shape to be representative of the macro-structure of the product. However, even when this condition is satisfied, each test may investigate the response of different features of the micro and macro-structures of geosynthetics. Indeed, changing a single test condition may result in a change in the load-strain response. (Kabir, 1984 and Yeo, 1985).

3.3.1 Constant Rate of Strain Test

This wide width tensile strength test for geotextile is very famous and widely performed since it involves very little time. A constant rate of strain is maintained while applying the load increment, until the specimen ruptures. Load verses strain is recorded and the ultimate load at the rupture is considered as ultimate strength. Different standards specify their own rate of strain at which the test is to be performed. For example, BS 6906, Part 5 specifies a rate of strain at 7-13% per minute and the temperature to be (20 ± 1)° C. According to ASTM D 4595 a relatively wide specimen is gripped, across its entire width in the clamps of a Constant Rate of Extension (CRE) type tensile strength testing machine. The machine operated at a prescribed rate of extension and continues to apply a longitudinal force to the specimen until the specimen ruptures. Tensile strength, elongation, initial and secant modulus and breaking toughness of the test specimen is then calculate from the load and deformation reading of the machine. It has load and elongation recorders and special jaws with serrated faces to firmly grip on the specimen to prevent slippage. These special jaws are capable of testing up to 200 mm wide specimens and no rotation is permitted about the grips. The test scheme is shown in Fig. 3.1 and Fig. 3.2.

The strain rate commonly used in this test should be given careful consideration. Haliburton et al., (1980) has suggested to use 150mm wide and 300 mm long specimens at a strain rate of 2%/min while Andrawes et al., (1984) recommended 200mm wide and 100 mm long specimen at a strain rate of 10%/min. The determined values of the wide-width strip's force-elongation properties of geotextiles, provide design parameters for reinforcement type applications.

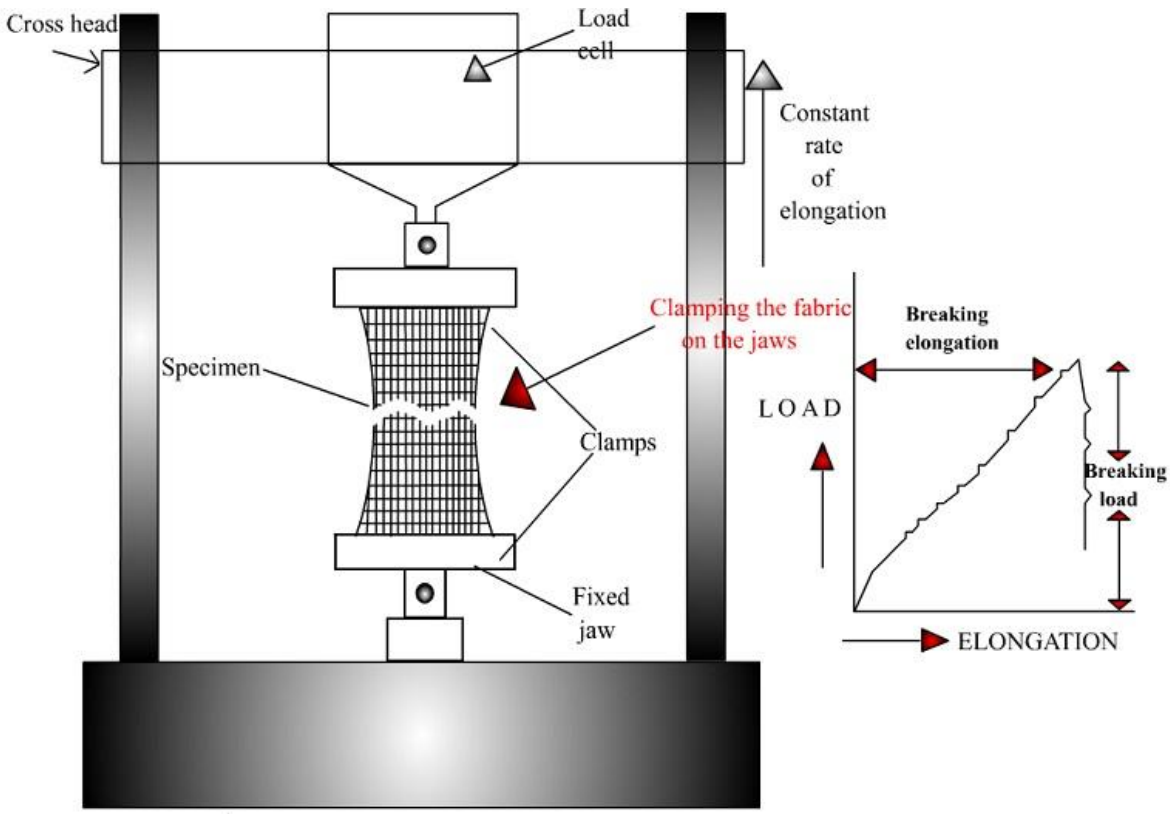

Fig. 3.1: Constant rate of strain test setup for geotextile

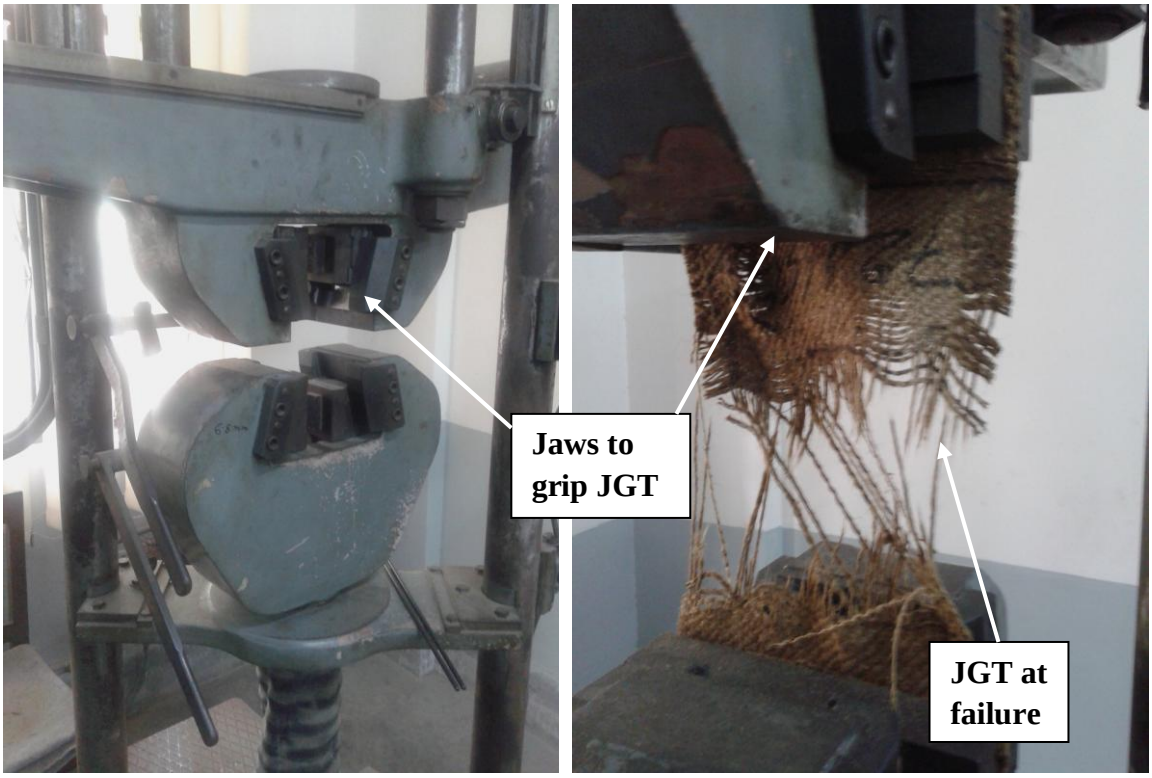

(a) (b)

Fig. 3.2: Constant rate of strain test of JGT: (a) Wolpert machine and (b) tested sample

(b)

(a)

Fig. 3.3: Creep test setup: (a) sample under loading and (b) setup to count deformation

The test specimens for wide-width test are cut with a width of 200 mm and length of 100 mm. The lengths of the specimen were parallel to the direction for which the tensile strength is being measured. The length of the specimen was selected such that, it fits the clamps being used. Nine specimens of each type JGT, viz. UT and AT of two different mass 627gsm and 724gsm in both direction MD and XMD, were prepared for testing. A set of three sample of each type JGT were tested at three different strain rate (10±3)%/min, (50±5)%/min and (100±10)%/min, to evaluate the strain rate sensitivity of JGTs.

3.3.2 Sustained Load Creep Test

The scheme of test apparatus used in sustained load creep test is shown in Fig. 3.3. This test involves very longer period of time compared to CRS test. The specimens were cut to shape and size as specified in ASTM D5262-07. The upper end was fixed to a clamp that is fixed to the main frame. The lower end is fixed to a clamp, where the load was applied. The loads for creep test were chosen based on a percentage of the geotextiles's wide width tensile strength. Creep tests were conducted using 10% (P_{10}), 20% (P_{20}), 30% (P_{30}) and 40% (P_{40}) of ultimate tensile strength (P_u) of a particular sample. Samples were loaded for 1000 hours and readings were taken at 0.01, 0.1, 0.25, 0.5, 1, 2, 5, 10, 30,100, 200, 500 and 1000 hour. After 1000 hours, the loads were removed and the elastic strain was also being measured. These data are used to plot strain-time plots to develop load strain curves for further usages.

3.4 Isochronous Load-Strain Curves

Each of the test methodologies involves different form of data presentation and for a particular test several forms of data presentation can be used. The most widely applicable form of presenting creep test data is in the form of isochronous load-strain curves at a constant temperature. Isochronous curves are the plots of load verses strain at the same temperature for different long term loading, such as creep test. In order to obtain isochronous (load-strain) curves, the materials (specimens) are subjected to a series of loads and sustained as shown in the Fig. 3.4.The plots of total strain ε_T against time for the above loadings are constructed as shown in the Fig. 3.5 for EVP materials. For any time t_1, total strain values, corresponding to the loads are scaled off from the Fig 3.5 (a). In the

same manner for any time t_2 and t_3, corresponding strain values to the loads are obtained from the same Fig.s and marked on the plots of load vs strain. These points corresponding to different time t_1, t_2 and t_3 respectively, are joined to produce curves for t_1, t_2 and t_3 respectively. Thus a family of curves is obtained. The typical isochronous curves for EVP materials are shown in the Fig. 3.5(b).

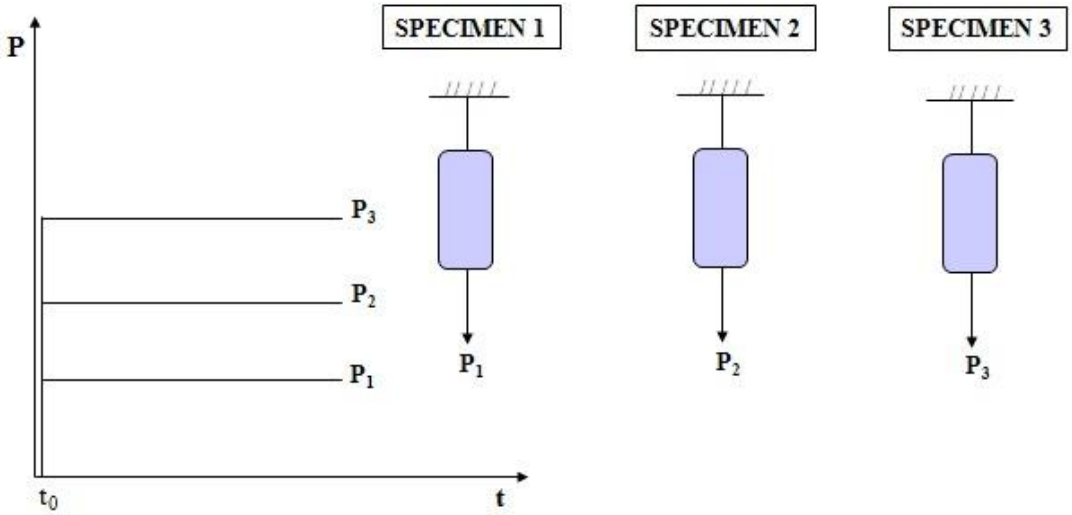

Fig. 3.4: Creep test setup, series of loading verses time (Mahaseth, 2002)

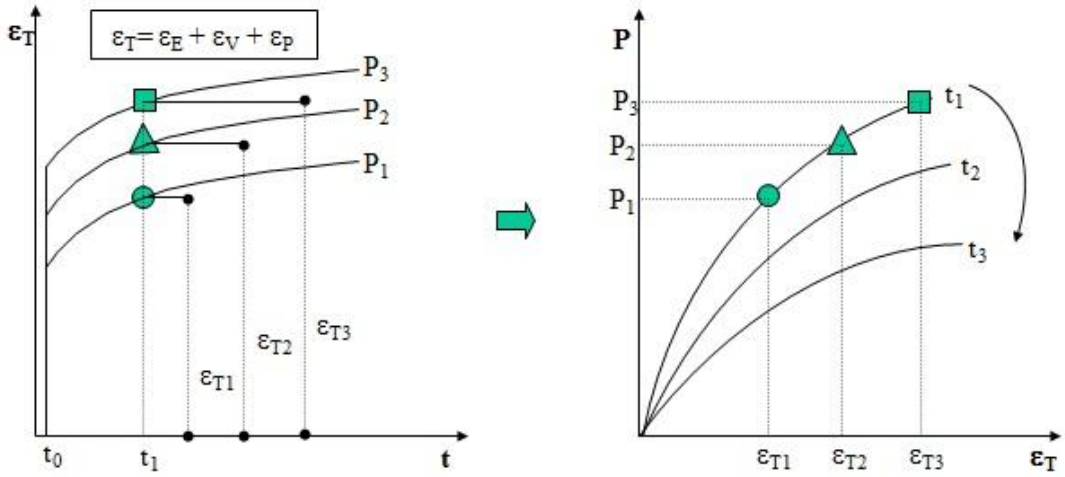

(a) (b)

Fig. 3.5: Deriving Isochronous load-strain curves for EVP geosynthetics: (a) total strain-time plot and (b) isochronous load-strain curves (Mahaseth, 2002)

3.5 Development of ε_R - ε_L Plot and Strain Envelope for EVP Material

The strain – time plots are presented in Fig. 3.6. From the Fig. the total strain can be calculated with various combinations of strain components, viz. locked and recoverable strain, for different loads and times.

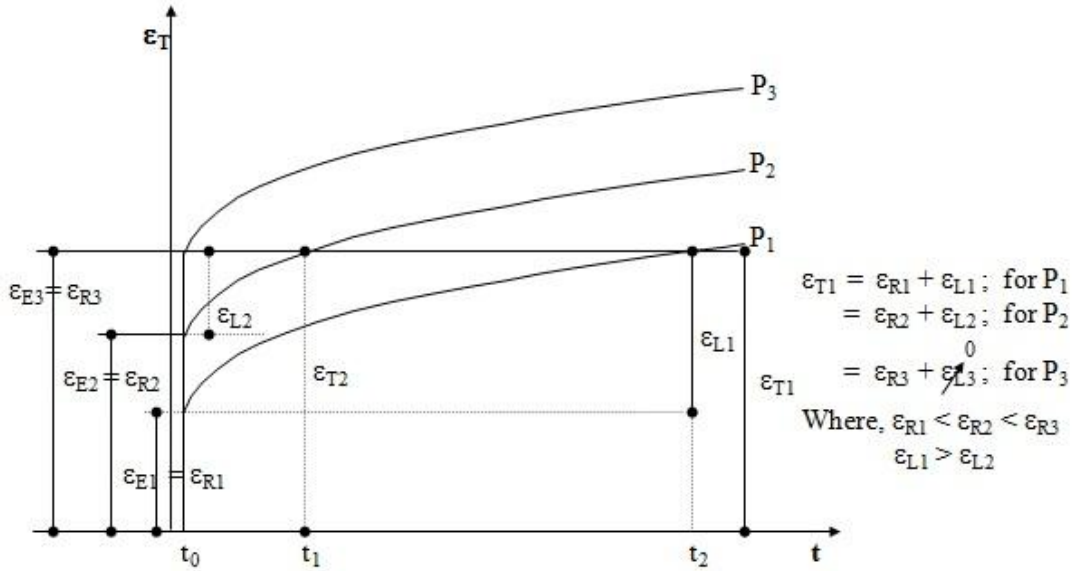

Fig. 3.6: Combinations of strain components for different sustained loadings to EVP material (Mahaseth, 2002)

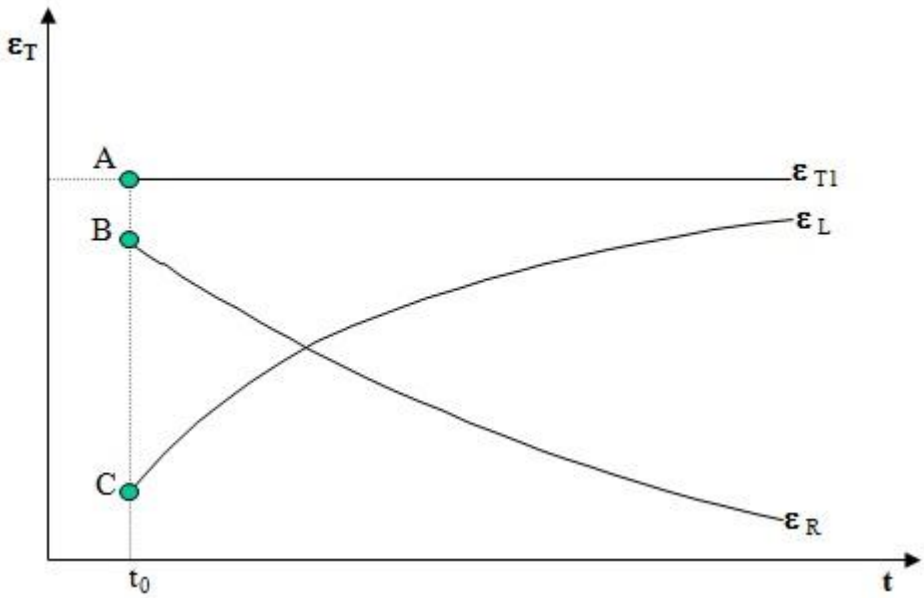

Fig. 3.7: Total strain, ε_T and its components with respect to time for EVP material (Mahaseth, 2002)

For example, if the material is to reach a total strain ε_{t1} at t_0, there can be only elastic strain ε_{E3} with load P_3, where as it may attain the same total strain ε_{t1} with load P_2 at time t_1, but with a combination of recoverable strain, $\varepsilon_{R2} = \varepsilon_{E2}$ and a small amount of locked in strain, ε_{L2}. However, it may also attain the same amount of strain ε_{t1} with load P_1 at time t_2 combining the recoverable strain $\varepsilon_{E1} = \varepsilon_{R1}$ and a greater locked in strain ε_{L1}.

Fig. 3.7 shows the curves for total strain ε_{T1} and its components (recoverable strain ε_R and locked in strain ε_L) plotted against time. It can be identified from this Fig. that, the total strain ε_T may be arrived at in various ways combining ε_R and ε_L depending on time. The features of the curves indicate that recoverable strain ε_R decreases with time while the locked in strain ε_L increases.

When the recoverable strain ε_R and locked in strain ε_L plotted against each other as shown in the Fig. 3.8, develop a strain envelop for a particular limiting strain ε_{T1}. Fig. shows that, for a specific limiting at point A, a higher value of recoverable strain ε_R and lower value of ε_L, or a lower value of ε_R and higher value of ε_L, at point B. In the other word it can be said that, at initial stages of the loading, the recoverable strain ε_R is greater than the locked in strain ε_L, but later on, it becomes vice versa.

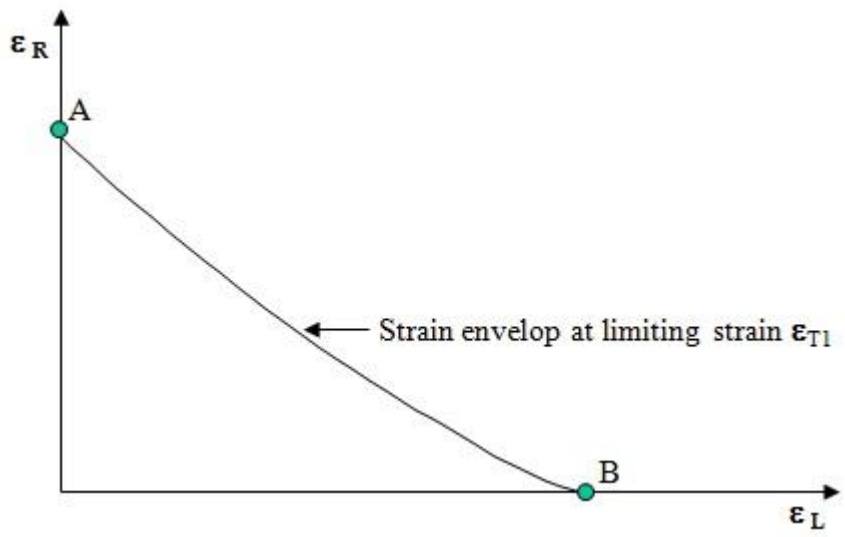

Fig. 3.8: Plot of ε_R - ε_L to develop strain envelope for EVP material (Mahaseth, 2002)

CHAPTER FOUR

RESULTS AND DISCUSSION

4.1 General

Test results of untreated and additive treated JGTs are presented in this chapter, which are narrated in chapter three, viz. mass per unit area, nominal thickness, wide-width tensile strength and sustained load creep test. The analyses of creep test data of selected JGTs are presented in this chapter. The extrapolation of creep test results by best curve fitting technique and formation of isochronous curves are also explained in chapter four. Derivation of strain components (ε_R and ε_L) from creep test result and the development of strain envelops for different limiting stain are presented here. Engineering applications of isochronous curve and variation in strain components are discussed in this chapter.

4.2 Physical Properties of JGT

Two physical properties that are mass per unit area and nominal thickness of selected JGTs were evaluated.

4.2.1 Mass per Unit Area

To determine the mass per unit area, five specimens of each type JGT, viz. untreated and additive treated of two masses 627gsm and 724gsm were cut in a manner that they represent the entire roll width. The length and width was measured at natural condition and then the masses were measured. The mass per unit area of JGTs are presented in Table 4.1. Mass per unit area of AT samples is found to be higher than that of the UT samples, due to the addition of chemicals through the treatment process.

Table 4.1: Average mass per unit area of untreated and additive treated JGTs

Type of JGT	Untreated		Additive Treated	
	627gsm	724gsm	627gsm	724gsm
Average mass per unit area (gsm)	611.2	742.2	828.9	1020.0

4.2.2 Nominal Thickness

Ten specimens of each type JGT, viz. UT and AT of two masses 627gsm and 724gsm, were tested to determine the nominal thickness of the selected JGTs. The test specimens were prepared in a randomly distributed pattern across the width. The thicknesses of JGTs are presented in Table 4.2. Thickness of AT samples is found to be higher than the UT samples due to the addition of chemicals through the treatment process.

Table 4.2: Average thickness of untreated and additive treated JGTs

Type of JGT	Untreated		Additive Treated	
	627gsm	724gsm	627gsm	724gsm
Average thickness (mm)	1.76	1.93	2.20	2.66

4.3 Mechanical Properties of JGT

Two mechanical properties, which are wide-width tensile strength and sustained load creep test, were performed for each type of selected JGT.

4.3.1 Wide-Width Tensile Strength

The equipment used in this test was a tensile testing machine named by Wolpert machine. It has load and elongation recorders and jaws with jagged faces for firmly grip on the specimen to prevent slippage.

A set of three sample of each type JGT were tested at three different strain rate (10±3)%/min, (50±5)%/min and (100±10)%/min. In total 72 samples were tested to determine the tensile strength and strain rate sensitivity of selected JGTs. The Ultimate Strength (US) in tension and elongation of JGTs are presented in Table 4.3, Table 4.4 and Table 4.5. The test results shown in the tables reveal that, effect of strain rate is insignificant on the strength of JGTs in MD as well as in XMD. The test results also show that the tensile strength of AT samples is almost equal to UT samples. This indicates that the additive treatment of JGTs, is not effective in enhancing the tensile strength. The treatment process decreases the biodegradability of JGTs only.

Table 4.3: Wide-width test results of untreated JGTs for different strain rate in machine direction and cross machine direction at constant temperature, 21°±2

Sample type	Strain rate	Wide width tensile strength (kN/m)		Average ultimate strength, P_u (kN/m)		Strain at breaking point (%)		Average strain at breaking point, ε_u (%)	
		MD	XMD	MD	XMD	MD	XMD	MD	XMD
UT 627gsm	(10±3) mm/min	24.7	10.1	24.2	10.4	12.2	10.2	11.7	9.8
	(50±5) mm/min	24.0	10.5			11.3	9.5		
	(100±10) mm/min	23.9	10.6			11.7	9.7		
UT 724gsm	(10±3) mm/min	28.0	12.1	27.4	12.5	13.2	11.3	12.5	11.0
	(50±5) mm/min	27.6	13.2			12.8	11.0		
	(100±10) mm/min	26.7	12.3			11.5	10.8		

Note: UT= Untreated; MD= Machine Direction; XMD= Cross Machine Direction.

Table 4.4: Wide-width test results of additive treated JGTs for different strain rate in machine direction and cross machine direction at constant temperature, 21°±2

Sample type	Strain rate	Wide width tensile strength (kN/m)		Average ultimate strength, P_u (kN/m)		Strain at breaking point (%)		Average strain at breaking point, ε_u (%)	
		MD	XMD	MD	XMD	MD	XMD	MD	XMD
AT 627gsm	(10±3) mm/min	22.7	9.3	23.3	9.6	12.7	12.0	12.3	11.0
	(50±5) mm/min	23.5	9.6			12.0	10.7		
	(100±10) mm/min	23.7	9.8			12.3	10.2		
AT 724gsm	(10±3) mm/min	25.0	12.1	25.1	11.1	10.6	12.0	12.2	11.8
	(50±5) mm/min	24.9	10.8			12.2	10.8		
	(100±10) mm/min	25.5	10.5			13.7	12.7		

Note: AT= Additive Treated; MD= Machine Direction; XMD= Cross Machine Direction.

Table 4.5: Summary of wide width test result of JGT untreated and additive treated JGTs at different strain rate in machine direction and cross machine direction

Sample type	Average ultimate strength, Pu (kN/m)		Average strain at breaking point, ε_u (%)	
	MD	XMD	MD	XMD
UT 627gsm	24.2	10.4	11.7	9.8
AT 627gsm	23.3	9.6	12.3	11.0
UT 724gsm	27.4	12.5	12.5	11.0
AT 724gsm	25.1	11.1	12.2	11.8

Note: UT= Untreated; AT= Additive Treated; MD= Machine Direction; XMD= Cross Machine Direction.

4.3.2 Sustained Load Creep Test

The loads for creep test were chosen based on the percentage of geotextiles's wide width tensile strength. Creep tests were conducted using 10%, 20%, 30% and 40% of Ultimate Strength (US) of a particular sample. Samples were loaded for 1000 hours and readings were taken at 0.01, 0.1, 0.25, 0.5, 1, 2, 5, 10, 30,100, 200, 500 and 1000 hour. After 1000 hours, the loads were removed and the elastic strain was measured. Fig. 4.1 shows the deformation of UT 627gsm sample with respect time and the recovery of the strain after unloading. Results of other samples are presented in Appendix B.

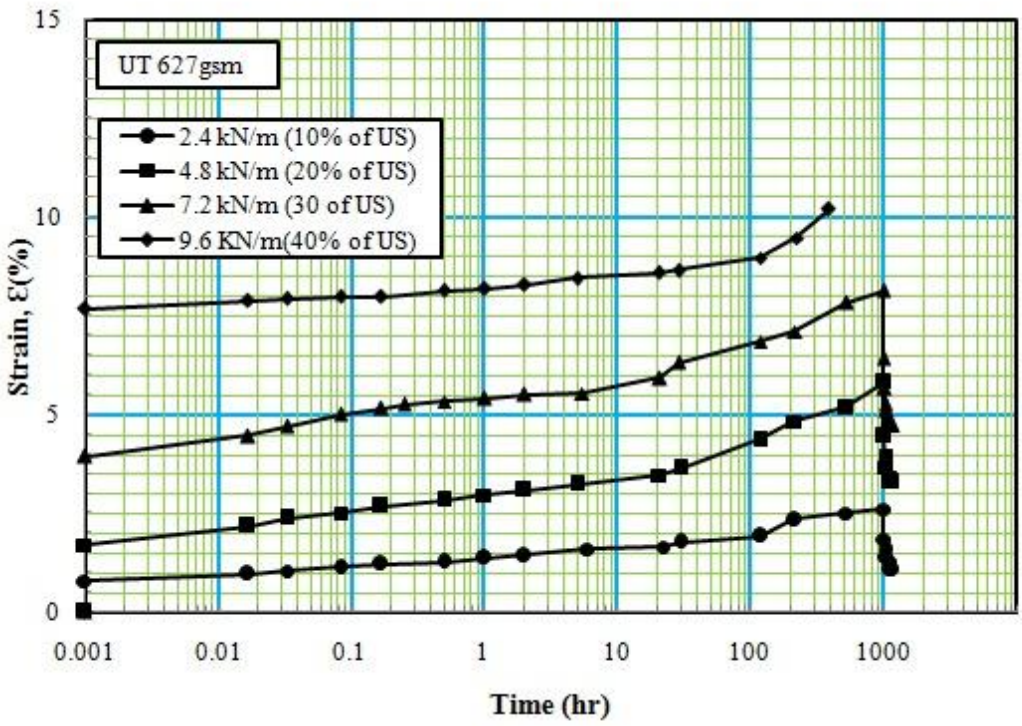

Fig. 4.1: Total strain vs log time (hr) for untreated 627gsm in machine direction

By considering the readings of loading and unloading, an average of 1200 hrs data were collected for each sample and in total almost 19200 hrs creep test data were collected for the research work. The atmospheric temperature was tried to keep at 21ºC, all through the test program. By using the test result a series of isochronous (load-strain) curves are prepared for the specimens. The elastic strain and visco-plastic strain for different time are calculated to develop strain envelops for different limiting strains.

4.4 Extrapolation of Creep Test Data

Mostly RSSs are designed for an operation period that is greater than the duration of creep tests. Therefore, it becomes necessary to extrapolate creep test data to the required design life of the structure. In the same manner, it also becomes essential to extrapolate creep test data at higher load levels other than those employed during the tests. Khan (1999) showed that, the data for larger duration than the creep test could be obtained by extrapolation using best curve fitting technique.

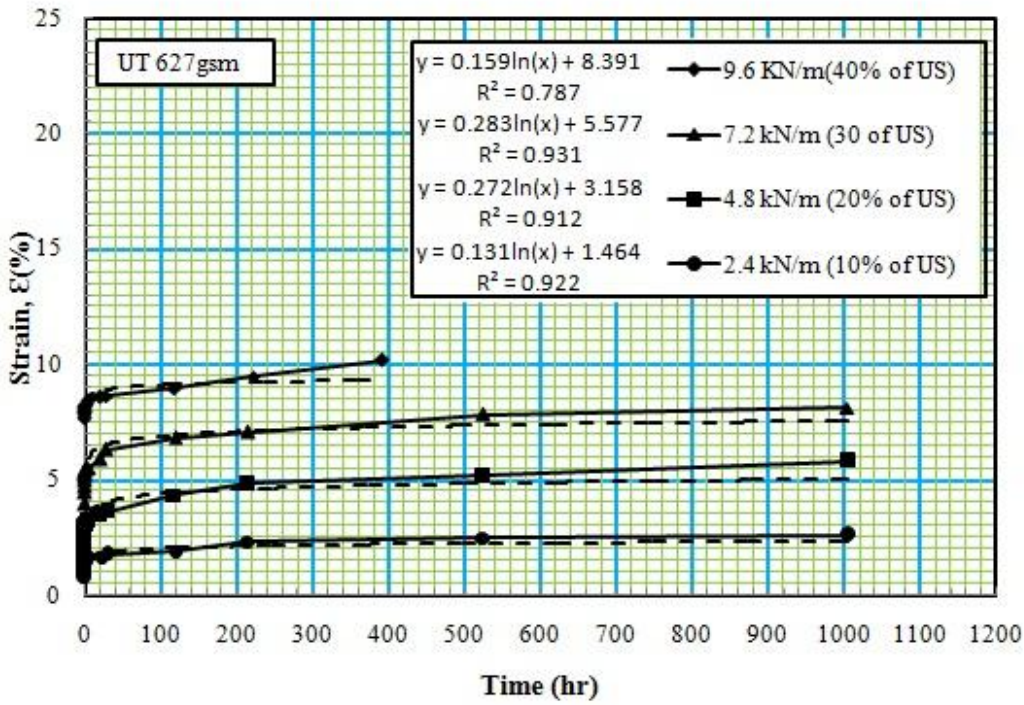

Fig. 4.2: Strain vs. time curves and best fitted curves for the strain vs. time relationships of untreated 627gsm in machine direction

The curves form test result fit logarithmic series as shown Fig.4.2. Results of other samples are presented in appendix B. The typical form of the curves can be express by the equation as follows:

$$y = A \, Ln(x) + B \qquad 4.1$$

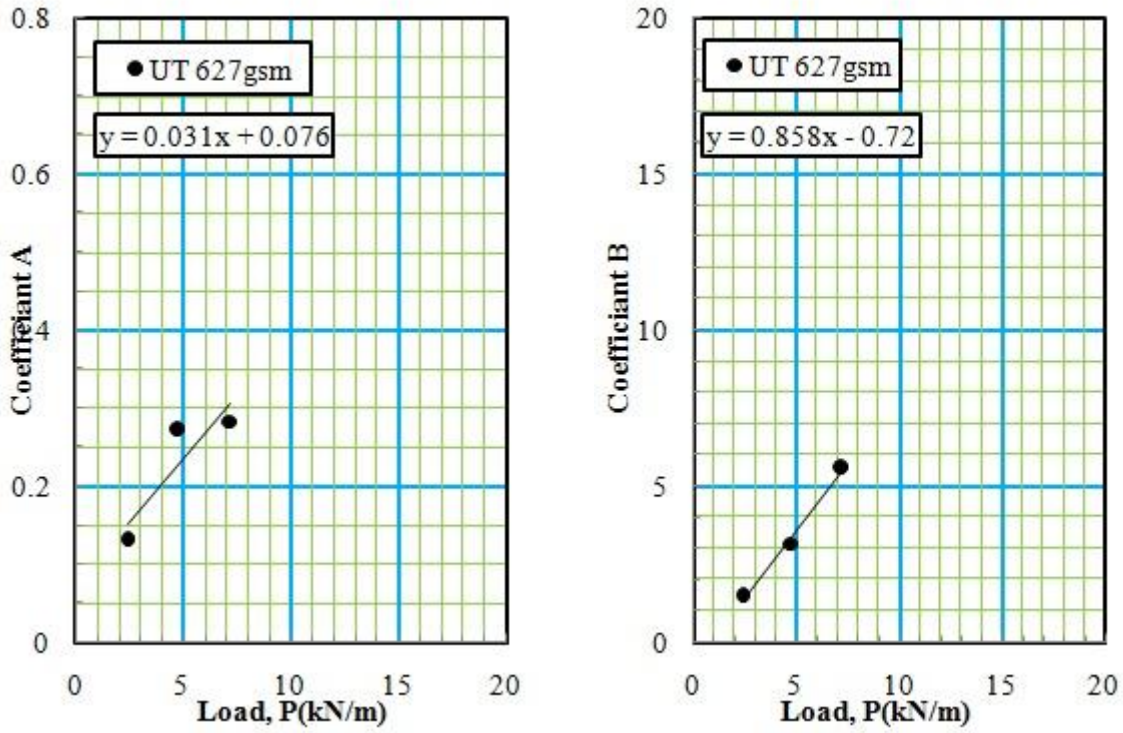

(a) (b)

Fig. 4.3: Trend line coefficients: (a) coefficient A obtained from linear fit curve and (b) coefficient B obtained from linear fit curve

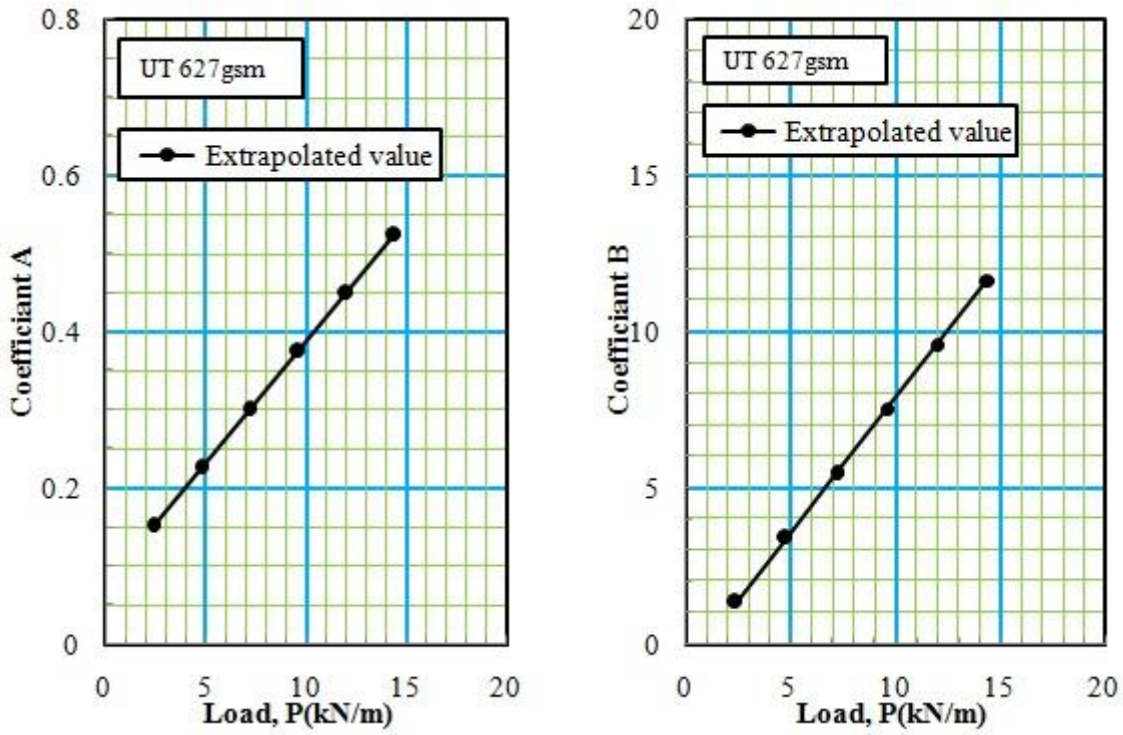

(c) (d)

Fig. 4.4: Extrapolation of coefficients: (a) coefficient A of linear fit curve and (b) coefficient B of linear fit curve

The coefficient A and B are separated and plotted at different load levels. The plot shows linear fit, as presented in Fig. 4.3. The equations of both parameters A and B are in the form of, y = ax + c. From these linear fits, the parameters A and B have been extrapolated at higher load levels as shown in Fig. 4.4. The extrapolated values are used to determine the total strain-time curves at higher load levels. The creep test results of UT 627gsm are extrapolated at higher load levels by using the extrapolated values of A and B as shown in Fig. 4.5. Results of other samples are presented in Appendix B.

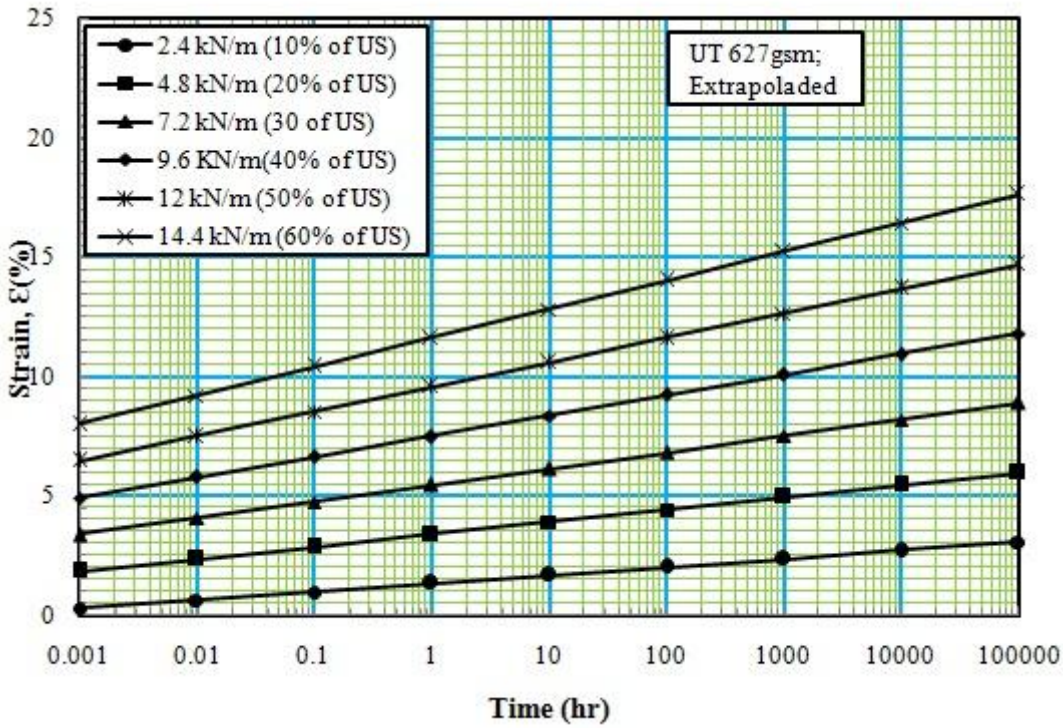

Fig. 4.5: Extrapolated total strain vs log time (hr) for untreated 627gsm in machine direction

4.5 Isochronous Curves of JGT

The most convenient and broadly accepted form to present creep test results is isochronous curves, which are applied here for JGT samples. Isochronous curves are the load–strain curve for different times at a constant temperature (Mahaseth, 2002). Fig. 4.6 represents the load-total strain plots derived from the total strain-time plots. Once the isochronous curves have been derived, the strain at any load level for any time could be found. Alternatively, the load corresponding to a particular strain for any time could be found from these curves. That means from the isochronous curves of selected JGTs, the load carrying capacity at the End of Design Life (EDL) or the possible design life for a particular load can be predicted for a particular strain in isothermal condition.

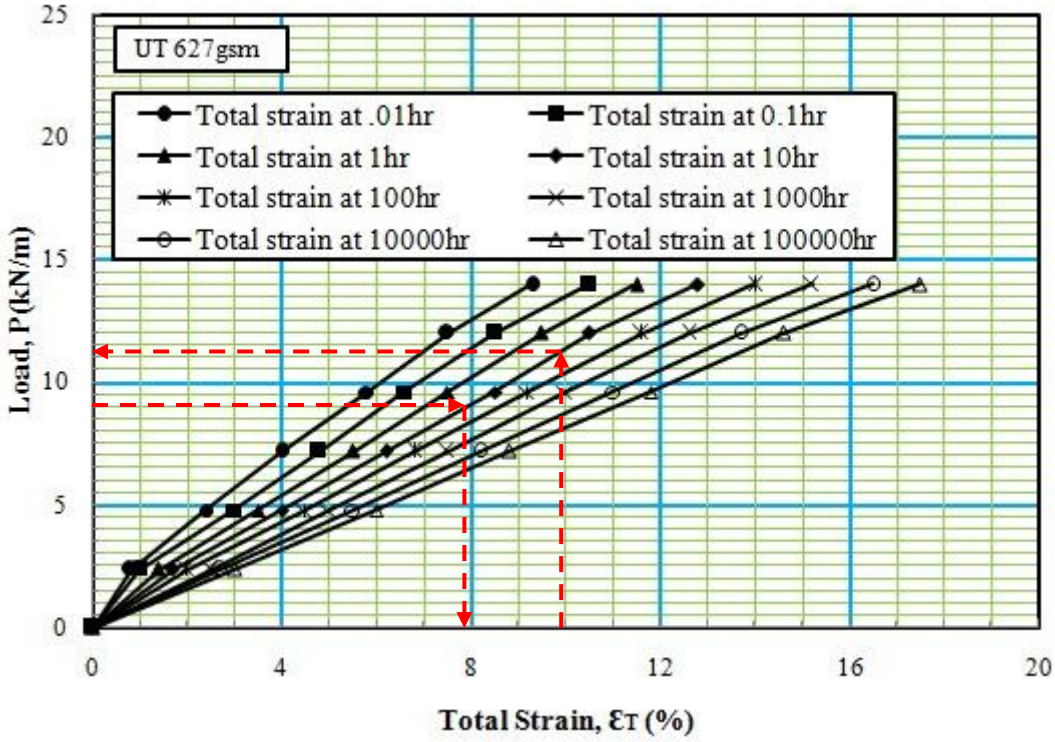

(a)

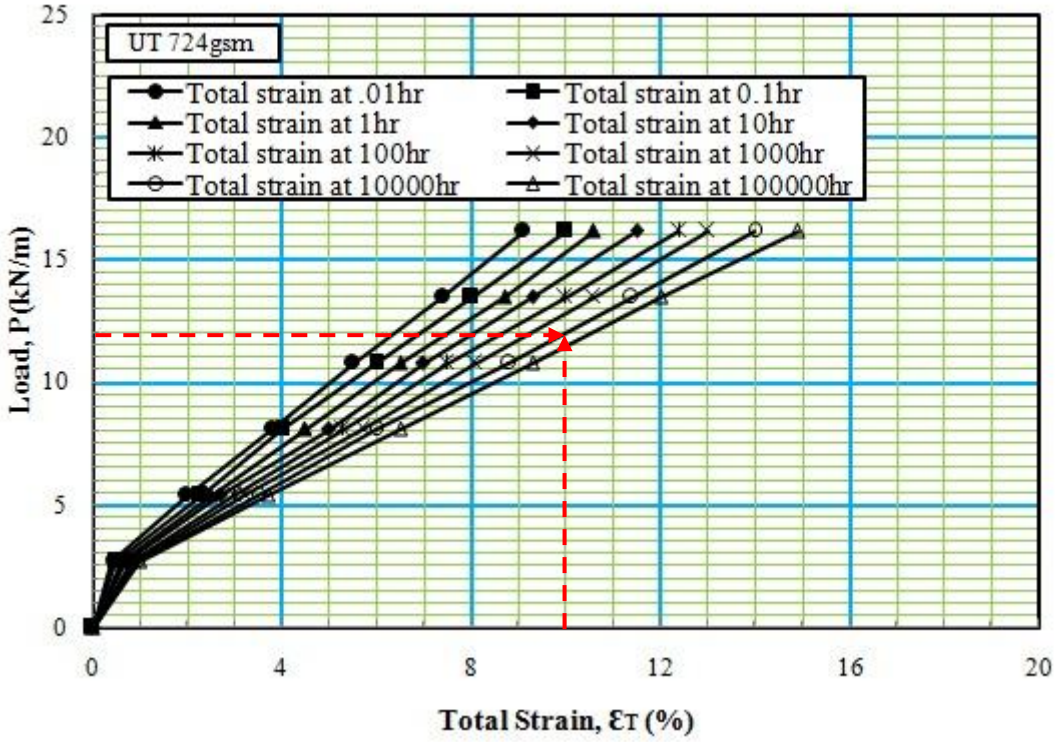

(b)

Fig. 4.6: Isochronous curves derived from creep test result: (a) untreated 627gsm and (b) untreated 724gsm

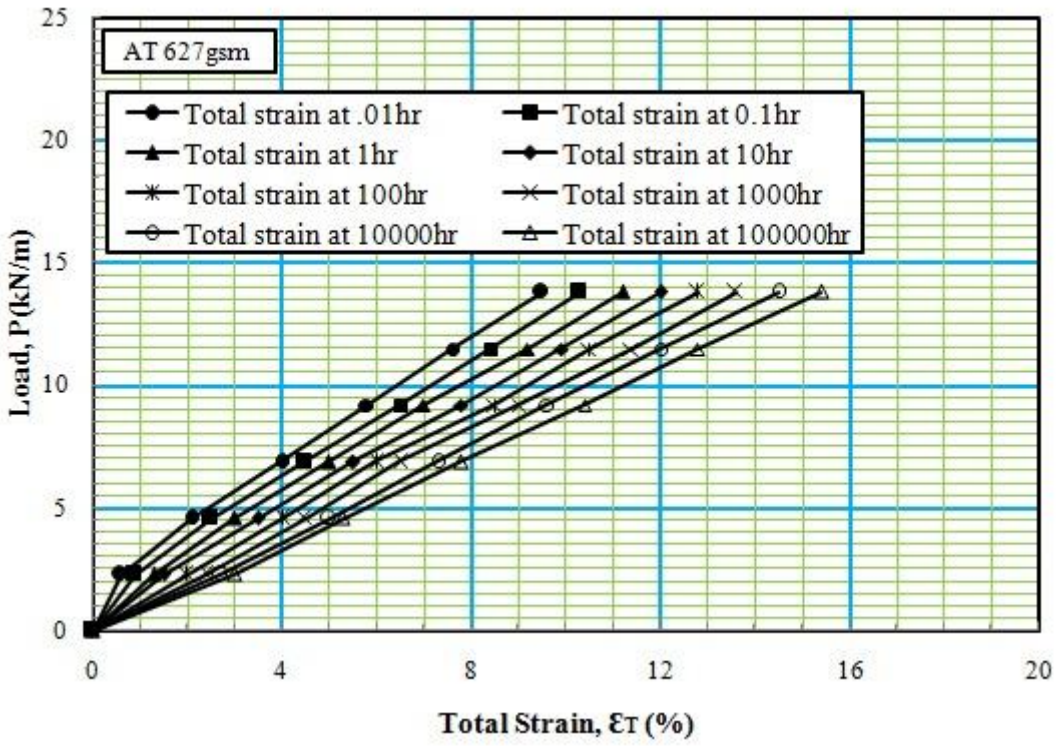

(a)

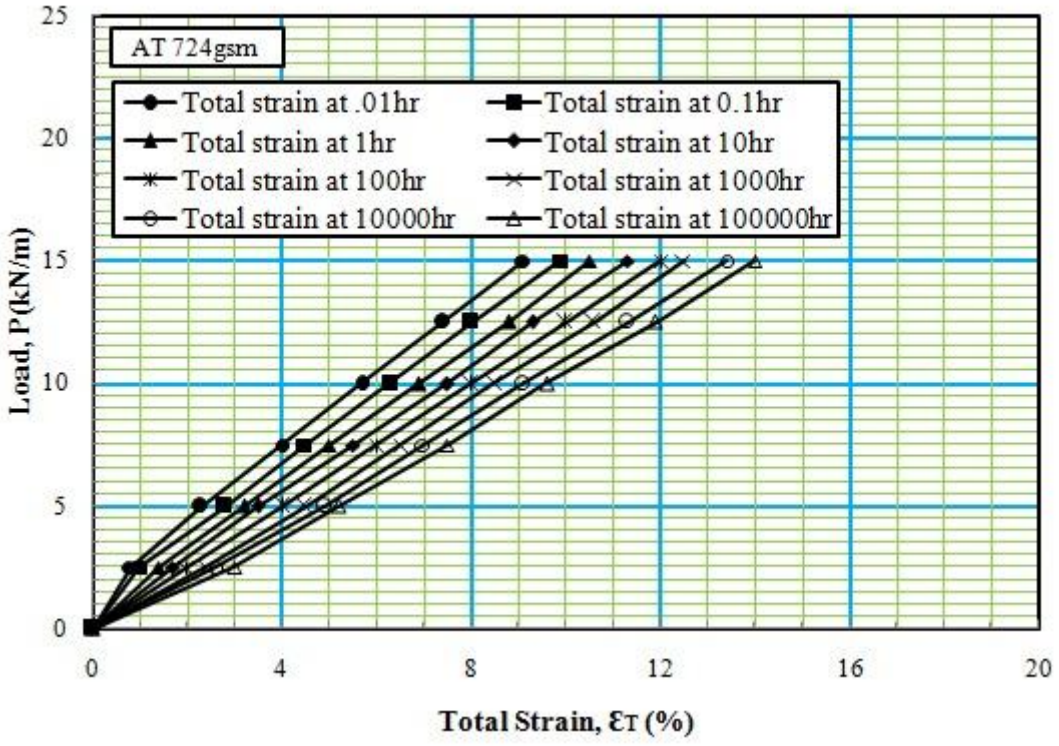

(b)

Fig. 4.7: Isochronous curves derived from creep test result: (a) additive treated 627gsm and (b) additive treated 724gsm

A design strain is considered as 10% for a specified load 9kN/m and the design life of JGT is considered as 10hr. From the isochronous curves as shown in Fig. 4.6(a) it is found that, after 10hr developed strain is 7.9%. That means a load greater than 9kN/m is required to develop the 10% limit strain at EDL. From the isochronous curve the required load could be calculated, which is 11kN/m.

On the other hand, a design strain is considered as 10% for a specified load 12kN/m. From Fig. 4.6(b), it is found that the specified strain and load indicate an isochronous curve of 10000hr. That means the specific type of JGT can be applied under 12kN/m loading for 10000hr, which will develop a strain of 10% at the end of 10000hr.

4.6 Development of ε_R - ε_L Plot and Strain Envelope for JGTs

To develop the load-recoverable strain curves, the unloading response of JGT samples are compiled. Recoverable strain ε_R is constant for a particular load level irrespective of time. Load-recoverable strain is developed and extrapolated as shown in Fig. 4.8. From Fig. 4.8, the recoverable strain at any load level could be found. The Fig. 4.9 represent the load-locked strain curves, which have been derived in a process, $\varepsilon_L = \varepsilon_T - \varepsilon_R$. For various limiting strains, viz. 2%, 5%, and 10%, the loads are obtained from the isochronous curves as shown in Fig. 4.10(a). The derived loads are then used to find the corresponding recoverable strains, Fig. 4.10(b). Thus the locked strain of a particular limiting strain is found by deducting the derived recoverable from limiting strain.

Fig. 4.17 to 4.18 shows the variation of total strain components, i.e. ε_R and ε_L with respect time for a specific limiting strain of UT 627gsm sample. Once the strain components obtained, they have been plotted against each other to develop strain envelope.

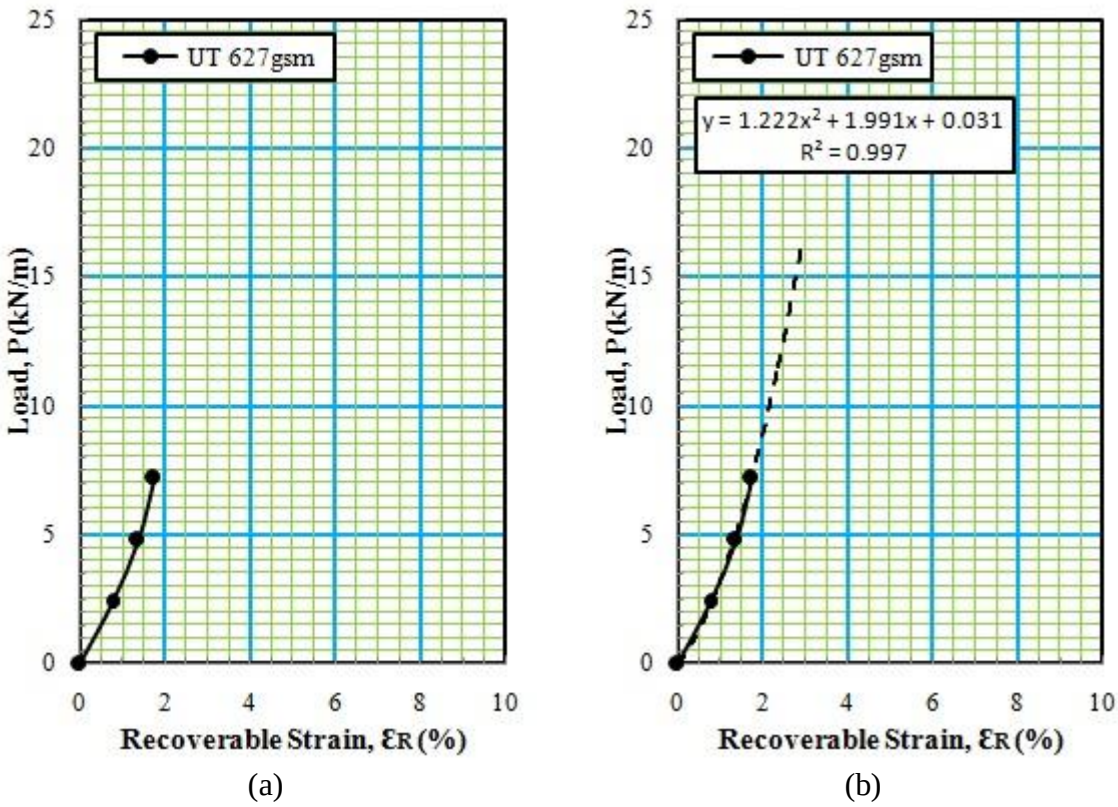

(a) (b)

Fig. 4.8: Load vs recoverable strain for untreated 627gsm in machine direction: (a) tested sample response and (b) extension of test result

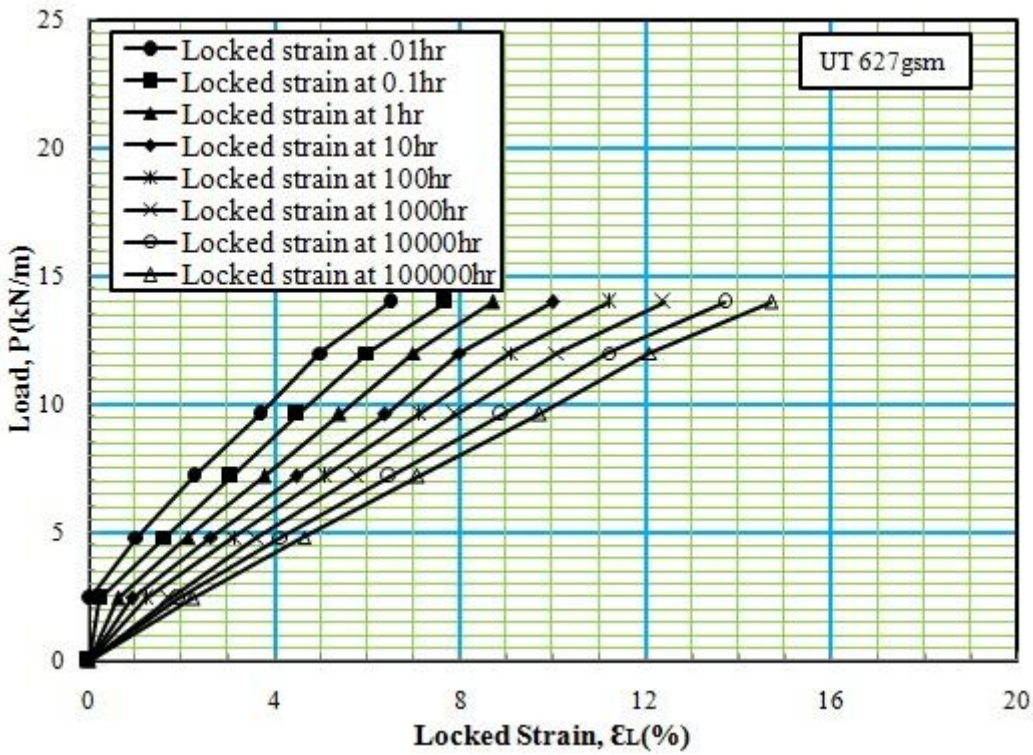

Fig. 4.9: Load vs locked strain for untreated 627gsm in machine direction

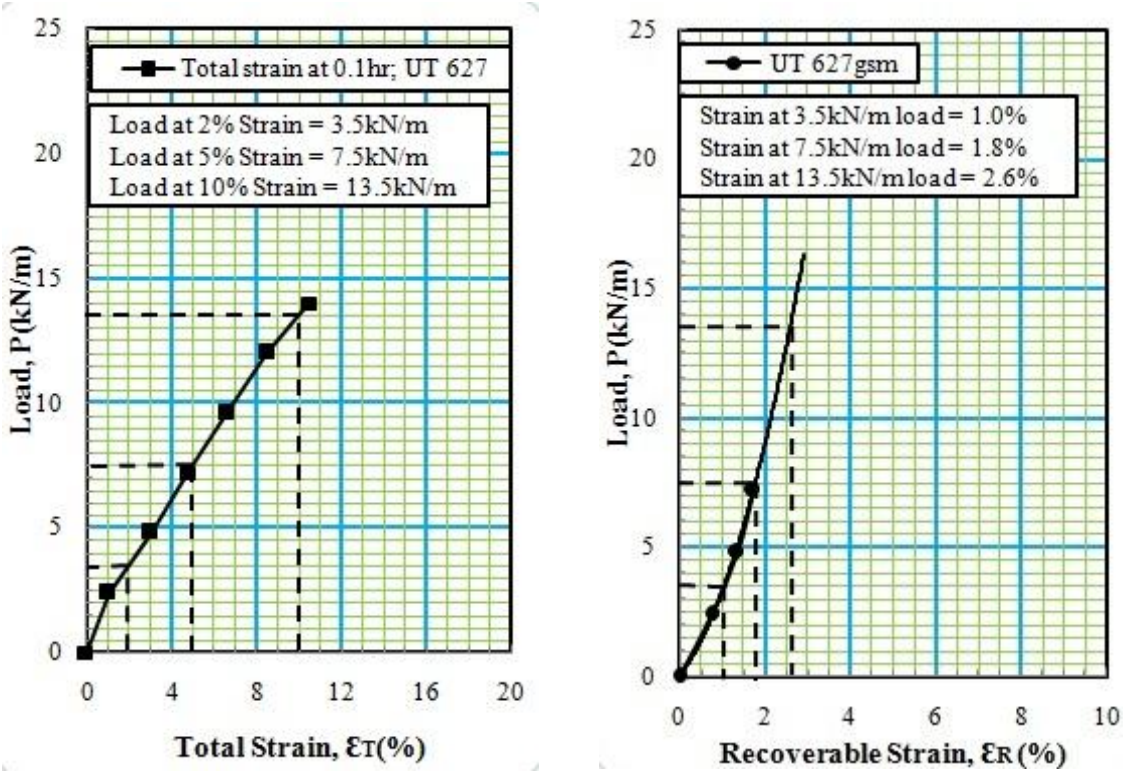

(a) (b)

Fig. 4.10: (a) Load vs. total strain graph and (b) load vs. recoverable strain graph for untreated 627gsm in machine direction at 0.1hr for different limiting strains

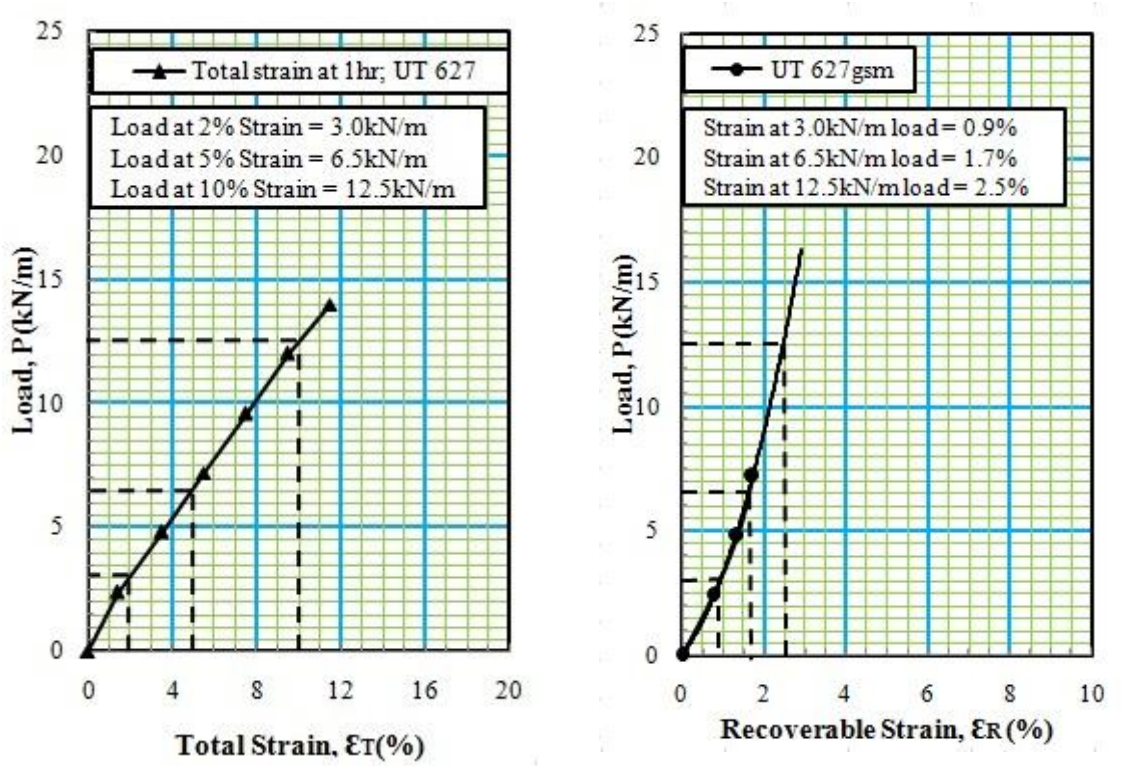

(a) (b)

Fig. 4.11: (a) Load vs. total strain graph and (b) load vs. recoverable strain graph for untreated 627gsm in machine direction at 1 hr for different limiting strains

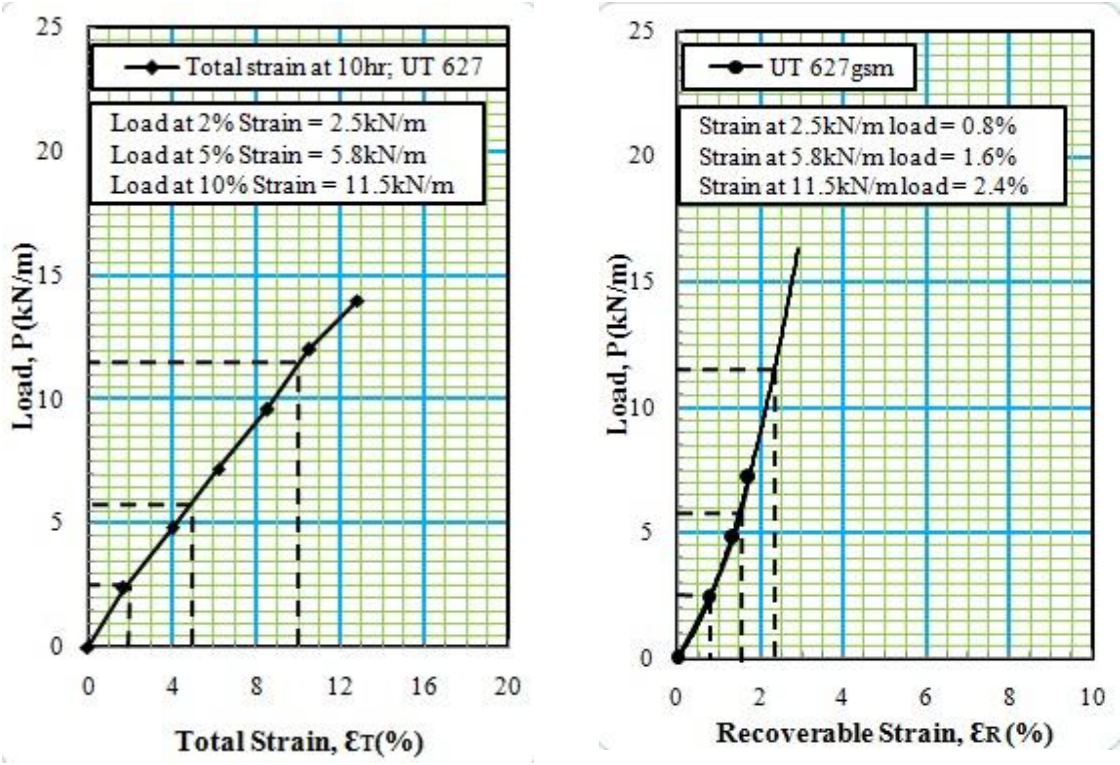

(a) (b)

Fig. 4.12: (a) Load vs. total strain graph and (b) load vs. recoverable strain graph for untreated 627gsm in machine direction at 10 hr for different limiting strains

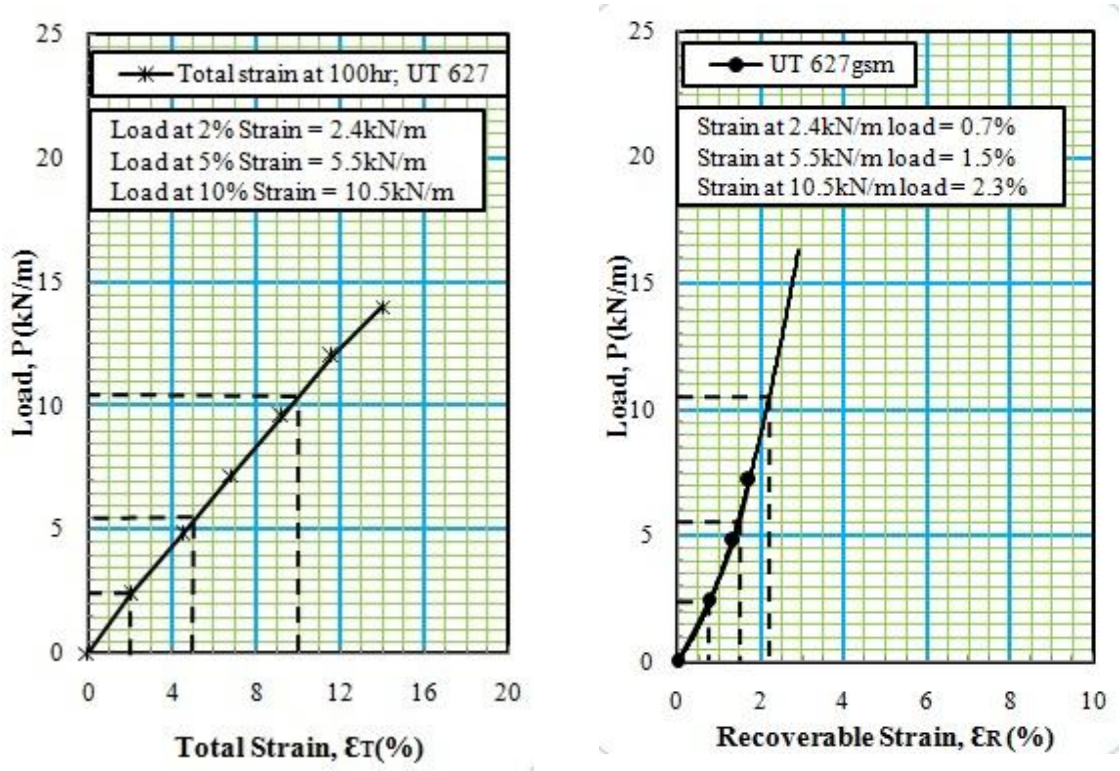

(a) (b)

Fig. 4.13: (a) Load vs. total strain graph and (b) load vs. recoverable strain graph for untreated 627gsm in machine direction at 100 hr for different limiting strains

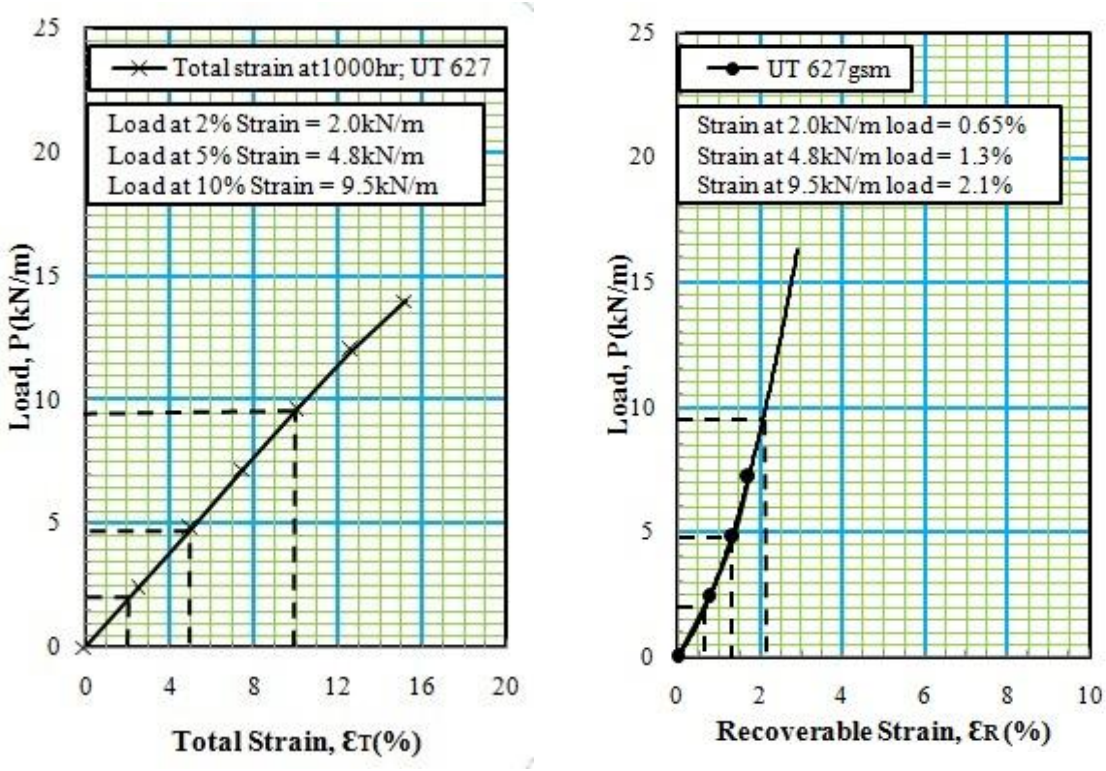

(a) (b)

Fig. 4.14: (a) Load vs. total strain graph and (b) load vs. recoverable strain graph for untreated 627gsm in machine direction at 1000 hr for different limiting strains

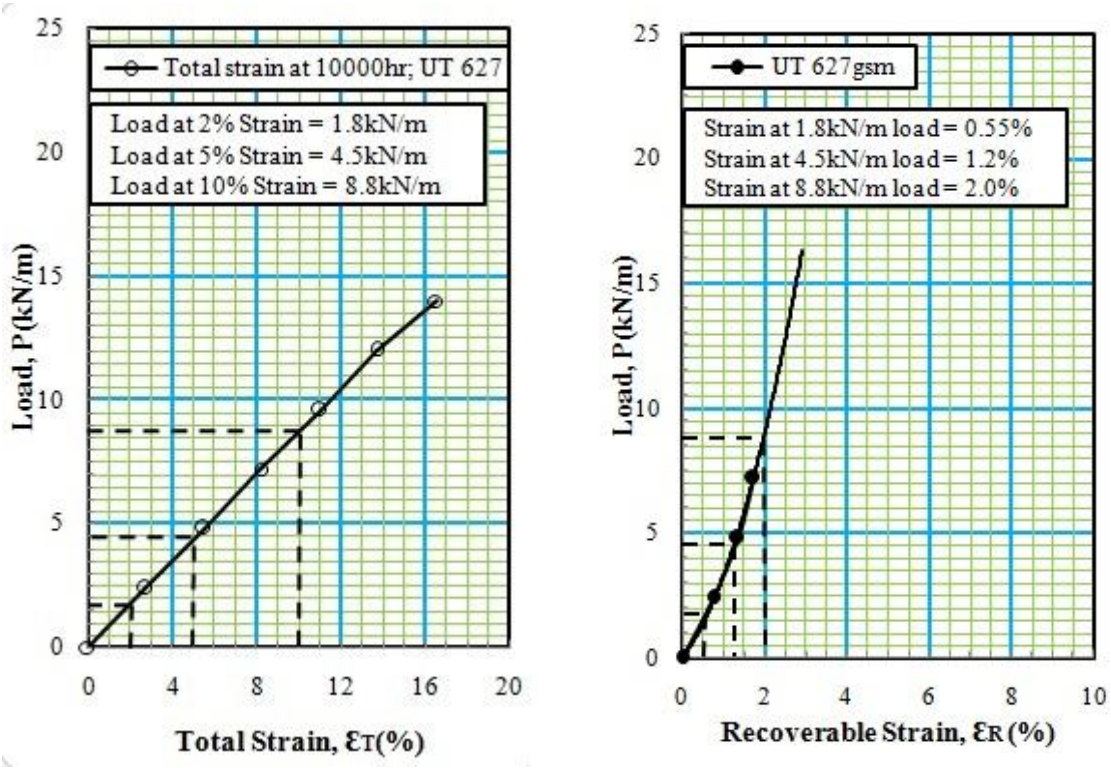

(a) (b)

Fig. 4.15: (a) Load vs. total strain graph and (b) load vs. recoverable strain graph for untreated 627gsm in machine direction at 10000 hr for different limiting strains

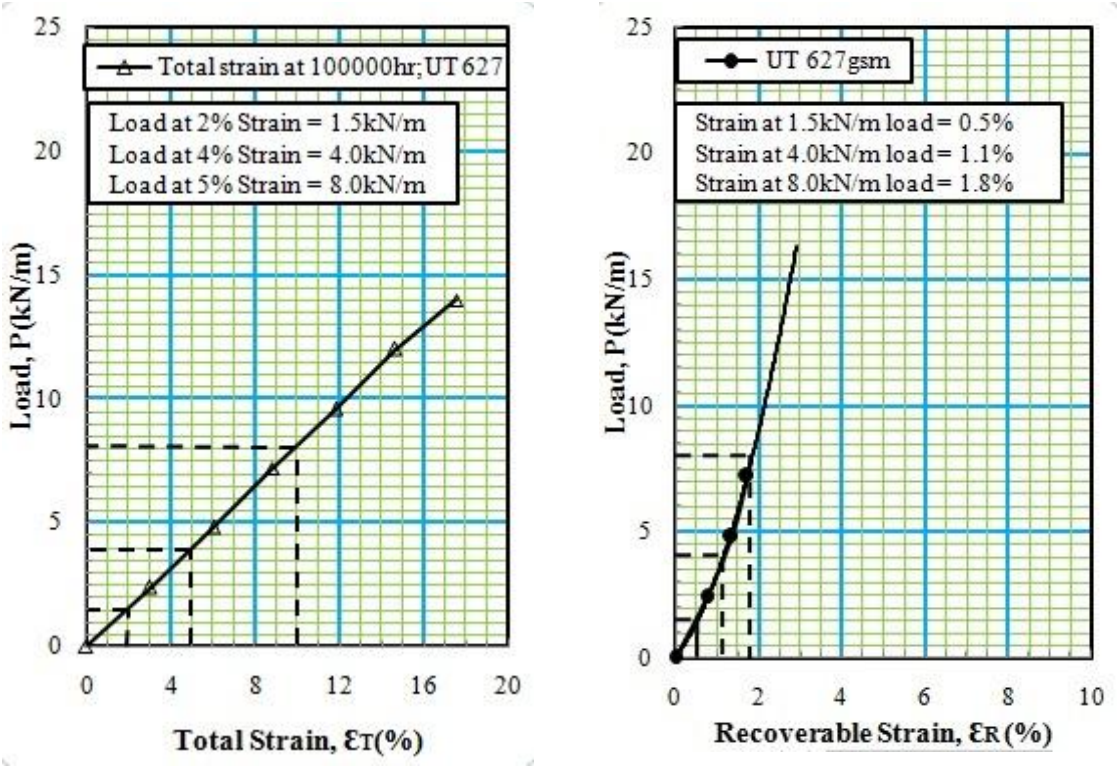

(a) (b)

Fig. 4.16: (a) Load vs. total strain graph and (b) load vs. recoverable strain graph for untreated 627gsm in machine direction at 100000 hr for different limiting strains

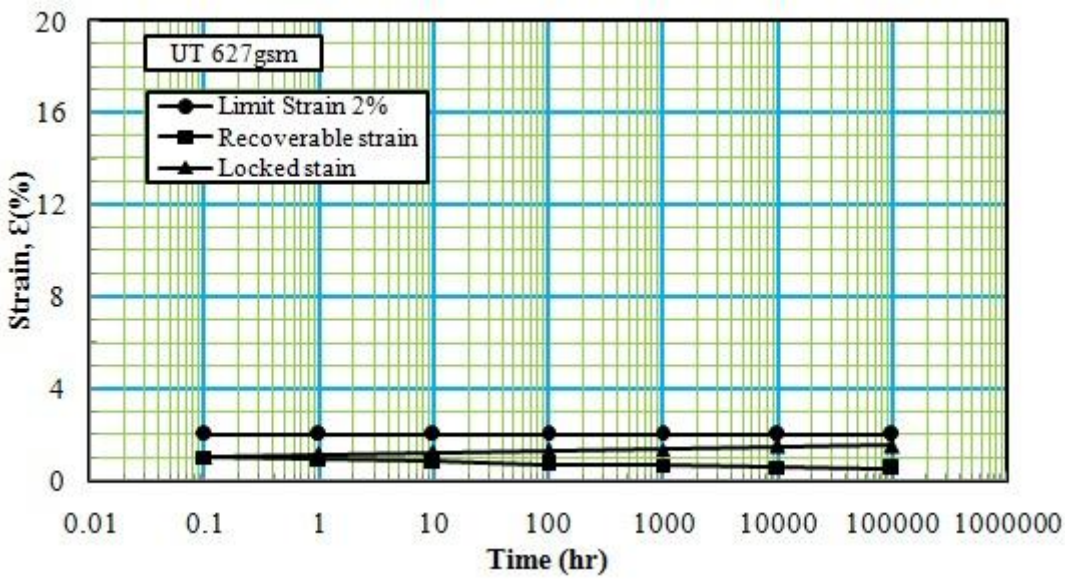

Fig. 4.17: 2% limit strain and it's component vs log time obtained from creep test of untreated 627gsm in machine direction

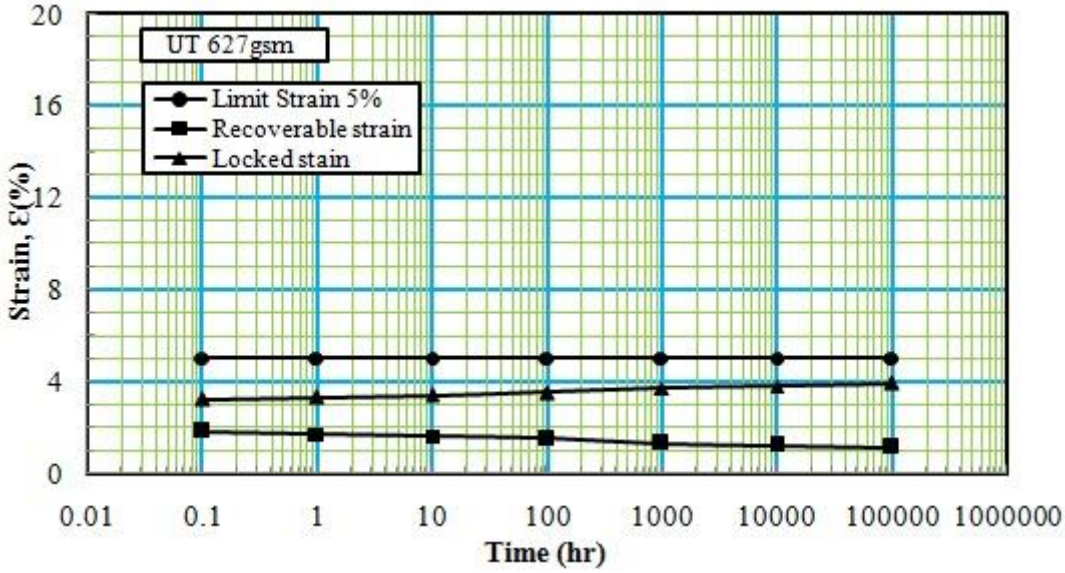

Fig. 4.18: 5% limit strain and it's component vs log time obtained from creep test of untreated 627gsm in machine direction

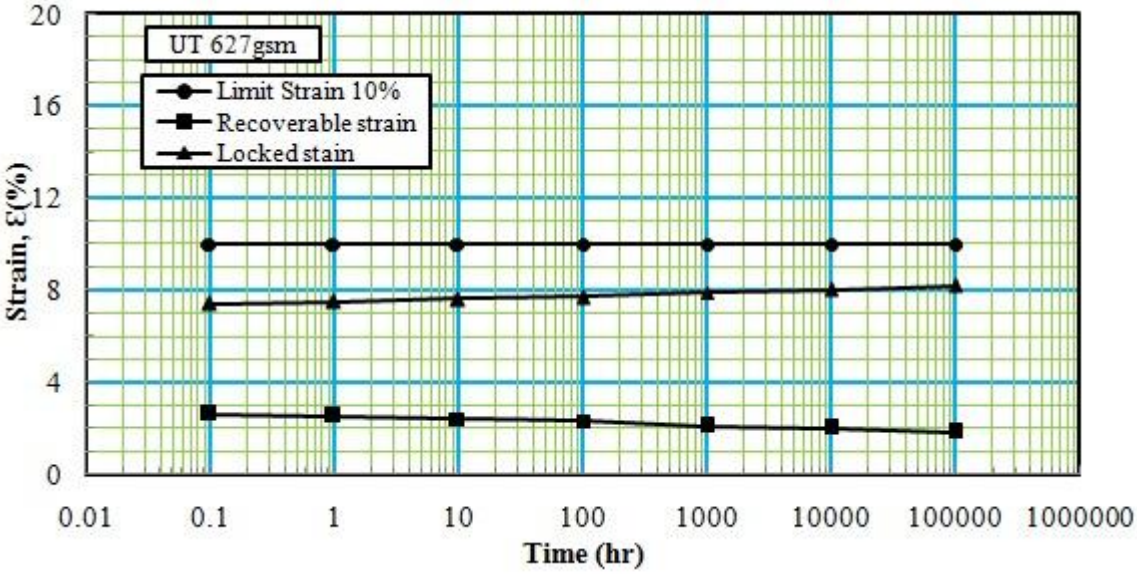

Fig. 4.19: 10% limit strain and it's component vs log time obtained from creep test of untreated 627gsm in machine direction

Fig. 4.20(a) shows the strain envelops for 2%, 5% and 10% limit strain of UT 627gsm sample. From the figure for 2% limit strain it is found that the ε_R decrease from 1.0% to 0.5% for time period 0.1hr to 100000hr, respectively. Whereas the ε_L increase from 1.0% to 1.5% for the same time period. For 5% limit strain it is found that the ε_R decrease from 1.8% to 1.1% for time period 0.1hr to 100000hr, respectively. Whereas the ε_L increase from 3.2% to 3.9% for the same time period. For 10% limit strain it found that the ε_R

decrease from 2.6% to 1.8% for time period 0.1hr to 100000hr respectively. Whereas the ε_L increase from 7.4% to 8.2% for the same time period.

Fig. 4.20(b) shows the strain envelops for 2%, 5% and 10% limit strain of UT 724gsm sample. From the figure for 2% limit strain it found that the ε_R decrease from 0.95% to 0.5% for time period 0.1hr to 100000hr respectively. Whereas the ε_L increase from 1.05% to 1.5% for the same time period. For 5% limit strain it is found that the ε_R decrease from 1.3% to 1.0% for time period 0.1hr to 100000hr, respectively. Whereas the ε_L increase from 3.7% to 4.0% for the same time period. For 10% limit strain it is found that the ε_R decrease from 2.1% to 1.5% for time period 0.1hr to 100000hr respectively. Whereas the ε_L increase from 7.9% to 8.5% for the same time period.

Fig. 4.21(a) shows the strain envelops for 2%, 5% and 10% limit strain of AT 627gsm sample. From the figure for 2% limit strain it found that the ε_R decrease from 0.9% to 0.4% for time period 0.1hr to 100000hr respectively. Whereas the ε_L increase from 1.1% to 1.4% for the same time period. For 5% limit strain it is found that the ε_R decrease from 1.6% to 1.0% for time period 0.1hr to 100000hr respectively. Whereas the ε_L increase from 3.4% to 4.0% for the same time period. For 10% limit strain it is found that the ε_R decrease from 2.5% to 1.8% for time period 0.1hr to 100000hr respectively. Whereas the ε_L increase from 7.5% to 8.2% for the same time period.

Fig. 4.21(b) shows the strain envelops for 2%, 5% and 10% limit strain of AT 627gsm sample. From the figure for 2% limit strain it found that the ε_R decrease from 1.08% to 0.5% for time period 0.1hr to 100000hr respectively. Whereas the ε_L increase from 0.92% to 1.5% for the same time period. For 5% limit strain it is found that the ε_R decrease from 1.9% to 1.1% for time period 0.1hr to 100000hr respectively. Whereas the ε_L increase from 3.1% to 3.9% for the same time period. For 10% limit strain it is found that the ε_R decrease from 2.6% to 1.95% for time period 0.1hr to 100000hr respectively. Whereas the ε_L increase from 7.4% to 8.05% for the same time period.

Strain envelops of selected JGTs show that, ε_L increases from its initial value with the increase of loading time. ε_R decreases from its initial value as with the increase of loading time. The results also indicate that when a particular strain developed within a shorter duration, it will develop comparatively greater value of ε_R and smaller value of ε_L. On the other hand, when relatively longer duration is taken to generate the same amount of strain, it will develop comparatively smaller value of ε_R and greater value of ε_L.

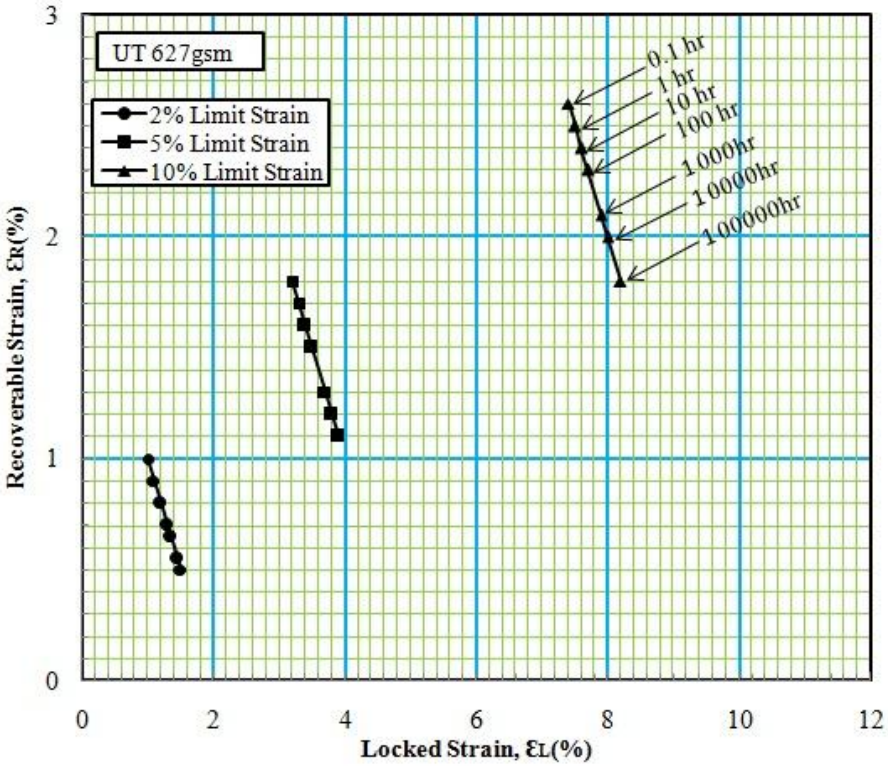

(a)

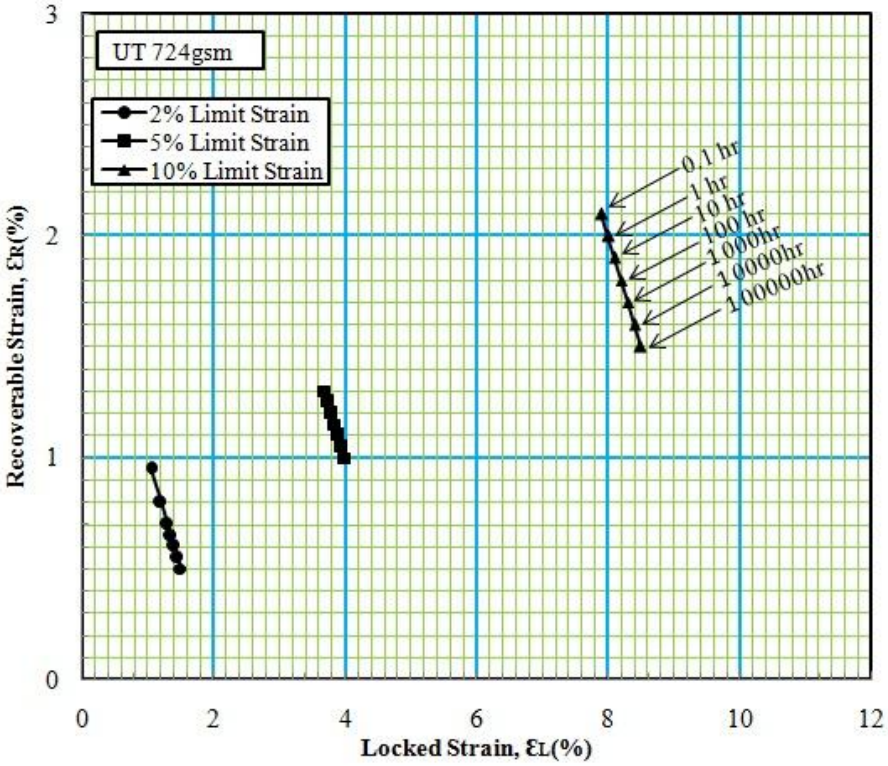

(b)

Fig. 4.20: Strain envelopes at different limit strain in machine direction for: a) untreated 627gsm, b) untreated 724gsm

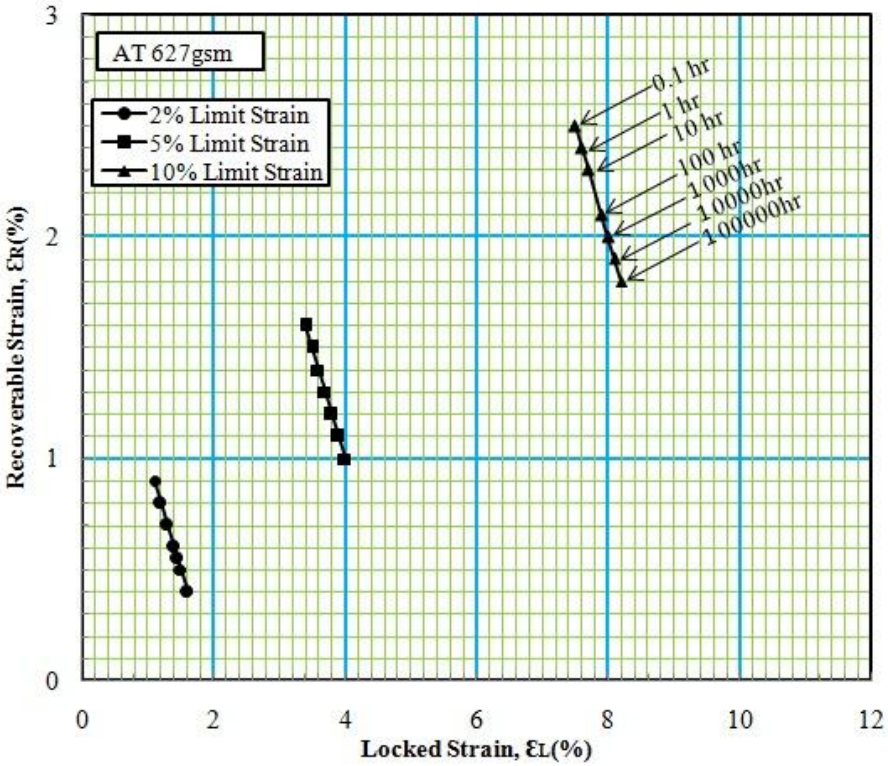

(a)

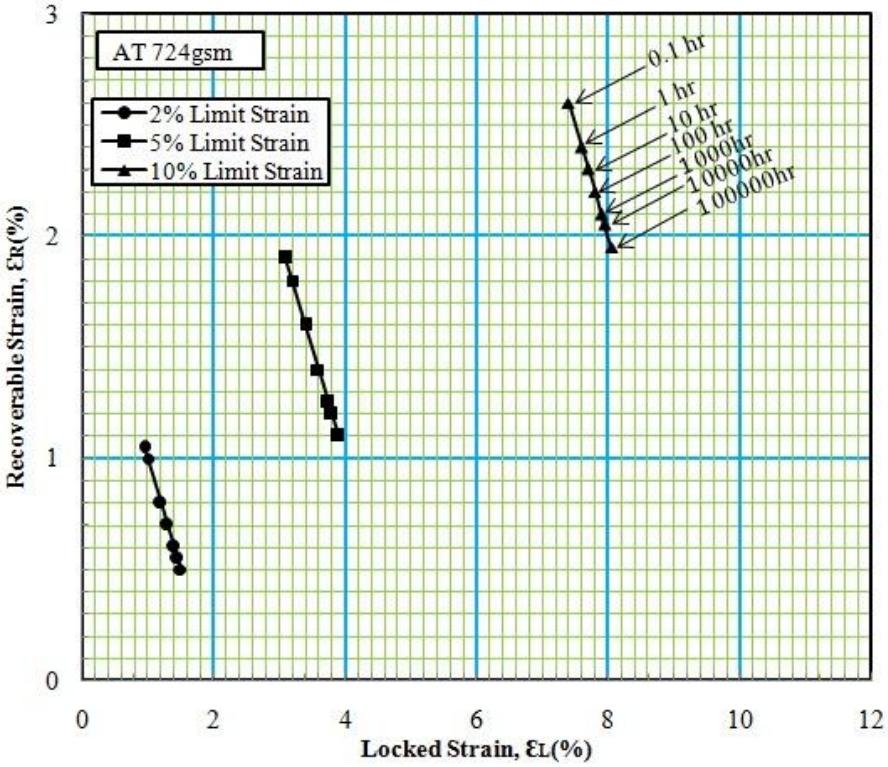

(b)

Fig. 4.21: Strain envelopes at different limit strain in machine direction for: a) additive treated 627gsm and b) additive treated 724gsm

CHAPTER FIVE

CONCLUSIONS AND RECOMMENDATIONS

5.1 General

The prime aim of this study was to analyze the creep behaviour of JGTs to evaluate the strain components: elastic strain (recoverable strain), ε_R and visco-plastic strain (locked strain), ε_L through isochronous curves and to develop strain envelop in isothermal condition. Four types of JGTs, untreated and additive treated of two different masses (627gsm and 724gsm) were selected for this study, which are commonly used in Bangladesh for different geotechnical purposes. Test results are summarized and discussed in Chapter Four and the findings of the test results are presented in this chapter.

5.2 Conclusions

From the analysis of test results, the following conclusions are drawn:

1) The isochronous curves of selected JGTs are developed in isothermal condition. The strain responses i.e., recoverable strain, locked strain and strain components at different limiting strain are developed through isochronous curves.

2) As discussed in Chapter Four, from isochronous curves of selected JGTs the possible design life for a particular load or the load carrying capacity at the End of Design Life (EDL) can be predicted for a limit strain in isothermal condition.

3) Interpretation of creep test result shows that elastic strain, ε_L is increases with the increase of loading time. On the other hand, recoverable strain, ε_R is decreases with the increase of loading time.

4) The results also indicate that when a particular strain developed within a shorter duration, it will develop comparatively larger value of ε_R and smaller value of ε_L. On the other hand, when relatively longer duration is taken to generate the same amount of strain, it will develop comparatively smaller value of ε_R and larger value of ε_L.

5) For a particular limit strain, the components, ε_R and ε_L at any stage of design life can be estimated from strain envelop.

6) The wide with test results reveal that the effect of strain rate is insignificant on the strength of JGTs in MD as well as in XMD. It means that the strain rate, 10±2%/min as specified in ASTM for synthetic geotextiles is not be a significant parameter for JGTs. Higher strain rate could be adopted for determining the tensile strength of JGTs.

5.3 Recommendations for Future Study

For the future researcher, the author is placing some recommendations which are as follows:

1) Similar strain envelopes (ε_R -ε_L) plots may be generated for other types of JGTs at isothermal conditions as in the present study.

2) The (ε_R -ε_L) strain envelopes from the creep test for JGTs in the present study may also be used to interpret the multi stage action (sustained plus cyclic loading) tests at isothermal conditions.

3) Strain rate sensitivity on the strength of other type of JGTs (treated by bitumen, latex and other common practices) need to be performed as in the present study for the standardization of JGT.

REFERENCES

AASHTO Standard Specifications for Highway Bridges, Division II, Section 7, Earth Retaining Systems (1997).

Abdullah, A. B. M., "A Hand Book on Synthetic Geotextiles Particularly Natural Synthetic Geotextiles from Jute and Other Vegetable Fibers," Bangladesh Jute Research Institute, Dhaka, pp. 33-87 (1999).

Andrawes, K. Z., McGown, A. and Kabir, M. H., "Uniaxial Strength Testing of Woven and Nonwoven Geotextiles," *Geotextiles and Geomembranes*, Vol. 1, pp. 41-56 (1984).

Andrawes, K. Z. and Yogarajah, I., "Effects of reinforcement connections on the behaviour of reinforced soil retaining walls," in *8th International. Conference of the Association for Computer Methods and Advances in Geomechanics*, pp. 1313-1318 (1994).

ASTM. Annual Book of ASTM Standard, Section 4, Vol. 04.13, Geosynthetics (2015).

BE3/78 *Reinforced earth retaining walls and bridge abutments for embankments.* Technical Memorandum, Department of Transport, UK (1987).

BS Code of Practice for Strengthened/Reinforced Soils and Other Fills. BSI (1995).

Collin, J. G., Chouery-curtis, V. E. and Berg, R. R., "Field observation of reinforced soil structures under seismic loading," in *Proc. International Symposium on Earth Reinforcement Practice*, Vol.1, pp.223-228 (1992).

Elias, V., Yuan, Z., Swan Jr., R. W. and Bachus, "Development of protocols for confined extension/creep testing of geosynthetics for highway applications," Publication No. FHWA-RD-97-143, U.S. Department of Transportation, USA (1998).

Fukuda, N., Yamanouchi, T., Sakai, N. and Shinatani, H, "Applicability of seismic design methods to geogrid reinforced embankment," in *Proc. 5th International Conference on Geotextiles, Geomembranes and Related Products*, Singapore, pp. 533-536 (1994).

Geoguide 1 *Guide to retaining wall design.* Geotechnical Engineering Office, Civil Engineering Department, Hong Kong (1993).

Geospec 2 *Model specification for reinforced fill structures.* Geotechnical Control Office, Civil Engineering Services Department, Hong Kong (1989).

Ghosh, S. K., Bhattacharyya, R., Mondal, M. M., " A Review on Jute Geotextile – Part 1," *International Journal of Research in Engineering and Technology,* Vol 3, Issue 2, pp.378-386 (2014).

Greenwood, J. H. and Jewell, R. A., "Strength and Safety: The Use of Mechanical Property Data. Reinforced Embankments: Theory and Practice in the British Isles," Thomas Telford, London, pp. 83-98 (1989).

HA 68/94 *Design methods for the reinforcement of highway slopes by reinforced soil and soil nailing*. Design Manual for Roads and Bridges, Vol. 4, Section 1, Part 4, HMSO (1997).

Haliburton, T. A., Fowler, J. and Langman, J. P. (1980) *Design and Construction of a Fabric Reinforced Test Section at Pinto Pass*, Mobile, Alabama‖, Trans Res. Record#79, Washington D.C.

Islam, M. S., Khan, A. J., Siddique, A., Saleh, A. M. and Nasrin, S., "Control of erosion of hill slope top soil using geo jute and vegetation," in *National Seminar on Jute Geotextiles*, Dhaka, pp. 27-34 (2014).

Islam, M. S., *Use of Vegetation and Geo-Jute for Slope Protection*, M.Sc. Engg. Thesis, Department of Civil Engineering, Bangladesh University of Engineering and Technology, 2013.

Islam, M. W., *Experimental Investigation of Prefabricated Vertical Jute Drain in Soft Soil*, M.Sc. Engg. Thesis, Department of Civil Engineering, Bangladesh University of Engineering and Technology, 2008.

Islam, S. S., *Laboratory Assessment of Soil-Jute Geotextile Interaction Behaviour*, M.Sc. Engg. Thesis, Department of Civil Engineering, Bangladesh University of Engineering and Technology, 2008.

Jewell, R. A., "Soil Reinforcement with Geotextiles," Special Publication 123, CIRIA, London, UK (1996).

Jewell, R. A., *Some Effects of Reinforcement on the Mechanical Behaviour of Soils*, Ph.D. Thesis, University of Cambridge, UK, 1980.

Jewell, R. A. and Greenwood, V. H., "Long Term Strength and Safety in Steep Soil Slopes Reinforced by Polymer Mat," *Geotextiles and geomembranes*, Vol. 7, pp. 81-118 (1988).

Jewell, R. A., Paine, N. and Woods, R. I., "Design method for steep reinforced slopes and embankments," in *Symposium of Polymer Grid Reinforcement in Civil Engineering*, London, UK, pp.70-81 (1984).

JMDC *A Manual on Use of Jute Geotextiles in Civil Engineering.* Ministry of Textiles, GoI (2008).

Jones, C. J. F. P., "Discussions: slopes and excavations," in *Proc. of International Symposium on Earth Reinforcement Practice*, Fukuoka/ Kyushu, Japan, 11-13 Nov.1992, Ochiai, Hayashi & Otani (eds), Balkema, pp.972-975 (1993).

Jones, C. J. F. P., “Earth Reinforcement and Soil Structures,” Thomas Telford Publishing, Thomas Telford Services Ltd., London, UK (1996).

Jones, C. J. F. P., Fakher, A., Hamir, R. and Nettleton, I.M., “Geosynthetic materials with improved reinforcement capabilities,” in *Proc. International Symposium on Earth Reinforcement*, Fukuoka, Japan, Vol.2, 12-14 Nov. 1996, pp. 865 – 883 (1996).

Jones, C. J. F. P., McGown, A. and Varney, D. J., “Construction Methods, Economics and Specifications,” *The Application of Polymeric Reinforced Soil Retaining Structure*, NATO ASI Series, Series E, Applied Sciences, Vol. 147, pp. 573-611(1988).

Kabir, M. H., *In-isolation and In-soil Behaviour of Geotextiles*, Ph.D. Thesis, University of Strathclyde, Glasgow, UK, 1984.

Kabir, R., *Effectiveness of Jute Geotextile Filter for River Bank Protection*, M.Sc. Engg. Thesis, Department of Civil Engineering, Bangladesh University of Engineering and Technology, 2015.

Khan, A. J., *A Reassessment of the Design of Geosynthetic Reinforced Soil Structures*, Ph. D. Thesis, University of Strathclyde, Glasgow, UK, 1999.

Khan, A. J., “Efficacy of jute geotextiles for hill slope erosion control, rural road construction and river bank protection,” in *6th Asian Regional Conference on Geosynthetics - Geosynthetics for Infrastructure Development*, New Delhi, India, pp. 689-695 (8-11 November, 2016).

Khan, A. J., “Quality control of jute geotextiles and development of testing facilities,” Presented in International Workshop on Jute Geotextiles Technical Potential and Commercial Prospects, Dhaka, Bangladesh (2008).

Khan, A. J., Huq, F. and Hossain, S. Z., “Application of Jute Geotextiles for Rural Road Pavement Construction,” ASCE, *Ground Improvement and Geosynthetics, Geotechnical Special Publications (GSP) 238*, pp. 370-379 (2014).

Khan, A. J., Islam, M. S. and Islam, S. S., “Laboratory Assessment of Soil-Jute Geotextile Interaction Behavior,” *Electronic Journal of Geotechnical Engineering*, Vol. 19, Issue. 16, pp. 3949-3962 (2014).

Khan, A. J., Islam, M. S., Siddique, A., Kabir, R., and Nasrin, S., “Performance evaluation of river bank protection jute geo-textiles,” in *National Seminar on the Project: Development and Application of Potentially Important Jute Geo-textiles*, JDPC, Dhaka, (2014).

Khan, A. J, Rahman, M. M., “Road subgrade reinforcement using jute geotextiles”, in *Proc. of Bangladesh Geotechnical Conference*, BUET, Dhaka, pp. 196-206 (2009).

Koerner, R. M. (1998) *Designing with Geosynthetics*. Fourth Edition, Prentice Hall Inc., New Jersey.

Kupec, J., *Combined Sustained and Short Term Load Testing of Geosynthetics*, M.Sc. Thesis, University of Strathclyde, Glasgow, UK, 2000.

Lee, K. L., "Mechanism, analysis and design of reinforced earth walls," in *ASCE Symposium on Earth Reinforcement* Pittsburgh, Pennsylvania, pp. 62-76 (1978).,

Mahaseth, B., *Isothermal Response of Geosynthetics to Different Loading Regimes*, M.Sc. Engg. Thesis, Department of Civil Engineering, Bangladesh University of Engineering and Technology, 2002.

McGown, A., Andrawes, K. Z., Paul, J. and Austin, R. A., "Limit State Design of Reinforced Soil Walls Slopes and Embankments," *Danish geotechnical society, ISLSD93*, Vol.1/3, pp. 275-284 (1993).

McGown, A., Andrawes, K. Z., Pradhan, S. and Khan, A. J., "Limit state design of geosynthetic reinforced soil structures," Keynote lecture in *6th International Conference on Geosynthetics*, Atlanta, Georgia, USA, Vol.1, 25-29 Mar. 1998, pp.143-179 (1998).

McGown, A., Khan, A. J. and Kupec, J., "Determining the Design Parameters for Geosynthetic Reinforcements Subject to Single-Stage Actions Using the Isochronous Strain Energy Approach," *Geosynthetics International*, Vol. 11, Issue 5, pp. 355–368 (2004).

Mohy, M. A, *Evaluation of Properties of Jute Geotextile and its Assessment for Short Term and Long Term Civil Engineering Applications*, M.Sc. Engg. Thesis, Department of Civil Engineering, Bangladesh University of Engineering and Technology, 2005.

NCMA *Segmental retaining wall seismic design procedure*. Final Draft (1997).

Pradhan, S., *The Design of Synthetic Polymeric Reinforced Soil Structures: A Limit State Design Approach*, Ph.D. Thesis, University of Strathclyde, Glasgow, UK, 1996.

Prodhan, Z. H., "Application of jute geotextile for different structures including rural roads with slope protection," Presented in International Workshop on Jute Geotextiles Technical Potential and Commercial Prospects, Dhaka, Bangladesh (2008).

Rahman, M. M., *Use of Jute Geotextiles in Road Construction*, M.Sc. Engg. Thesis, Department of Civil Engineering, Bangladesh University of Engineering and Technology, 2009.

Tatsuoka, F., "Roles of facing rigidity in soil reinforcing," Keynote lecture in *Proc. of International Symposium on Earth Reinforcement Practice*, Fukuoka/Kyushu/Japan/11-13 Nov.1992, Ochiai, Hayashi & Otani (eds), Balkema, 1993, pp. 831-870 (1993).

Tatsuoka, F., Koseri, J., Tateyama, M., "Performance of Reinforced Soil Structures During the 1995 Hyogo-ken Nanbu Earthquake," Earth Reinforcement, Ochiai, Yasufuku & Omine (eds), Balkema, Rotterdam, pp. 973-1008 (1995).

Troost, G. H. and Ploeg, N. A., "Influence of weaving structure and coating on the degree of mechanical damage of reinforcing mats and woven geogrids caused by different

fills during installation," in *4th International Conference on Geotextiles, Geomembranes and Related products*, Hague, Nederlands, Vol.3, pp. 609 –614 (1990).

Voskamp, W. and Risseeuw, P., "Method to Establish the Maximum Allowable Load Under Working Conditions of Polyester Reinforcing Fabrics," *Geotextiles and geomembranes*, Vol. 6, pp. 173-184 (1987).

White, D. M., Holtz, R. D., "Performance of Geosynthetic-reinforced Slopes and Walls During Northridge, California Earthquake of January 17, 1997," Earth Reinforcement, Ochiai, Yasufuku & Omine (eds), Balkema, Rotterdam, pp. 965-972 (1997).

www. jutegeotech.com, 10.09.2016, 10:30pm.

Yeo, K. C., *The Behaviour of Polymeric Grids Used for Soil Reinforcement*, Ph.D. Thesis, University of Strathclyde, Glasgow, UK, 1985.

Yogarajah, I., *Effects of Construction Procedures on the Behaviour of Geogrid Reinforced soil Walls*, Ph.D. thesis, University of Strathclyde, Glasgow, UK, 1993.

Appendix A

Table 1: Mass per unit area of untreated and additive treated JGTs.

Type of JGT	Specimen No.	Mass of specimen (gm)	Length of specimen (m)	Width of specimen (m)	Mass per unit area (gsm)	Average mass per unit area (gsm)
UT 627gsm	1	51	0.3	0.3	567	**611.2**
	2	55	0.3	0.3	611	
	3	53	0.3	0.3	589	
	4	60	0.3	0.3	667	
	5	56	0.3	0.3	622	
UT 724gsm	1	70	0.3	0.3	777.78	**742.224**
	2	68	0.3	0.3	755.56	
	3	73	0.3	0.3	811.11	
	4	63	0.3	0.3	700	
	5	60	0.3	0.3	666.67	
AT 627gsm	1	80	0.3	0.3	888.89	**828.89**
	2	77	0.3	0.3	855.56	
	3	70	0.3	0.3	777.78	
	4	72	0.3	0.3	800	
	5	74	0.3	0.3	822.22	
AT 724gsm	1	95	0.3	0.3	1055.56	**1020**
	2	88	0.3	0.3	977.78	
	3	92	0.3	0.3	1022.22	
	4	99	0.3	0.3	1100	
	5	85	0.3	0.3	944.44	

Table 2: Thickness of untreated and additive treated JGTs.

Type of JGT	Specimen No.	Initial reading of dial gauge (0.01mm)	Final reading of dial gauge (0.01mm)	Thickness of specimen= (Final reading - Initial reading)x0.01	Average thickness (mm)
UT 627gsm	1	165	340	1.75	1.76
	2	165	351	1.86	
	3	165	345	1.8	
	4	165	336	1.71	
	5	165	337	1.72	
	6	165	342	1.77	
	7	165	335	1.7	
	8	165	340	1.75	
	9	165	336	1.71	
	10	165	348	1.83	
UT 724gsm	1	165	360	1.95	1.93
	2	165	354	1.89	
	3	165	365	2	
	4	165	352	1.87	
	5	165	359	1.94	
	6	165	355	1.9	
	7	165	361	1.96	
	8	165	368	2.03	
	9	165	356	1.91	
	10	165	350	1.85	
AT 627gsm	1	173	390	2.17	2.196
	2	173	398	2.25	
	3	173	388	2.15	
	4	173	392	2.19	
	5	173	397	2.24	
	6	173	381	2.08	
	7	173	400	2.27	
	8	173	391	2.18	
	9	173	396	2.23	
	10	173	393	2.2	
AT 724gsm	1	173	435	2.62	2.665
	2	173	443	2.7	
	3	173	425	2.52	
	4	173	440	2.67	
	5	173	445	2.72	
	6	173	430	2.57	
	7	173	450	2.77	
	8	173	440	2.67	
	9	173	434	2.61	
	10	173	453	2.8	

Table 4.3: Wide Width test Results for JGTs (UT 627gsm and UT 724 gsm) at constant temperature, 20°±2 and different strain rate in MD and XMD.

Sample type	Strain rate	Wide width tensile strength (kN/m)				Average ultimate strength, Pu (kN/m)		Strain at breaking point (%)				Average strain at breaking point, ε_u (%)	
		MD		XMD				MD		XMD			
		Strength (kN/m)	Average **strength (kN/m)**	**Strength (kN/m)**	Average **strength (kN/m)**	**MD**	**XMD**	Strain (%)	Average strain (%)	Strain (%)	Average strain (%)	**MD**	**XMD**
UT 627gsm	**(10±2) mm/min**	22.6	24.7	10.8	10.1	**24.2**	**10.4**	12	12.2	10	10.2	**11.7**	**9.8**
		25.5		9.3				13		11.5			
		26		10.3				11.5		9			
	(50±5) mm/min	23.5	24	8.8	10.5			12	11.3	9.5	9.5		
		24.5		11.8				11.5		10.5			
		24		10.8				10.5		8.5			
	(100±10) mm/min	25	23.9	10.8	10.6			12	11.7	9.5	9.7		
		23		11.3				11		10			
		23.5		9.8				12		9.5			
UT 724gsm	**(10±2) mm/min**	28.5	28	13.2	12.1	**27.4**	**12.5**	13	13.2	10.5	11.3	**12.5**	**11**
		27.5		11.8				14		11.5			
		28		11.3				12.5		12			
	(50±5) mm/min	28.5	27.6	12.3	13.2			12	12.8	12	11		
		27		14.2				13.5		10			
		27.5		13.2				13		11			
	(100±10) mm/min	26.5	26.7	10.3	12.3			11.5	11.5	13.5	10.8		
		27.5		12.8				11		10			
		26		13.7				12		9			

Table 4.4: Wide Width test Results for JGTs (AT 627gsm and UT 724 gsm) at constant temperature, 20°±2 and different strain rate in MD and XMD.

Sample type	Strain rate	Wide width tensile strength (kN/m)				Average ultimate strength, Pu (kN/m)		Strain at breaking point (%)				Average strain at breaking point, ε_u (%)	
		MD		XMD				MD		XMD			
		Strength (kN/m)	Average strength (kN/m)	Strength (kN/m)	Average strength (kN/m)	MD	XMD	Strain (%)	Average strain (%)	Strain (%)	Average strain (%)	MD	XMD
AT 627gsm	(10±2) mm/min	24	22.7	9.8	9.3	23.3	9.6	13	12.7	12	12	12.3	11
		21		9.3				13		13.5			
		23		8.8				12		10.5			
	(50±5) mm/min	24	23.5	9.3	9.6			12.5	12	10.5	10.7		
		23		8.8				12		12			
		23.5		10.8				11.5		9.5			
	(100±10) mm/min	24	23.7	8.3	9.8			12.5	12.3	11	10.2		
		24.5		11.3				13		9.5			
		22.6		9.8				11.5		10			
AT 724gsm	(10±2) mm/min	26	25	10.8	12.1	25.1	11.1	14	10.6	11	12	12.2	11.8
		25		9.8				14		12.5			
		24		11.3				12.5		12.5			
	(50±5) mm/min	26	24.9	9.8	10.8			12.5	12.2	10	10.8		
		23.5		11.8				11		11			
		25		10.8				13		11.5			
	(100±10) mm/min	26.5	25.5	11.8	10.5			14	13.7	13.5	12.7		
		24.5		10.3				13.5		13.5			
		25.5		9.3				13.5		11			

Appendix B

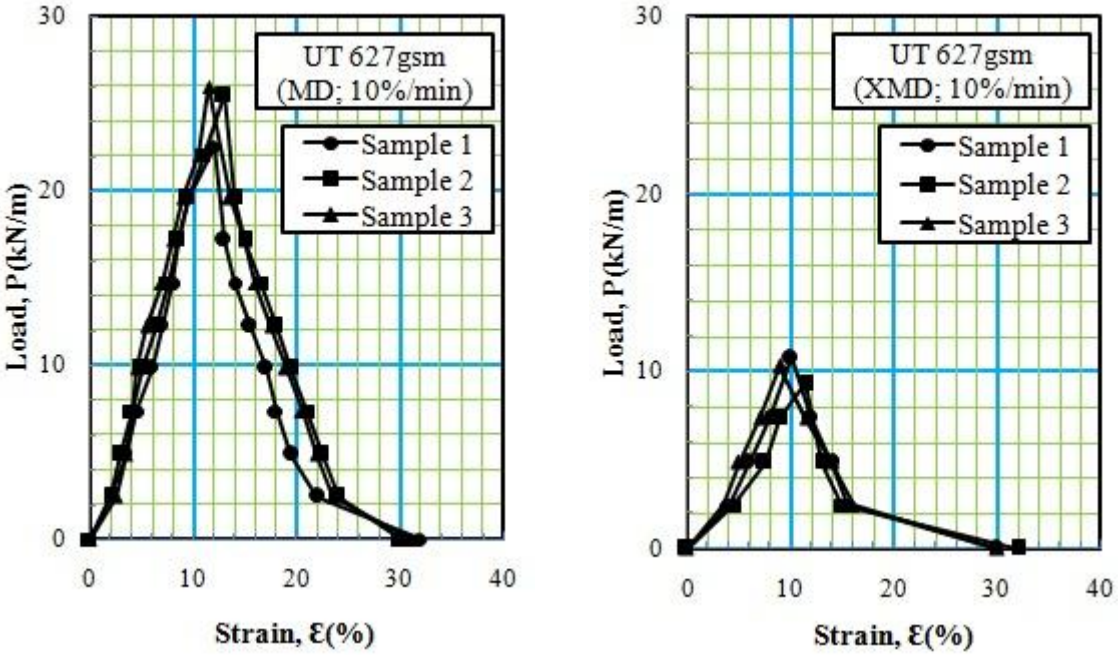

(a) (b)

Fig. 1: Wide-width test result of untreated 627gsm at the strain rate of (10±3)%/min: (a) machine direction and (b) cross machine direction

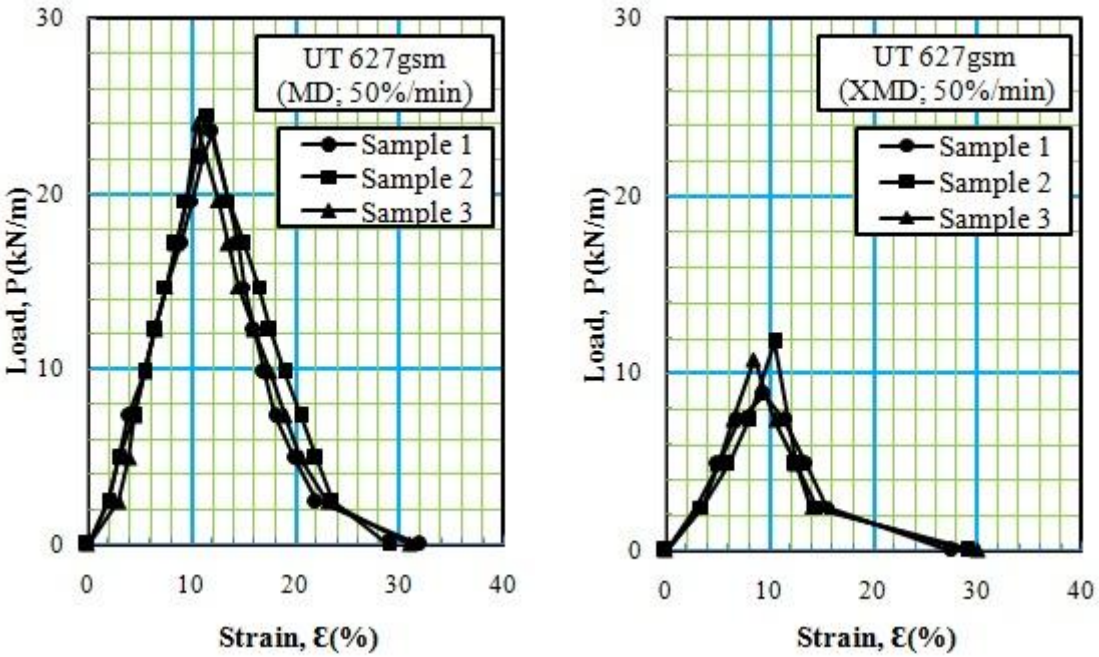

(a) (b)

Fig. 2: Wide-width test result of untreated 627gsm at the strain rate of (50±5)%/min: (a) machine direction and (b)cross machine direction

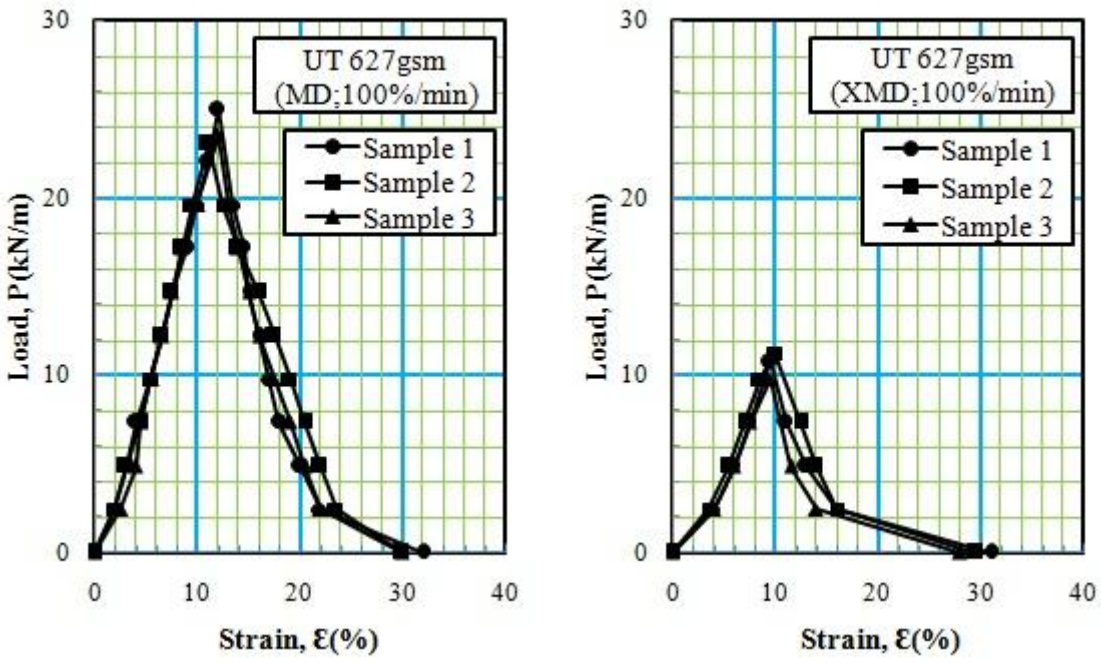

(a) (b)

Fig. 3: Wide-width test result of untreated 627gsm at the strain rate of (100±10)%/min: (a) machine direction and (b) cross machine direction

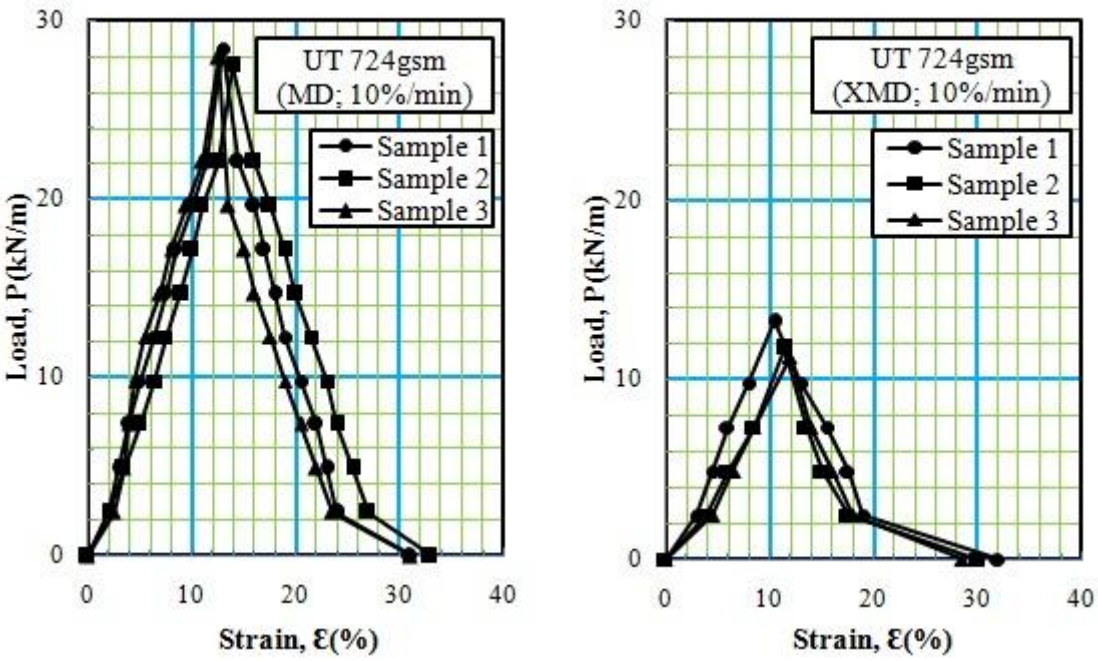

(a) (b)

Fig. 4: Wide-width test result of untreated 724gsm at the strain rate of (10±3)%/min: (a) machine direction and (b) cross machine direction

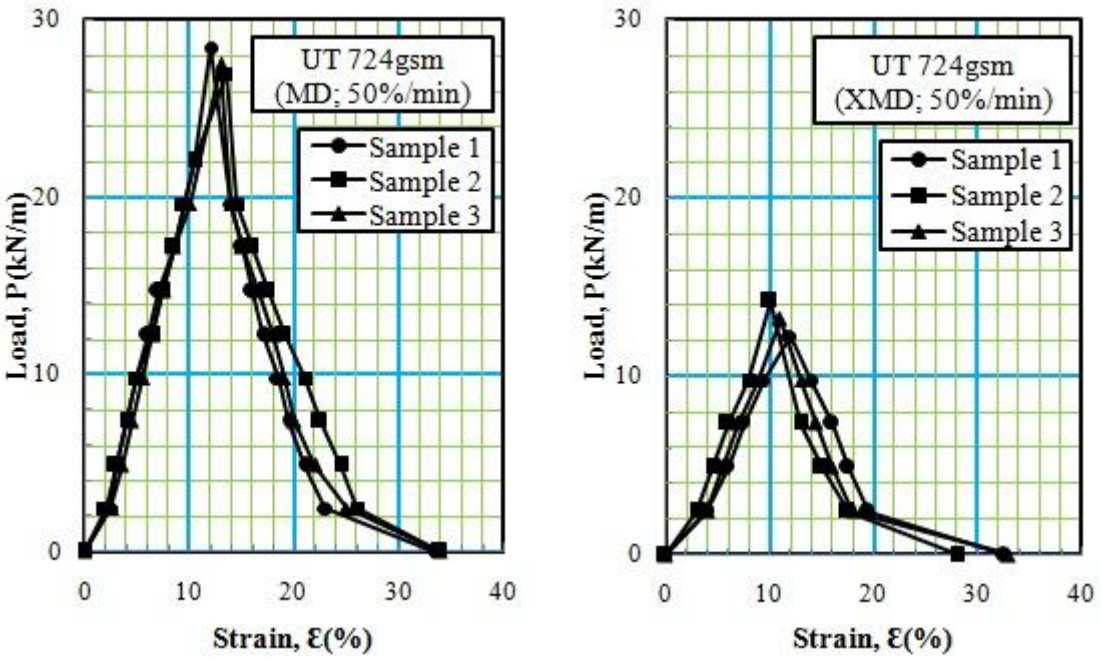

(a) (b)

Fig. 5: Wide-width test result of untreated 724gsm at the strain rate of (50±5)%/min: (a) machine direction and (b) cross machine direction

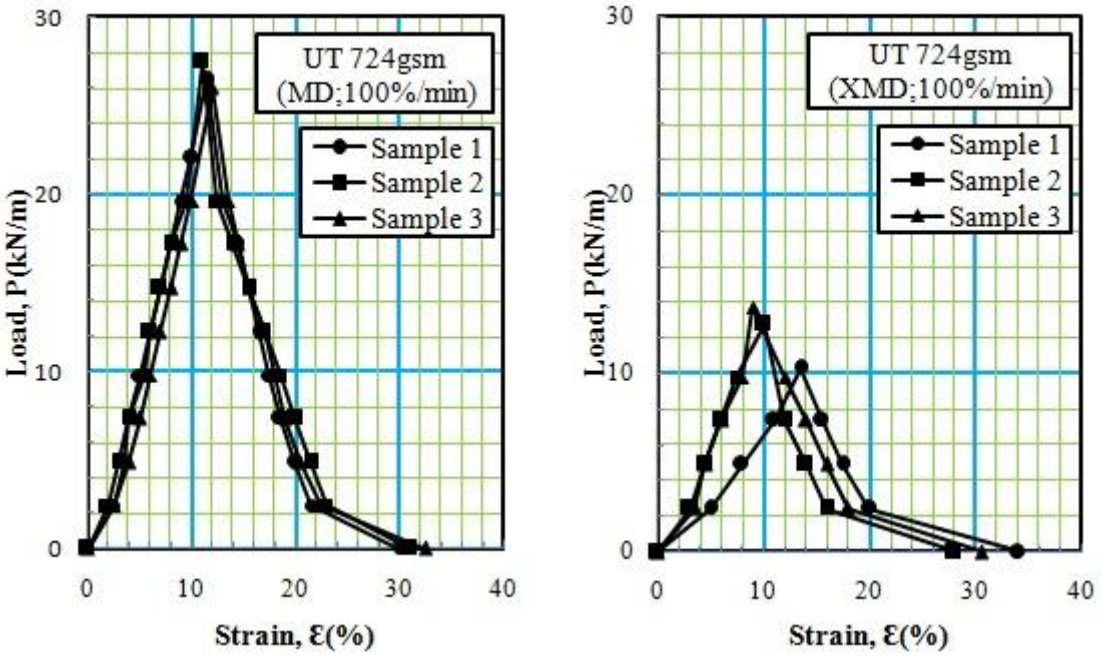

(a) (b)

Fig. 6: Wide-width test result of untreated 724gsm at the strain rate of (100±10)%/min: (a) machine direction and (b) cross machine direction

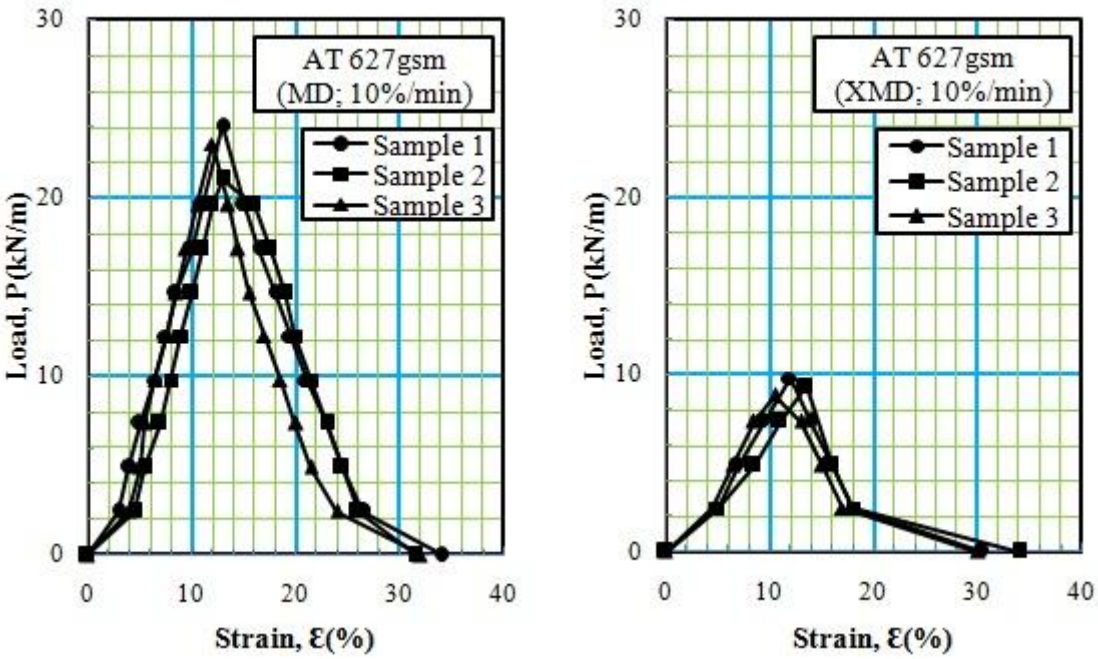

(a) (b)

Fig. 7: Wide-width test result of additive treated 627gsm at the strain rate of (10±3)%/min: (a) machine direction and (b) cross machine direction

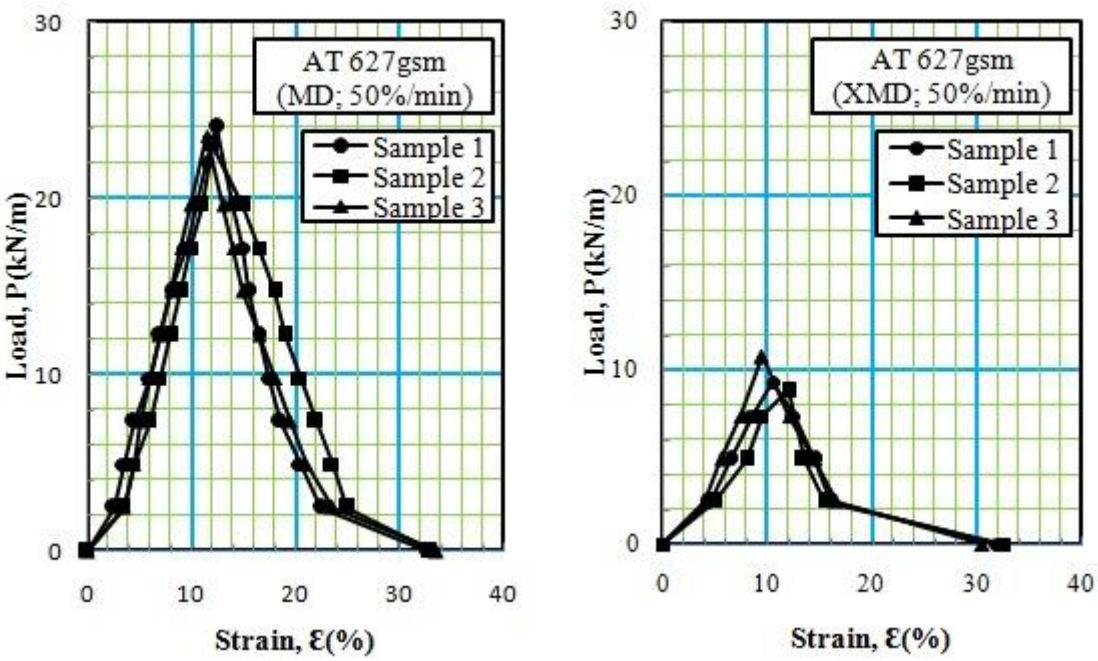

(a) (b)

Fig. 8: Wide-width test result of additive treated 627gsm at the strain rate of (50±5)%/min: (a) machine direction and (b) cross machine direction

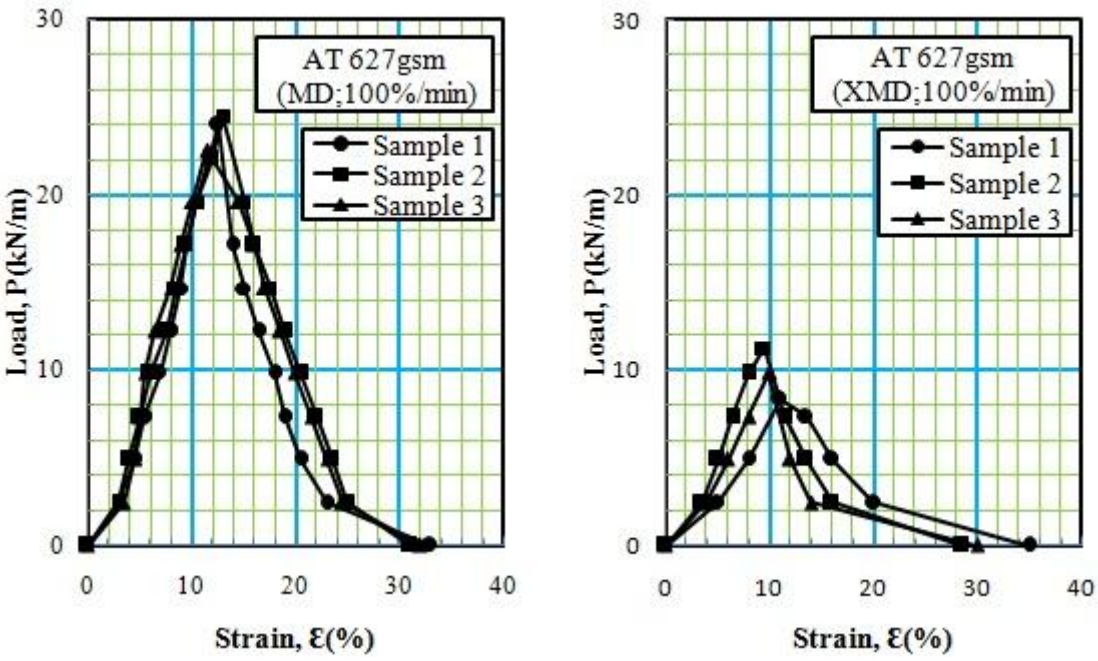

(a) (b)

Fig. 9: Wide-width test result of additive treated 627gsm at the strain rate of (100±10)%/min: (a) machine direction and (b) cross machine direction

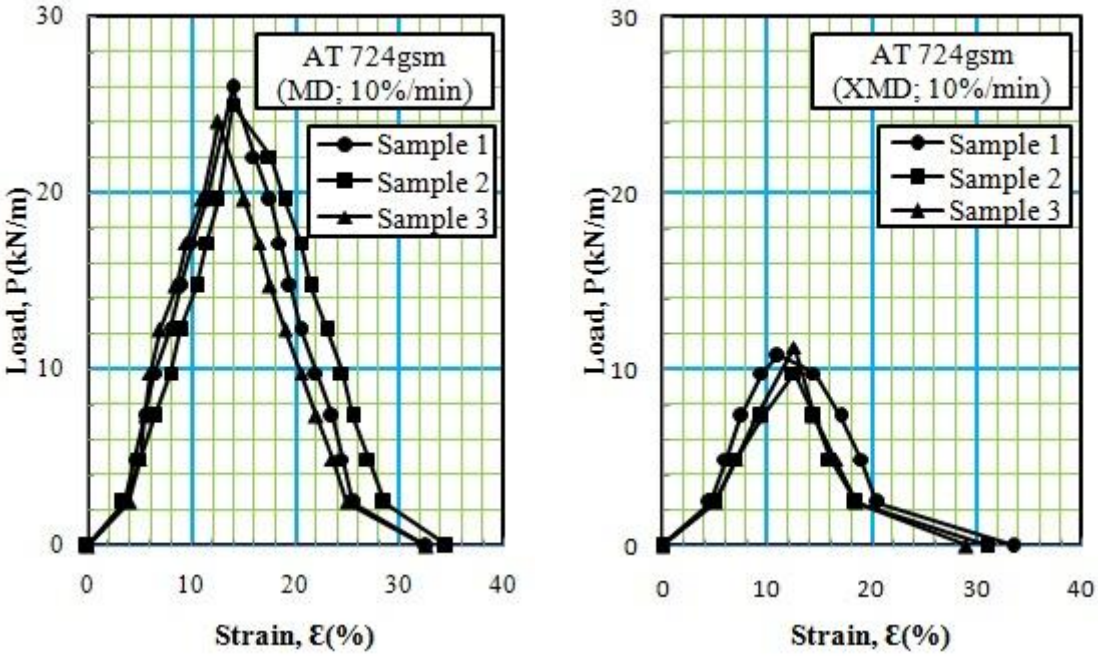

(a) (b)

Fig. 10: Wide-width test result of additive treated 724gsm at the strain rate of (10±3)%/min: (a) machine direction and (b) cross machine direction

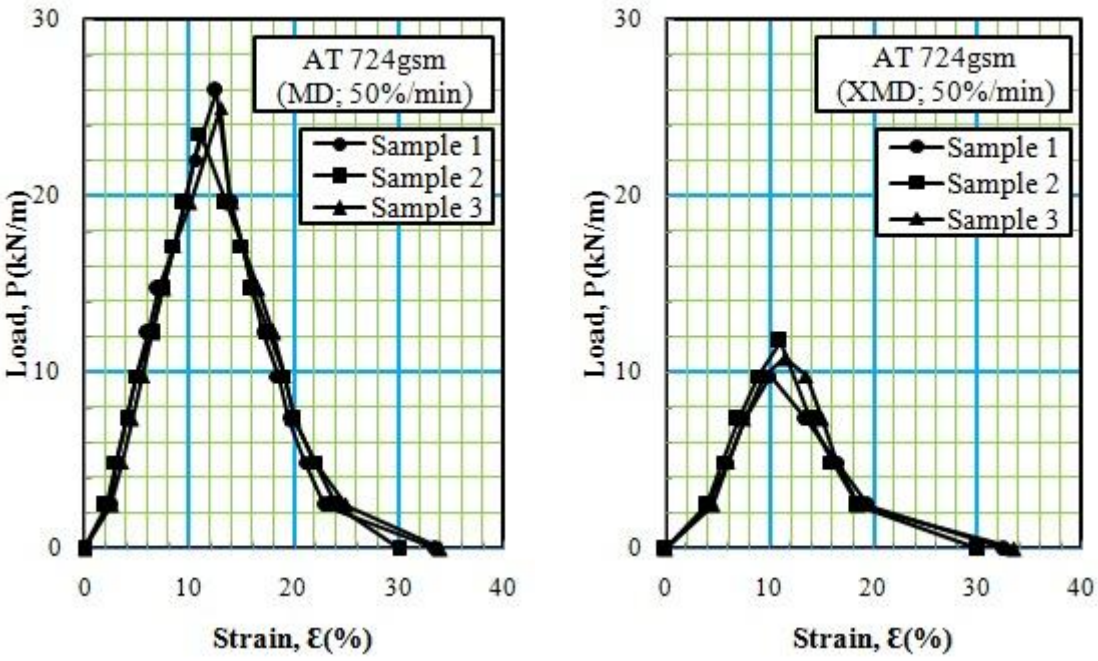

(a) (b)

Fig. 11: Wide-width test result of additive treated 724gsm at the strain rate of (50±5)%/min: (a) machine direction and (b) cross machine direction

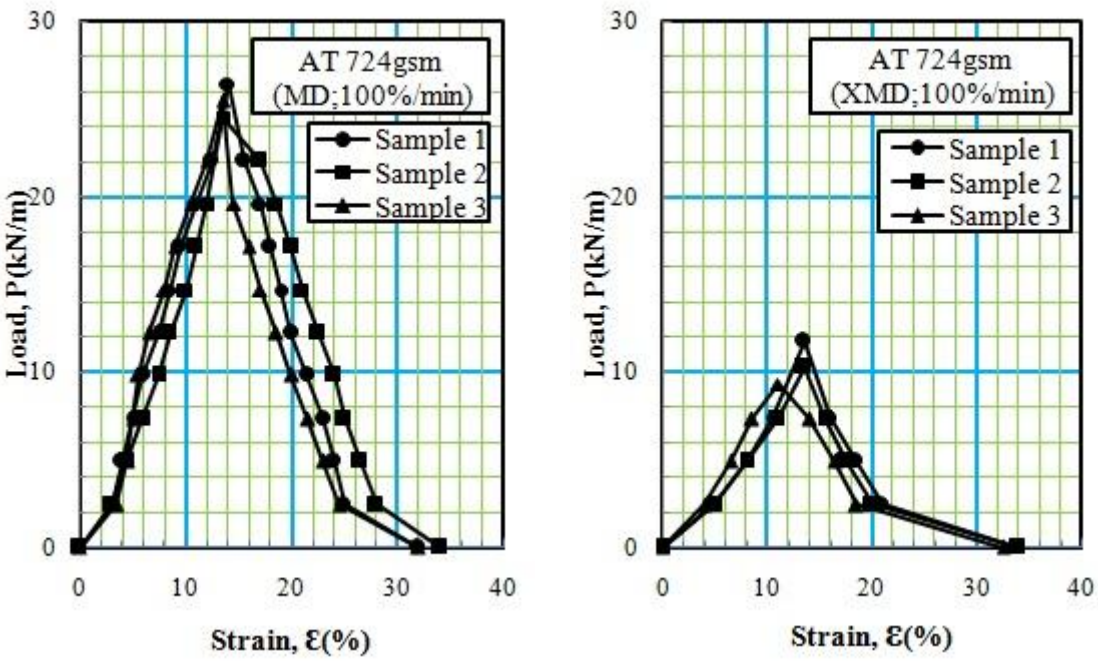

(a) (b)

Fig. 12: Wide-width test result of additive treated 724gsm at the strain rate of (100±10)%/min: (a) machine direction and (b) cross machine direction

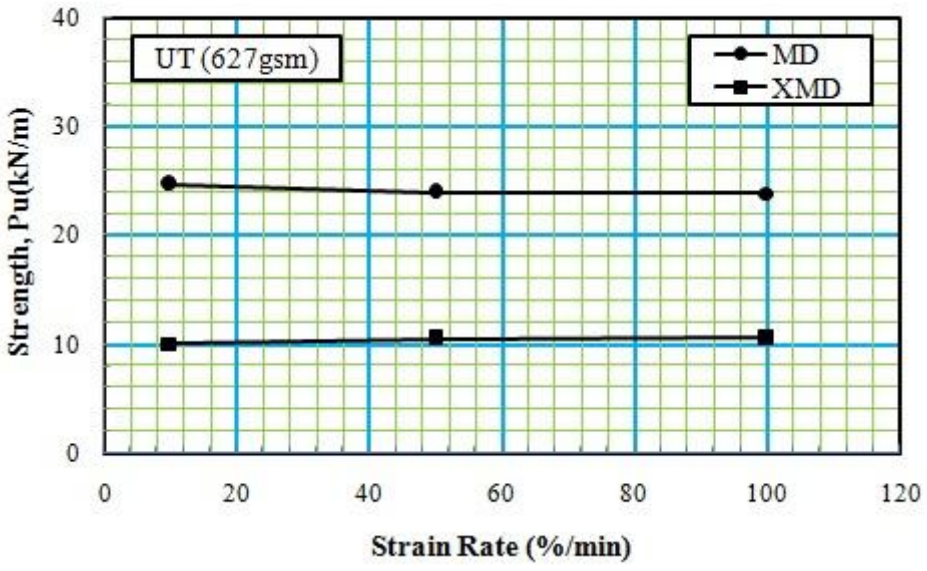

(a)

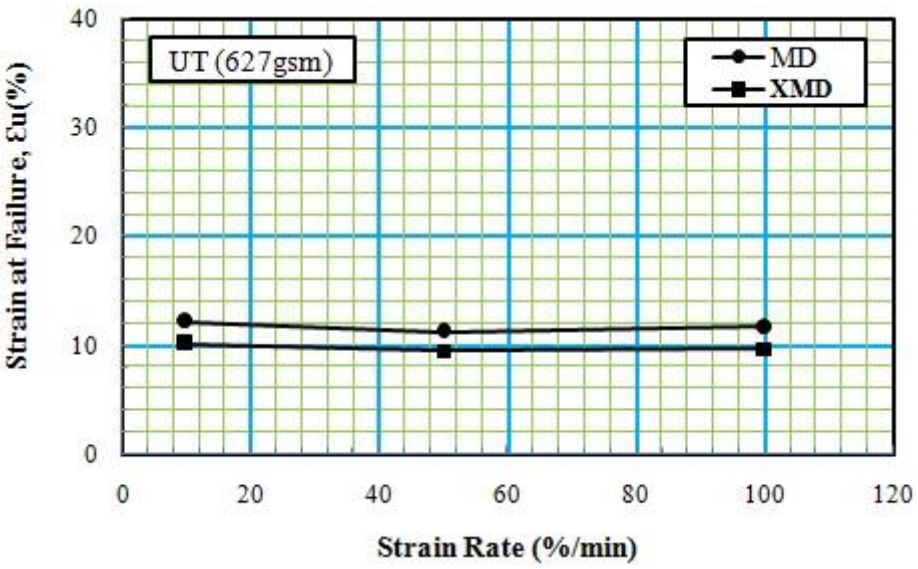

(b)

Fig. 13: Effect of different strain rate on wide-width test result of untreated 627gsm: (a) variation of strength and (b) variation of strain

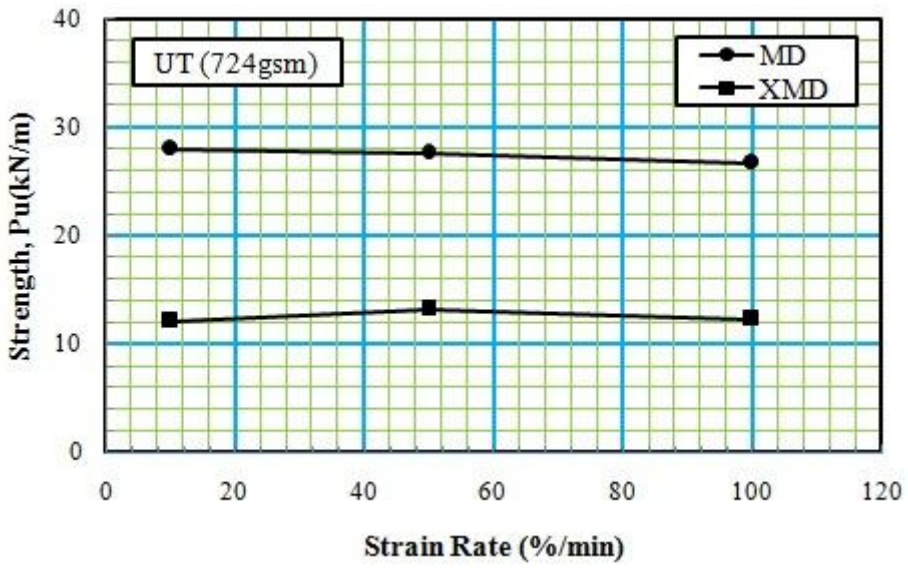

(a)

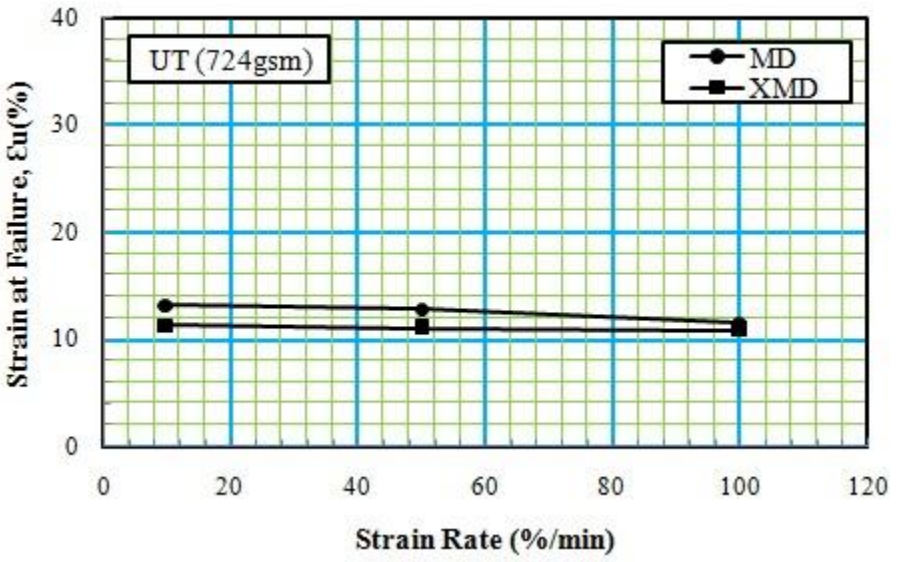

(b)

Fig. 14: Effect of different strain rate on wide-width test result of untreated 724gsm: (a) variation of strength and (b) variation of strain

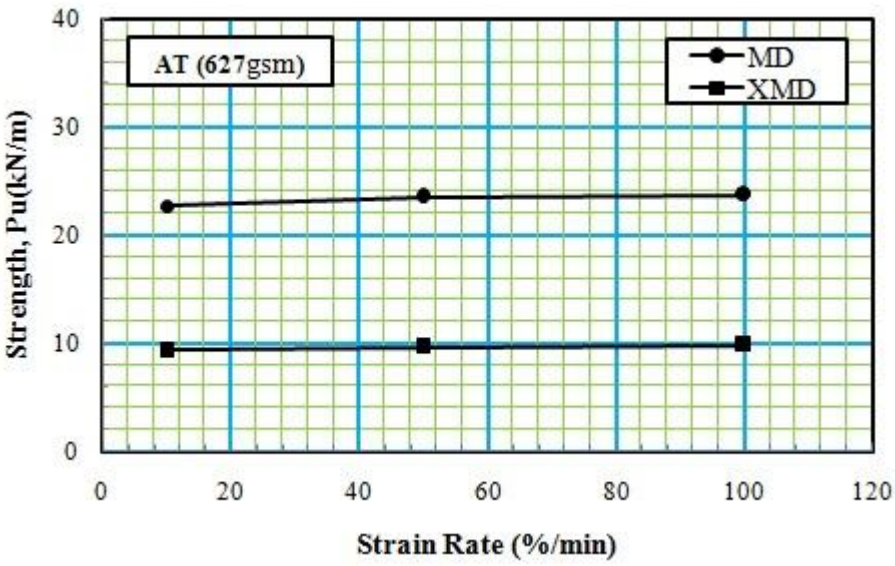

(a)

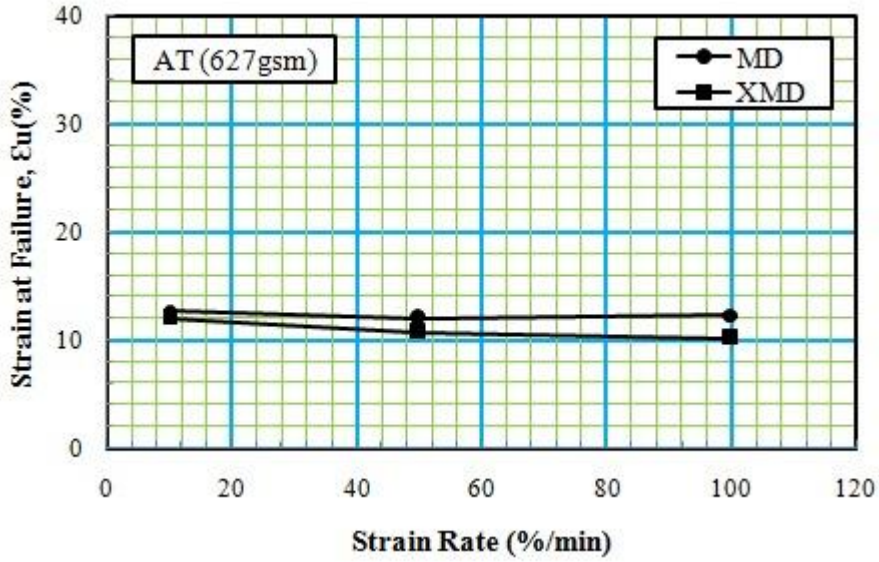

(b)

Fig. 15: Effect of different strain rate on wide-width test result of additive treated 627gsm: (a) variation of strength and (b) variation of strain

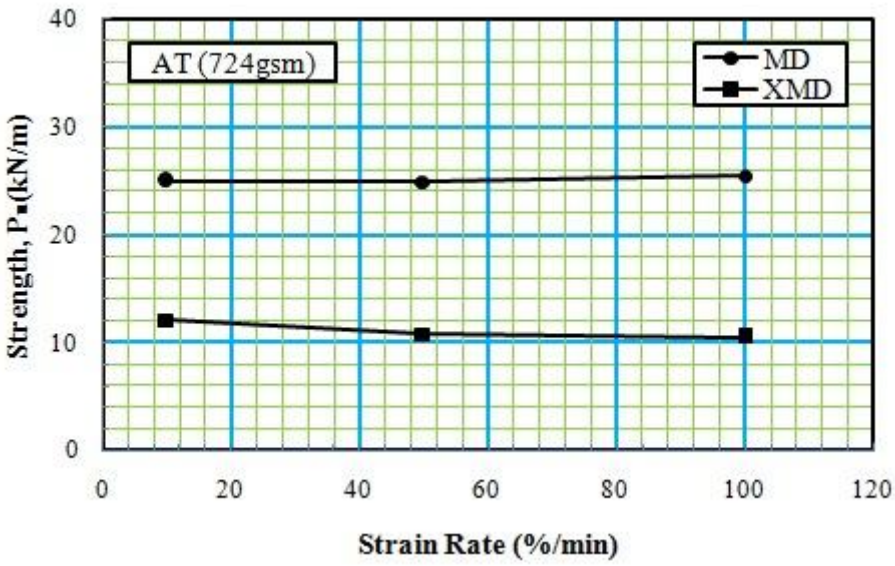

(a)

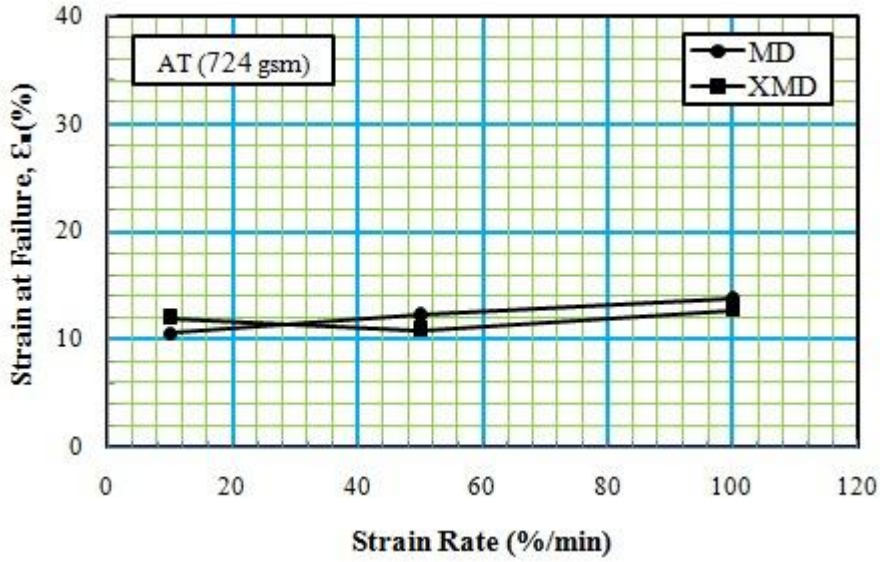

(b)

Fig. 16: Effect of different strain rate on wide-width test result of additive treated 724gsm: (a) variation of strength and (b) variation of strain

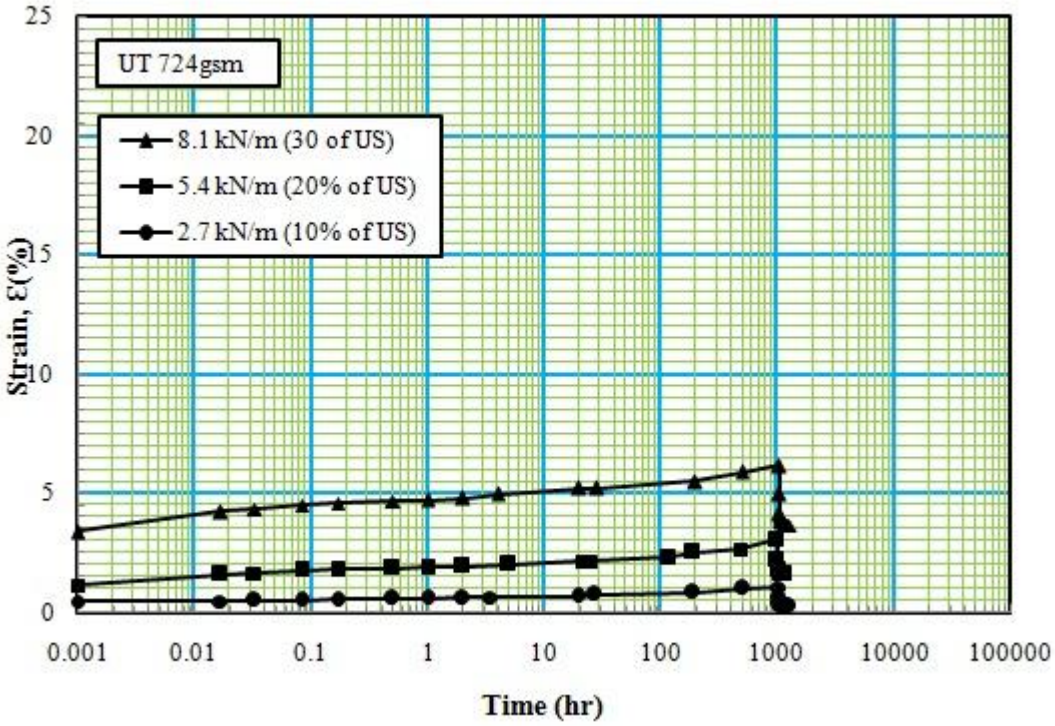
UT 724gsm
8.1 kN/m (30 of US)
5.4 kN/m (20% of US)
2.7 kN/m (10% of US)
Strain, ε(%)
Time (hr)
0
5
10
15
20
25
0.001
0.01
0.1
1
10
100
1000
10000
100000

(a)

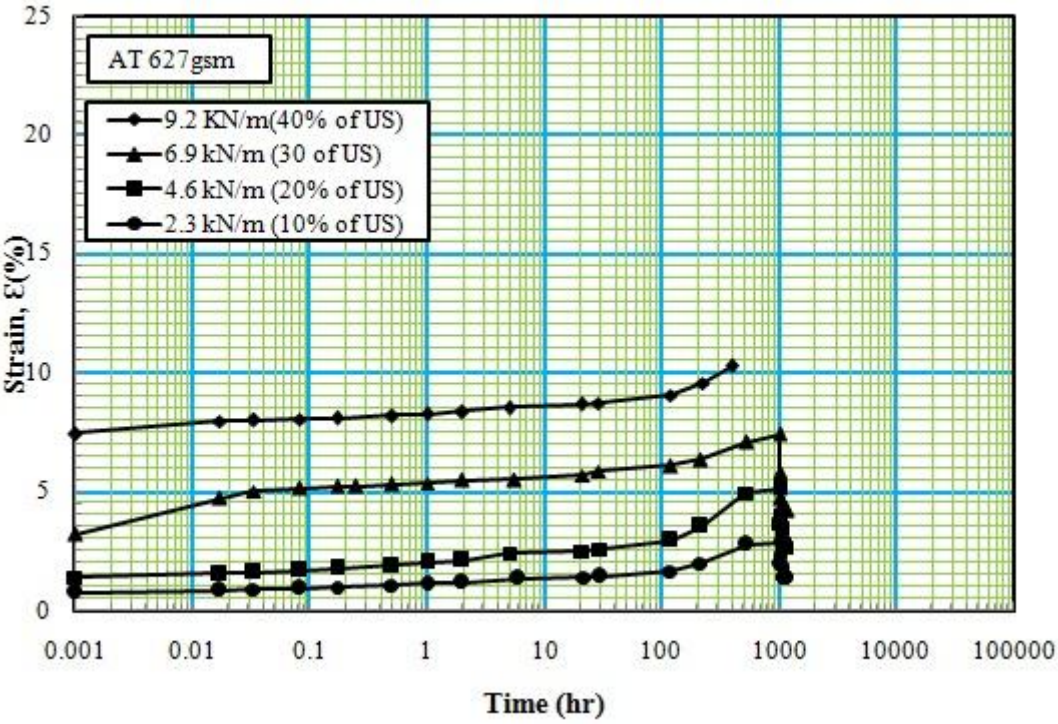
AT 627gsm
9.2 KN/m(40% of US)
6.9 kN/m (30 of US)
4.6 kN/m (20% of US)
2.3 kN/m (10% of US)
Strain, ε(%)
Time (hr)
0
5
10
15
20
25
0.001
0.01
0.1
1
10
100
1000
10000
100000

(b)

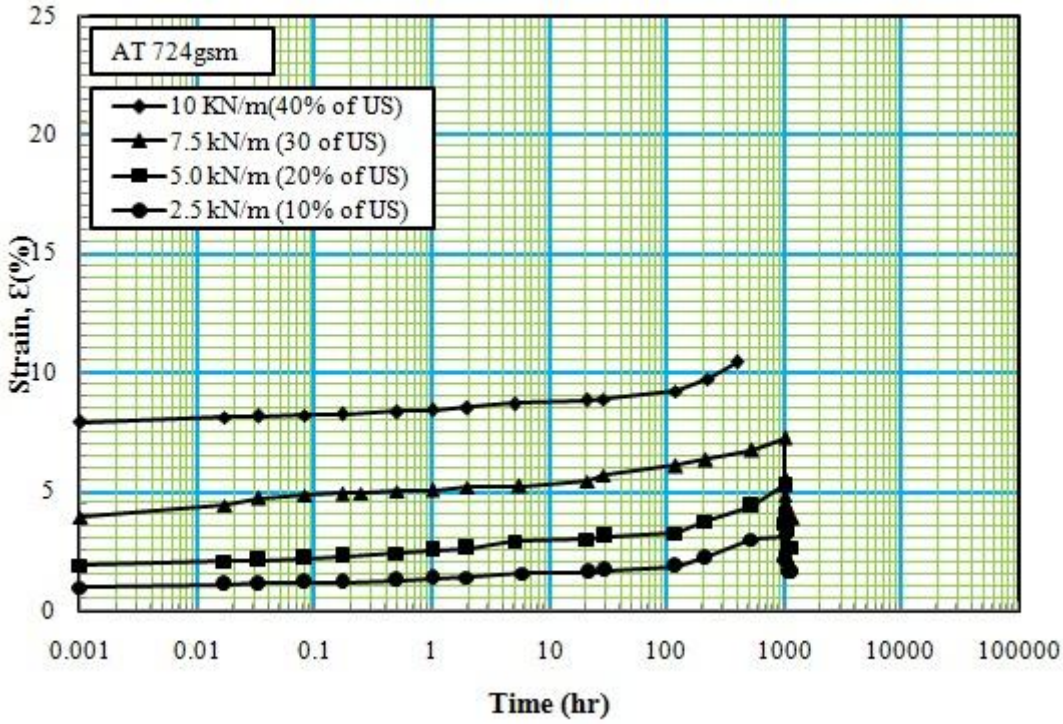

(c)

Fig. 17: Total strain vs log time (hr) in machine direction: (a) untreated 724gsm, (b) additive treated 627gsm and (c) additive treated 724gsm

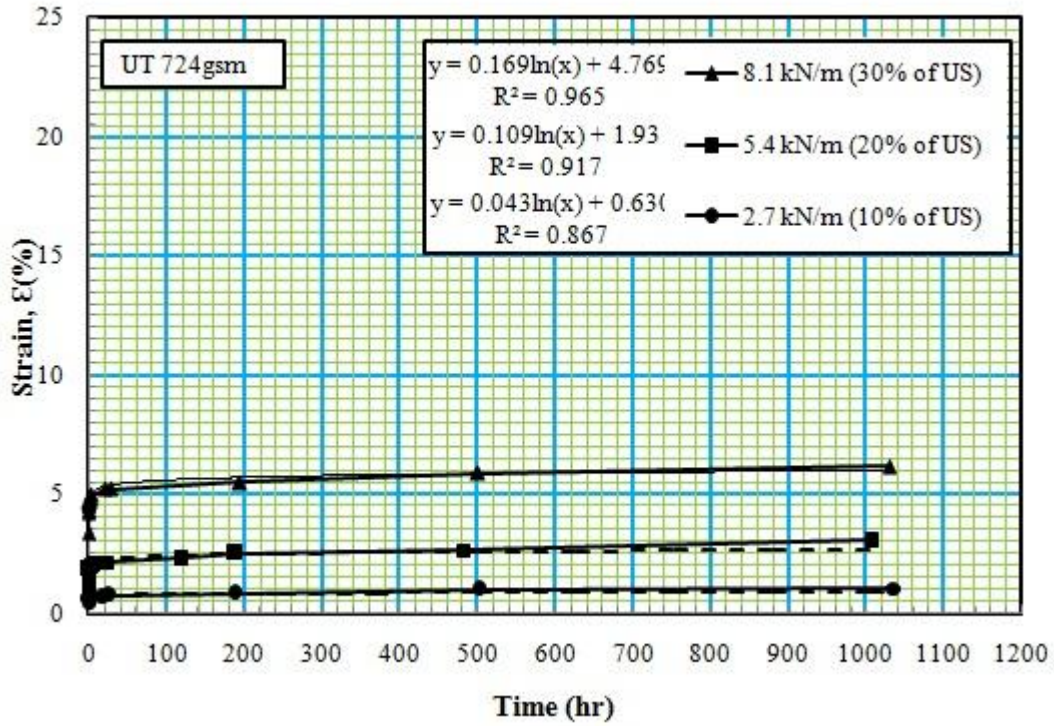

(a)

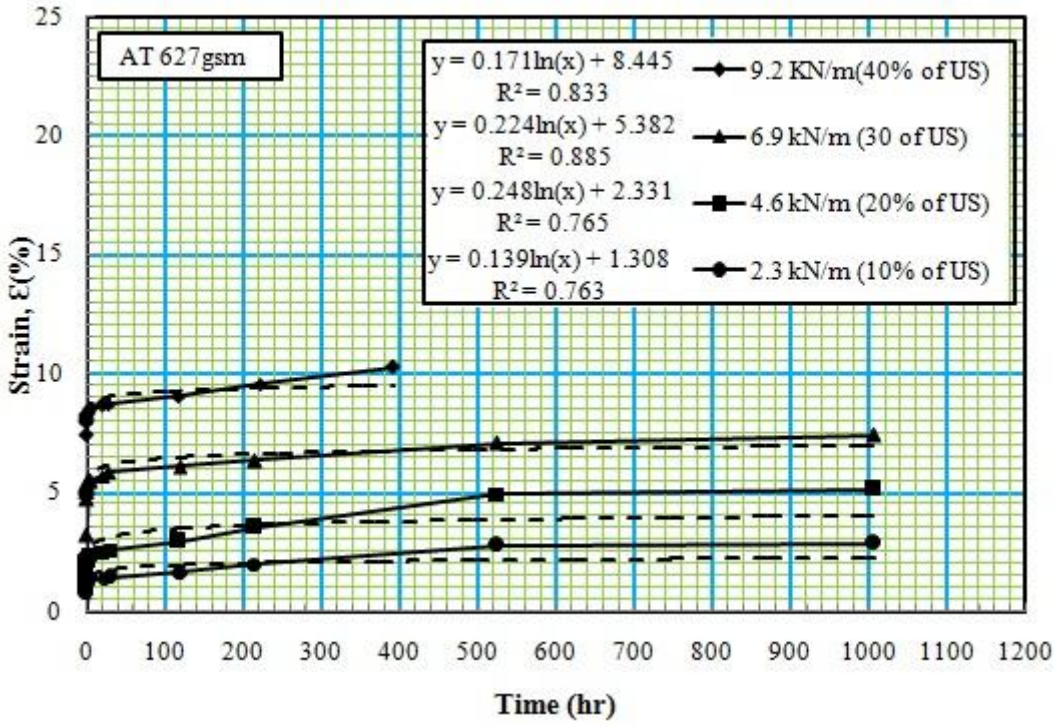

(b)

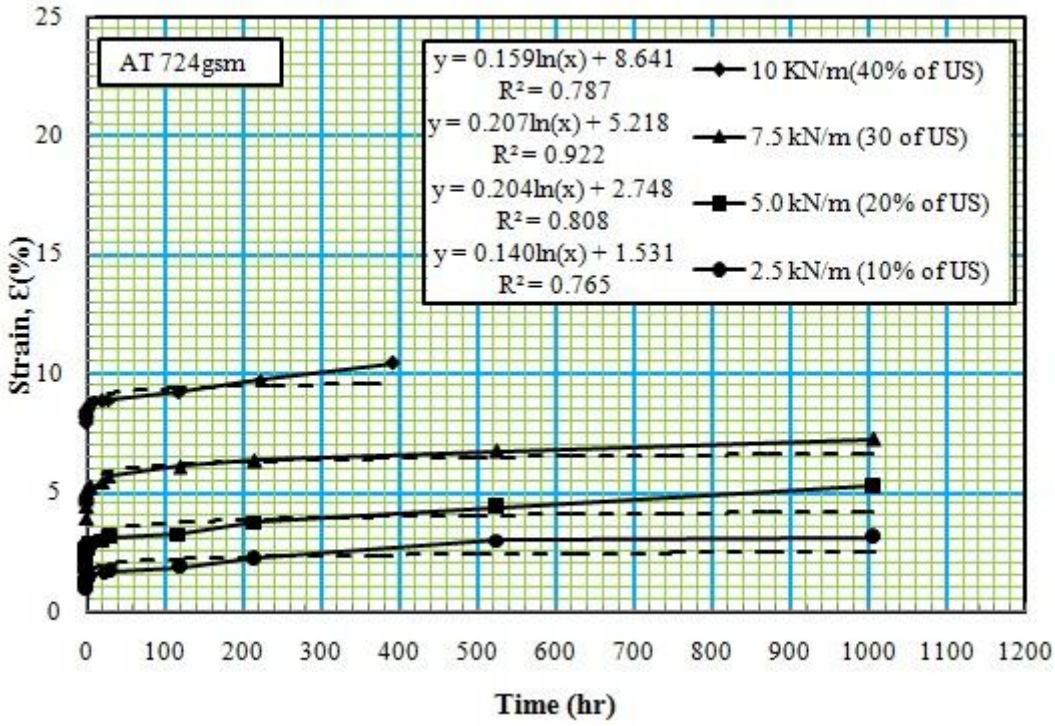

(c)

Fig. 18: Strain vs. time curves and best fitted curves for the strain vs. time relationships in machine direction: (a) untreated 724gsm, (b) additive treated 627gsm and (c) additive treated 724gsm

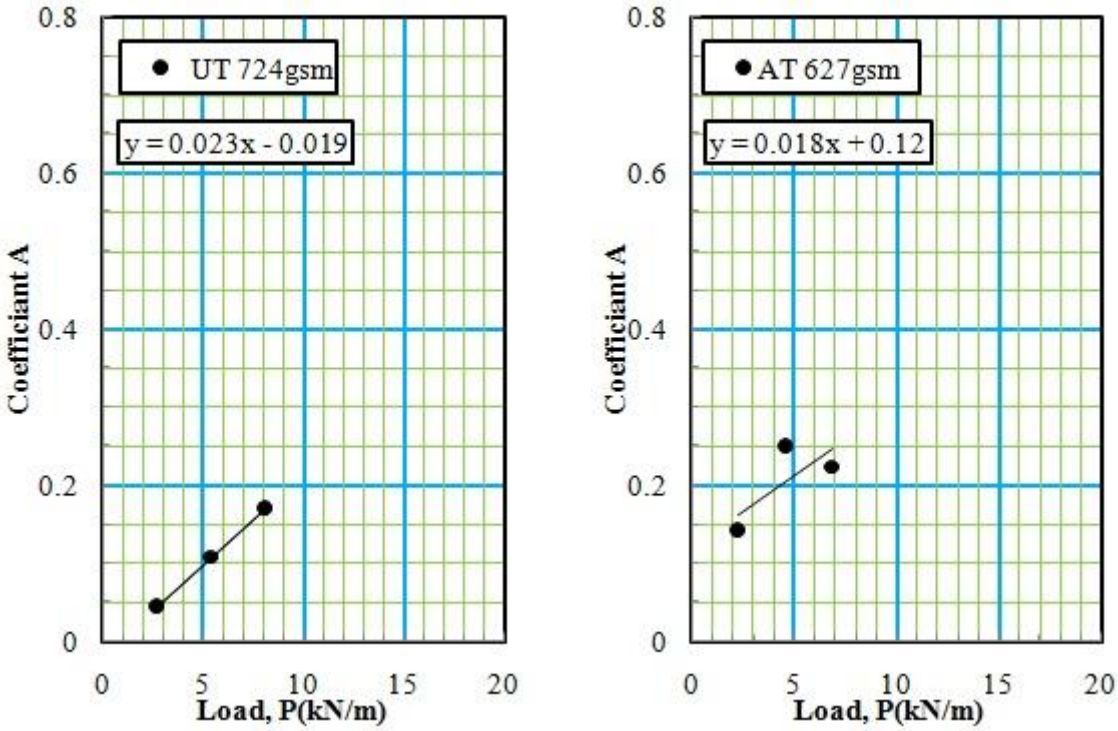

(a)

(b)

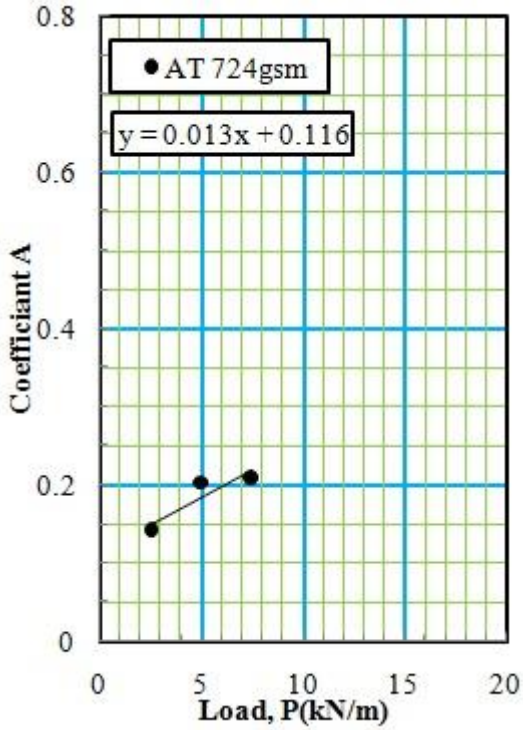

(c)

Fig. 19: Trend line coefficient A obtained from linear fit curve : (a) untreated 724gsm, (b) additive treated 627gsm and (c) additive treated 724gsm

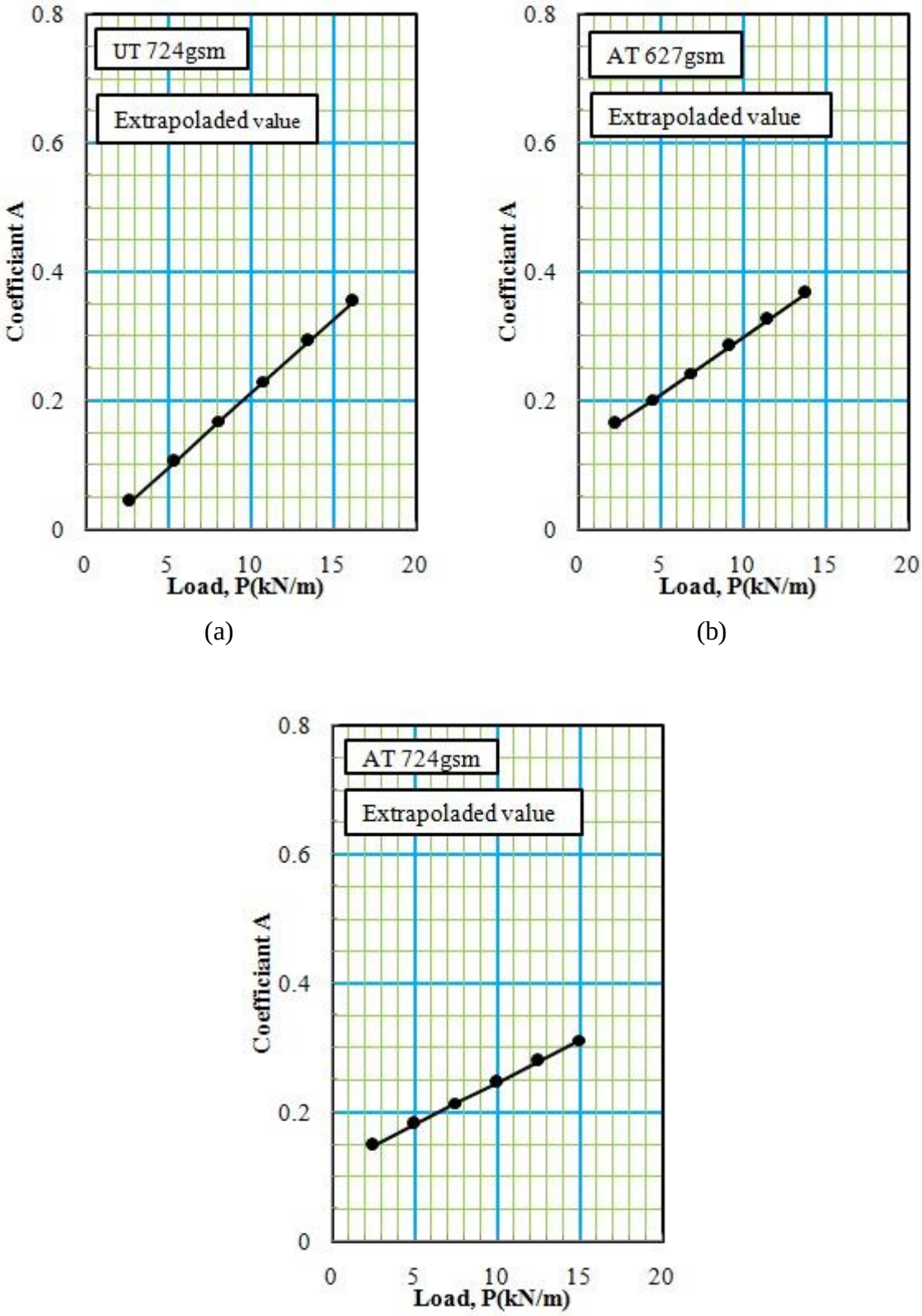

Fig. 20: Extrapolation of coefficient A obtained from linear fit curve: (a) untreated 724gsm, (b) additive treated 627gsm and (c) additive treated 724gsm

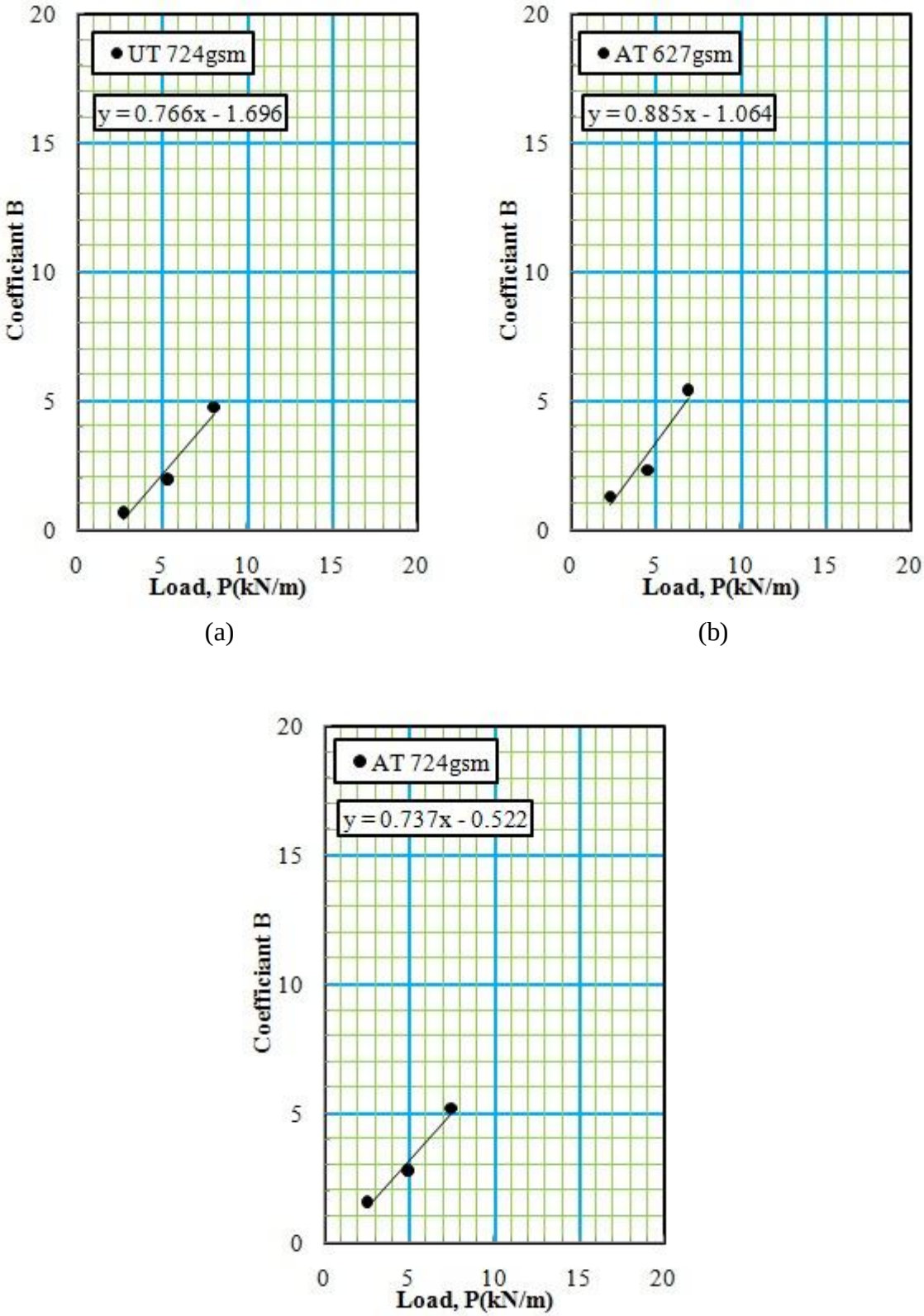

Fig. 21: Trend line coefficient B obtained from linear fit curve: (a) untreated 724gsm, (b) additive treated 627gsm and (c) additive treated 724gsm

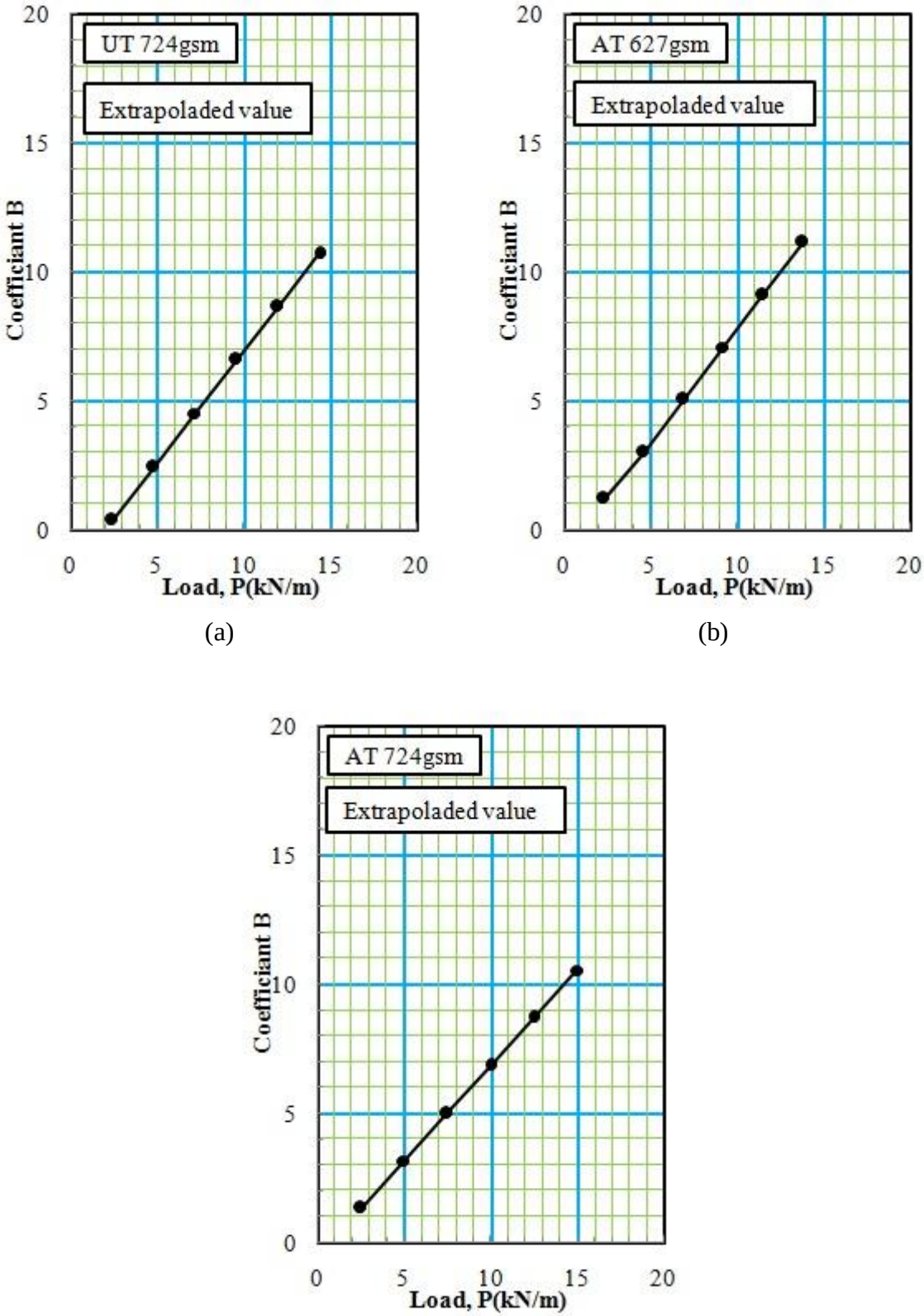

Fig. 22: Extrapolation of coefficient B obtained from linear fit curve: (a) untreated 724gsm, (b) additive treated 627gsm and (c) additive treated 724gsm

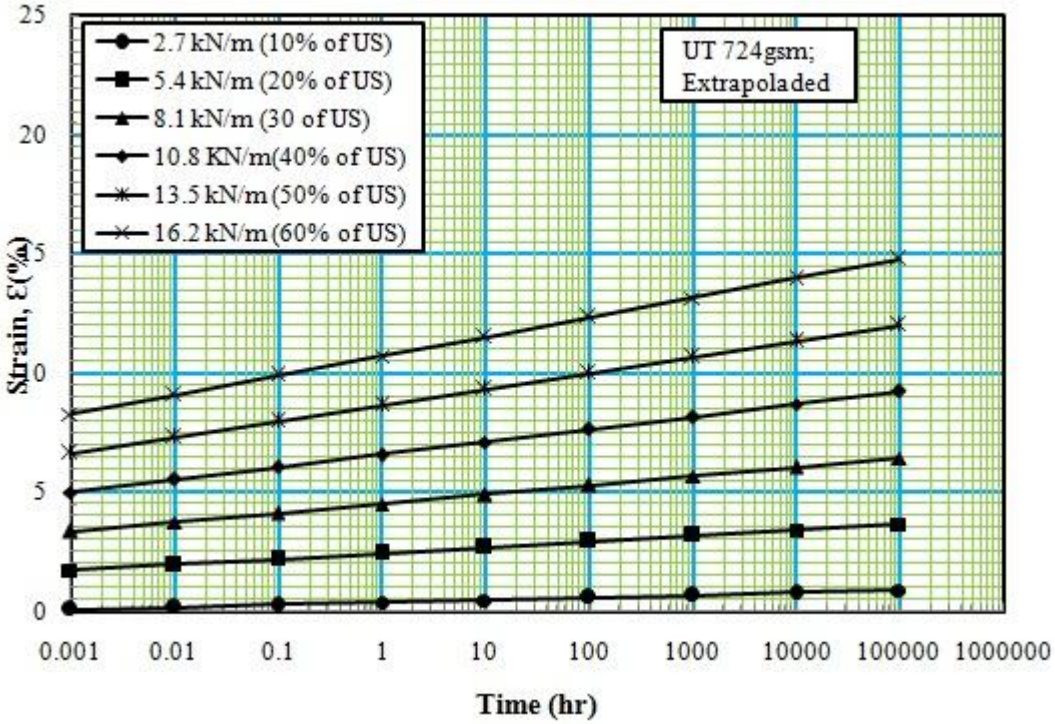
2.7 kN/m (10% of US)
5.4 kN/m (20% of US)
8.1 kN/m (30 of US)
10.8 KN/m(40% of US)
13.5 kN/m (50% of US)
16.2 kN/m (60% of US)
UT 724gsm;
Extrapoladed
Strain, ε(%)
Time (hr)
0
5
10
15
20
25
0.001
0.01
0.1
1
10
100
1000
10000
100000
1000000

(a)

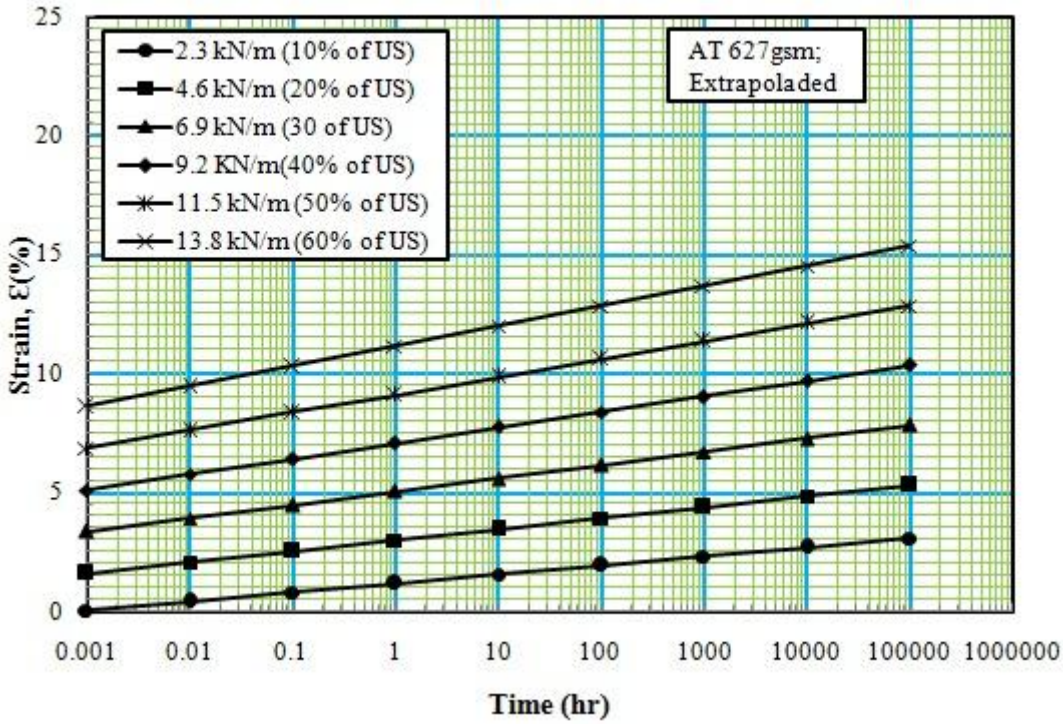
2.3 kN/m (10% of US)
4.6 kN/m (20% of US)
6.9 kN/m (30 of US)
9.2 KN/m(40% of US)
11.5 kN/m (50% of US)
13.8 kN/m (60% of US)
AT 627gsm;
Extrapoladed
Strain, ε(%)
Time (hr)
0
5
10
15
20
25
0.001
0.01
0.1
1
10
100
1000
10000
100000
1000000

(b)

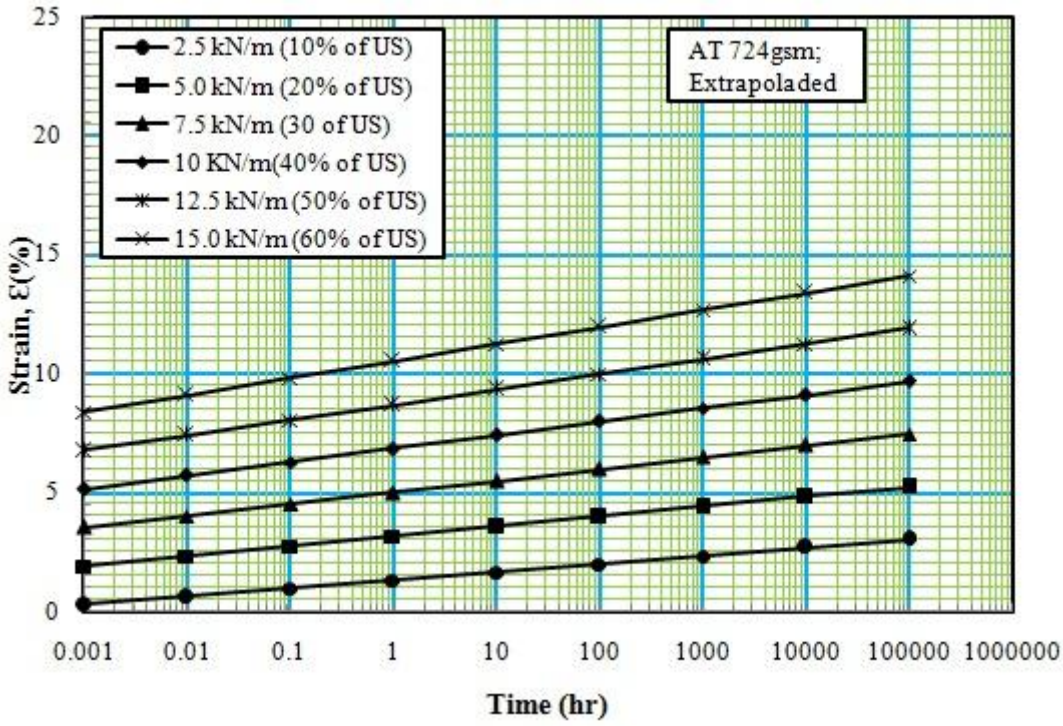

(c)

Fig. 23: Extrapolated total strain vs log time (hr) in machine direction: (a) untreated 724gsm, (b) additive treated 627gsm and (c) additive treated 724gsm

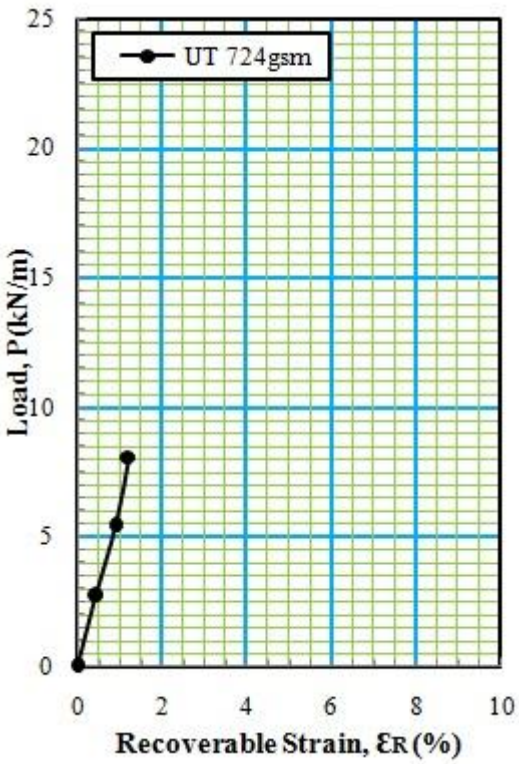

(a)

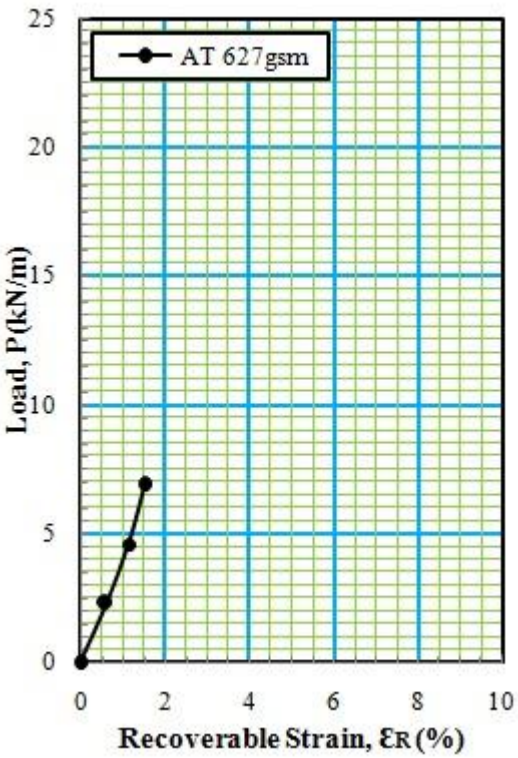

(b)

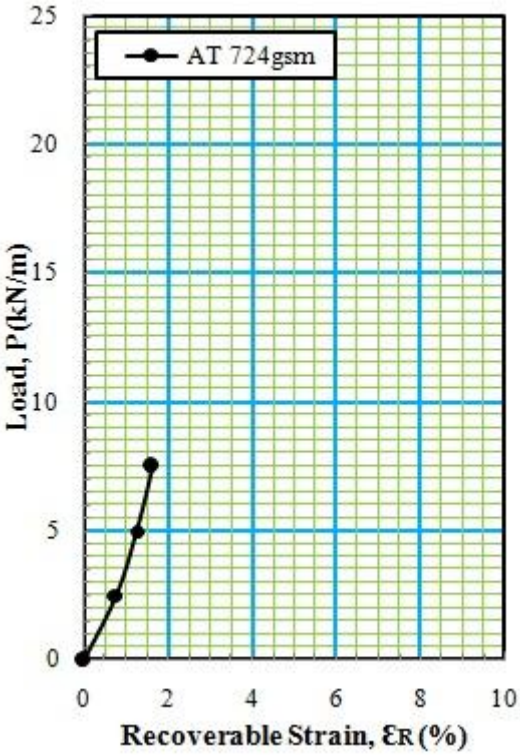

(c)

Fig. 24: Load vs recoverable strain in machine direction: (a) untreated 724gsm, (b) additive treated 627gsm and (c) additive treated 724gsm

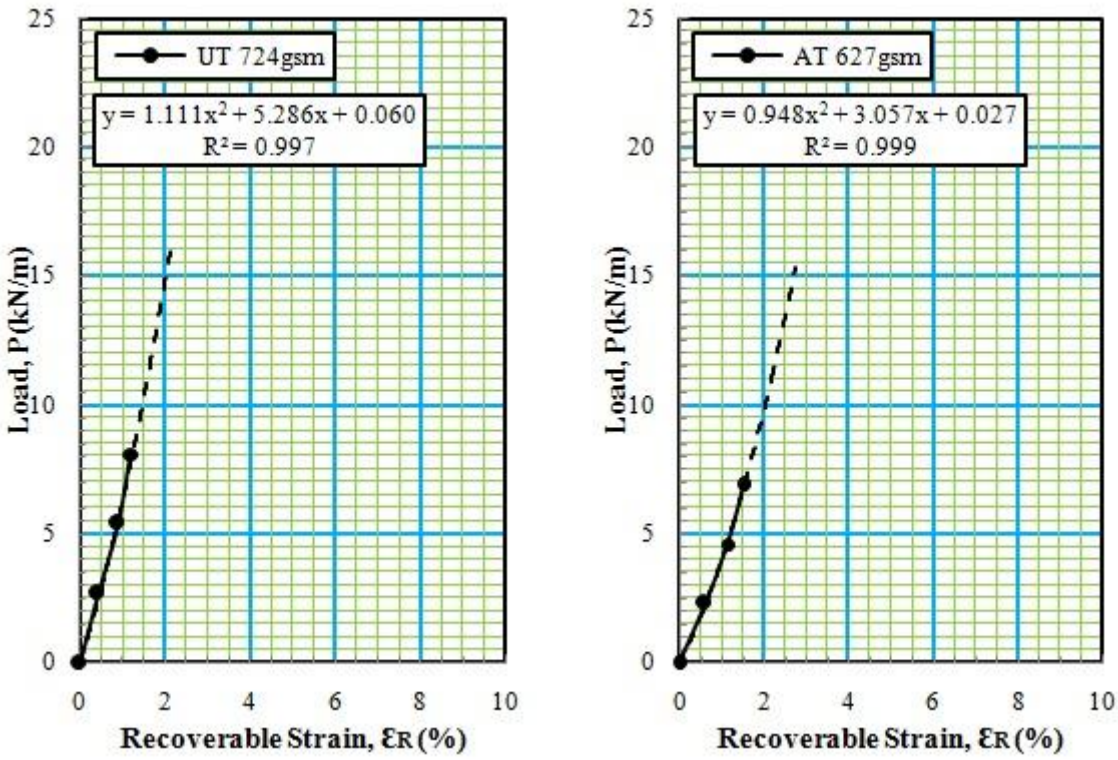

(a) (b)

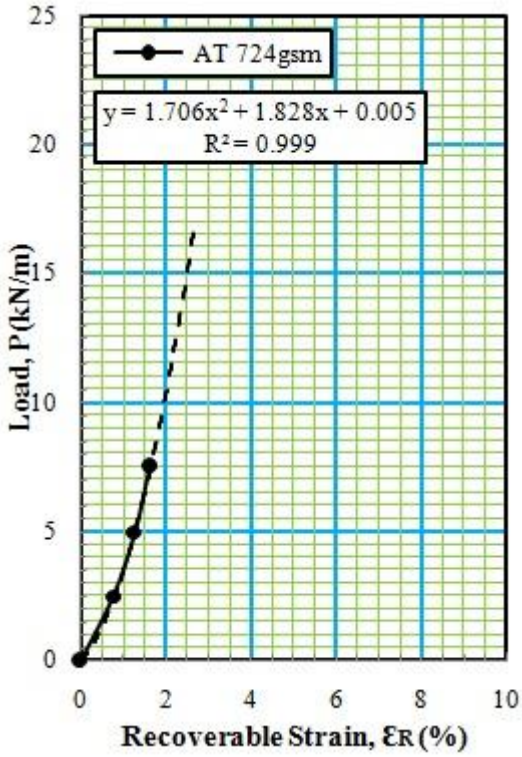

(c)

Fig. 25: Extrapolation of load vs recoverable strain in machine direction: (a) untreated 724gsm, (b) additive treated 627gsm and (c) additive treated 724gsm

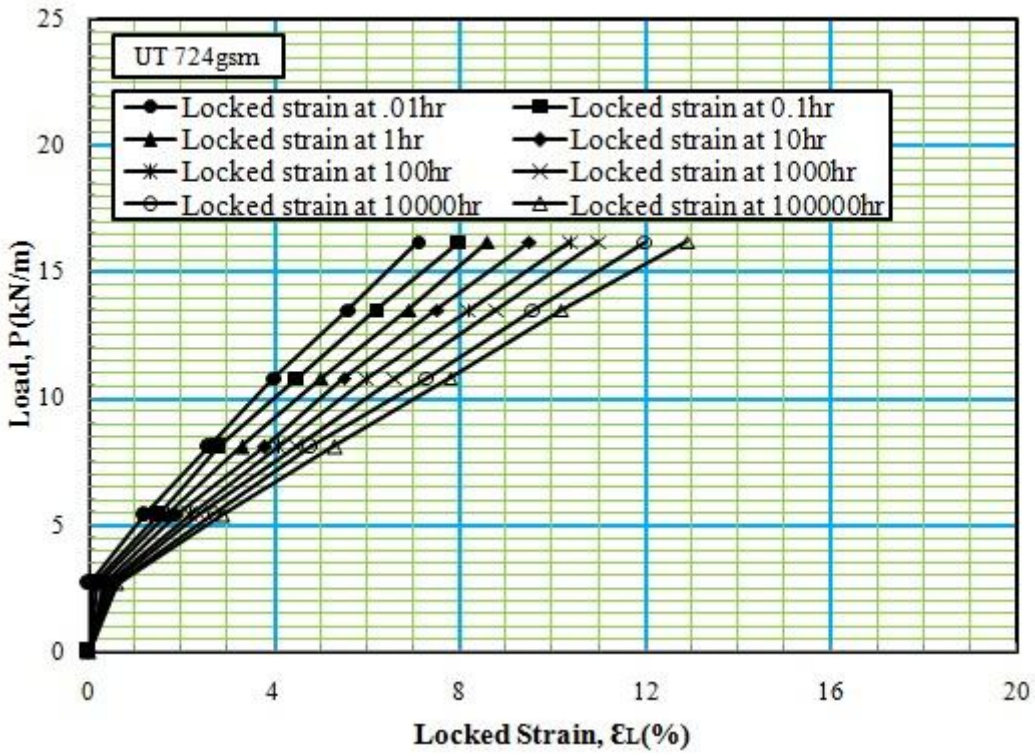
UT 724gsm
Locked strain at .01hr
Locked strain at 0.1hr
Locked strain at 1hr
Locked strain at 10hr
Locked strain at 100hr
Locked strain at 1000hr
Locked strain at 10000hr
Locked strain at 100000hr
Load, P(kN/m)
Locked Strain, εL(%)
0
5
10
15
20
25
0
4
8
12
16
20

(a)

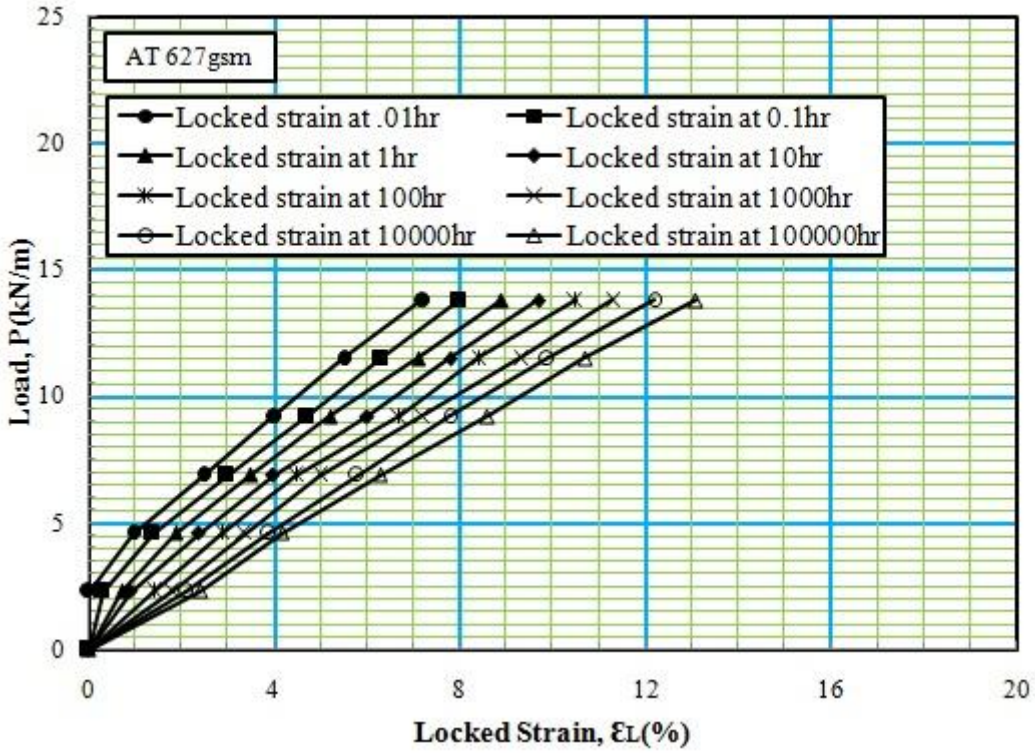
AT 627gsm
Locked strain at .01hr
Locked strain at 0.1hr
Locked strain at 1hr
Locked strain at 10hr
Locked strain at 100hr
Locked strain at 1000hr
Locked strain at 10000hr
Locked strain at 100000hr
Load, P(kN/m)
Locked Strain, εL(%)
0
5
10
15
20
25
0
4
8
12
16
20

(b)

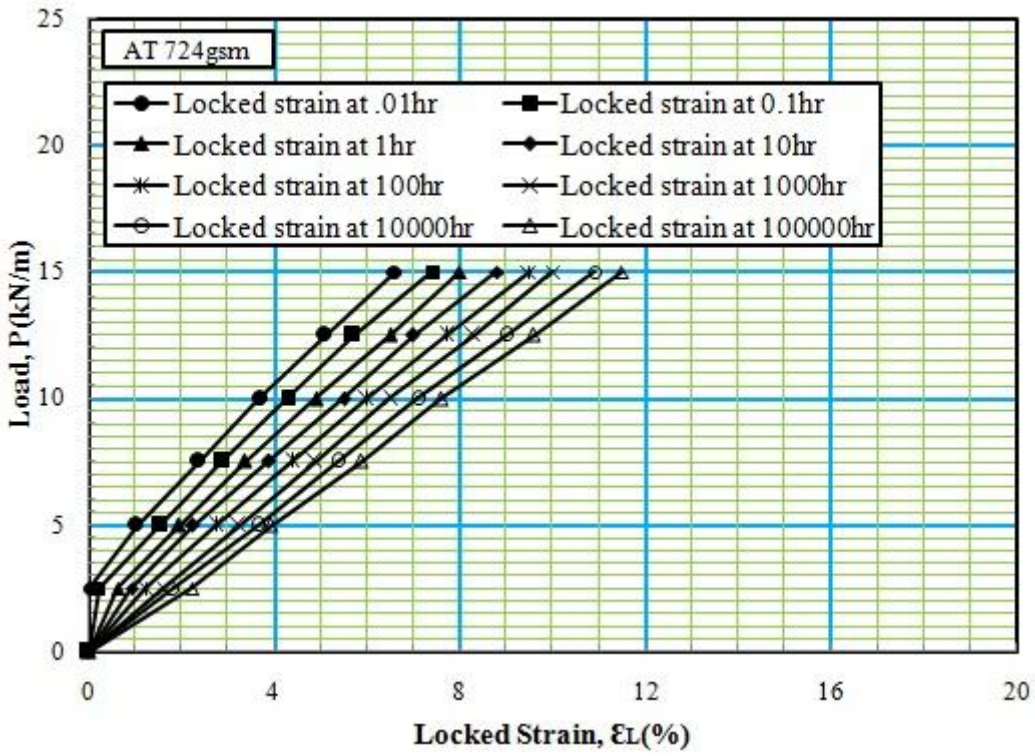

(c)

Fig. 26: Load vs locked strain in machine direction: (a) untreated 724gsm, (b) additive treated 627gsm and (c) additive treated 724gsm

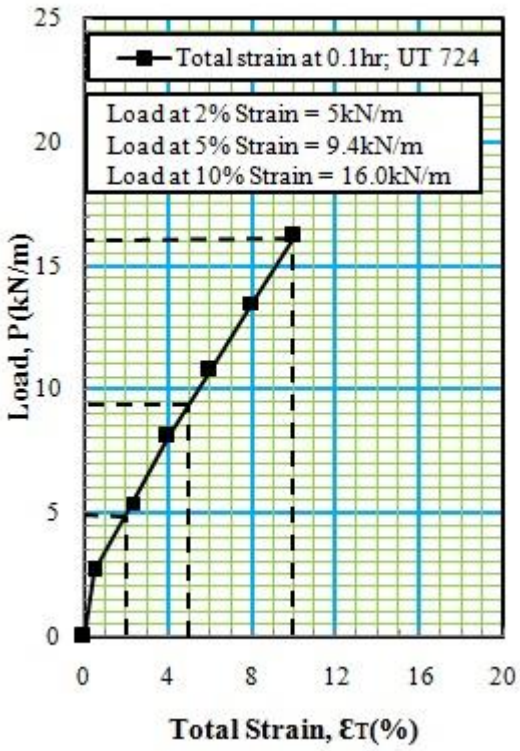

(a)

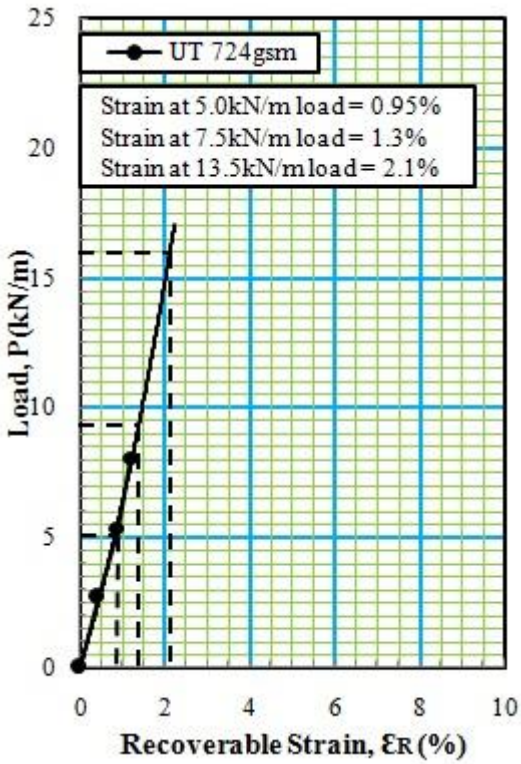

(b)

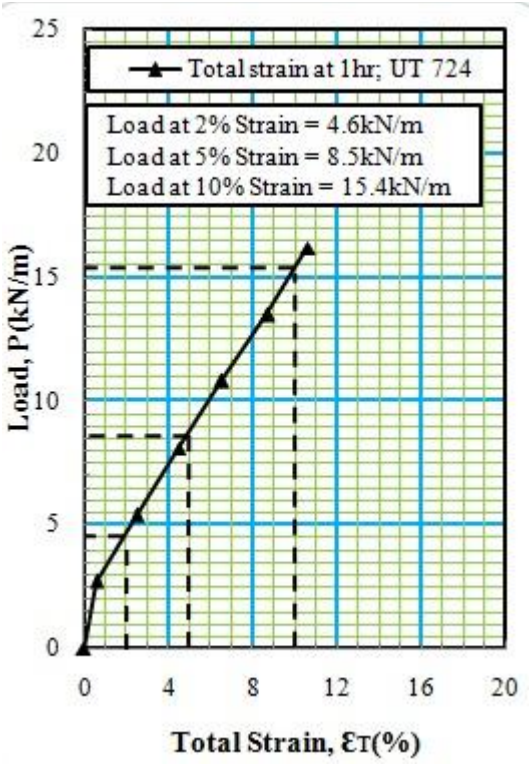
Total strain at 1hr; UT 724
Load at 2% Strain = 4.6kN/m
Load at 5% Strain = 8.5kN/m
Load at 10% Strain = 15.4kN/m
Load, P(kN/m)
Total Strain, εT(%)

(c)

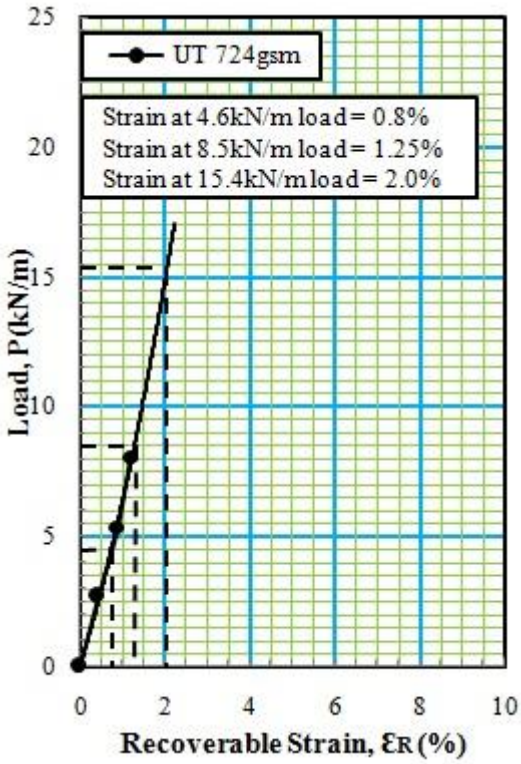
UT 724gsm
Strain at 4.6kN/m load= 0.8%
Strain at 8.5kN/m load= 1.25%
Strain at 15.4kN/m load= 2.0%
Load, P(kN/m)
Recoverable Strain, εR (%)

(d)

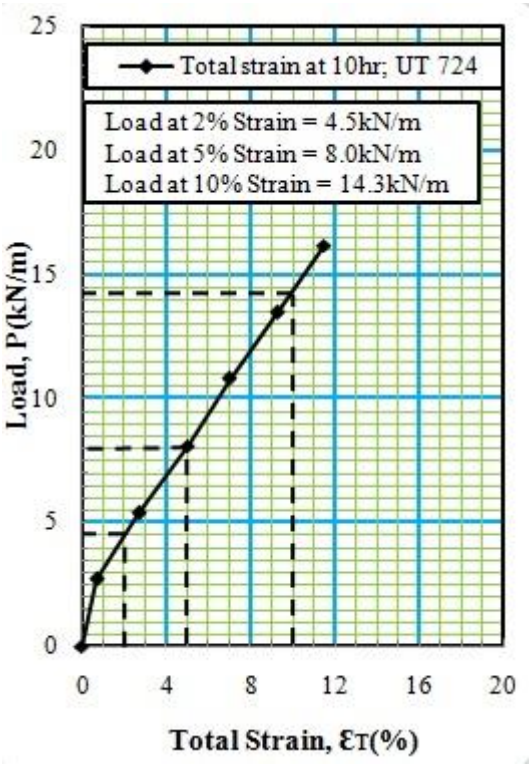
Total strain at 10hr; UT 724
Load at 2% Strain = 4.5kN/m
Load at 5% Strain = 8.0kN/m
Load at 10% Strain = 14.3kN/m
Load, P(kN/m)
Total Strain, εT(%)

(e)

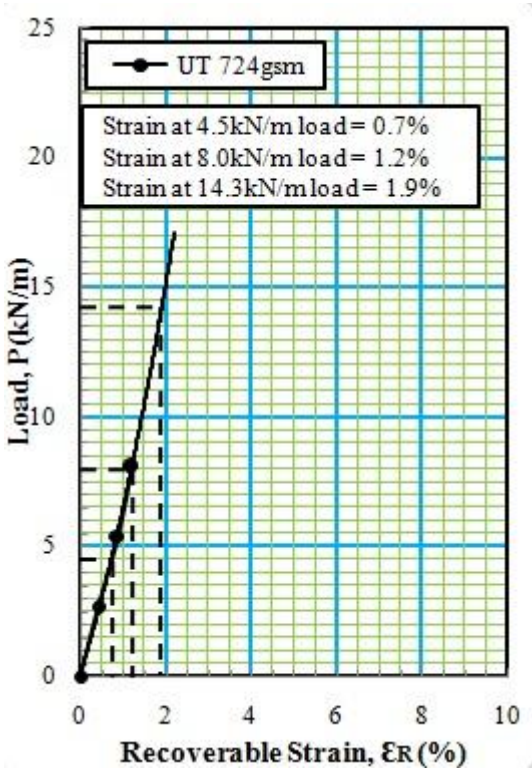
UT 724gsm
Strain at 4.5kN/m load= 0.7%
Strain at 8.0kN/m load= 1.2%
Strain at 14.3kN/m load= 1.9%
Load, P(kN/m)
Recoverable Strain, εR (%)

(f)

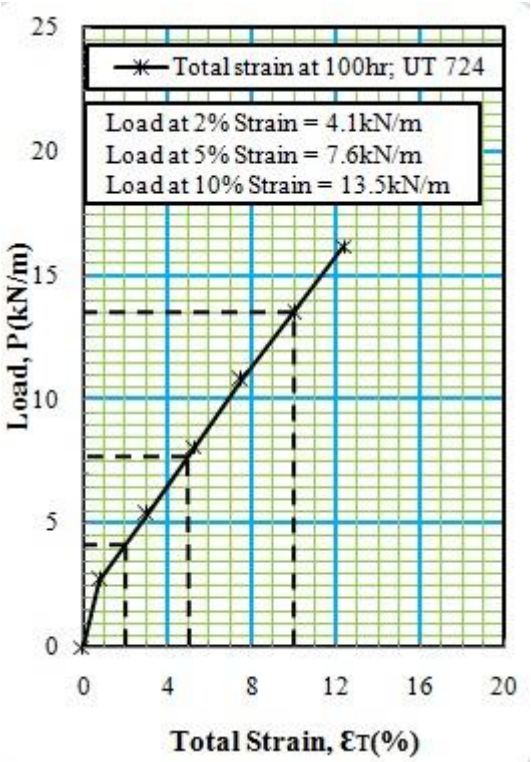
Total strain at 100hr; UT 724
Load at 2% Strain = 4.1kN/m
Load at 5% Strain = 7.6kN/m
Load at 10% Strain = 13.5kN/m
Load, P(kN/m)
Total Strain, εT(%)

(g)

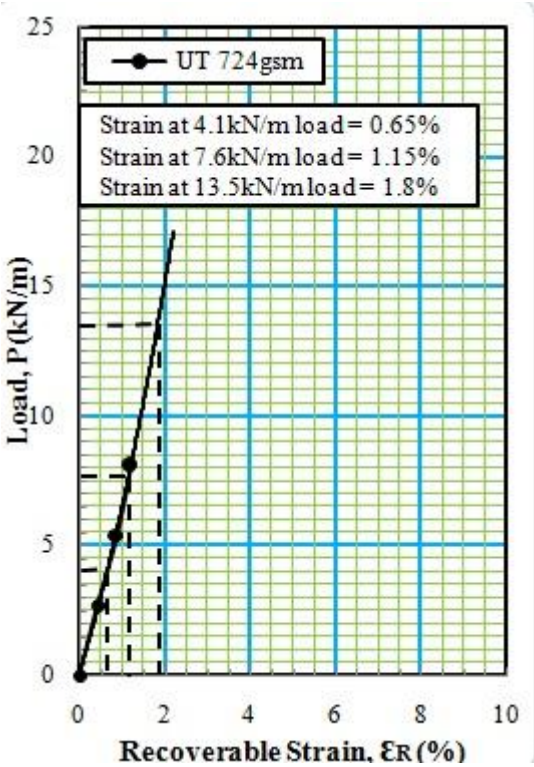
UT 724gsm
Strain at 4.1kN/m load = 0.65%
Strain at 7.6kN/m load = 1.15%
Strain at 13.5kN/m load = 1.8%
Load, P(kN/m)
Recoverable Strain, εR (%)

(h)

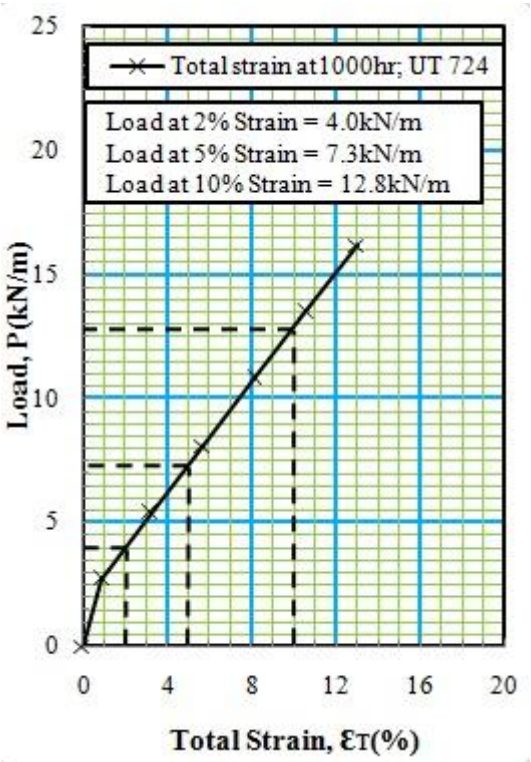
Total strain at 1000hr; UT 724
Load at 2% Strain = 4.0kN/m
Load at 5% Strain = 7.3kN/m
Load at 10% Strain = 12.8kN/m
Load, P(kN/m)
Total Strain, εT(%)

(i)

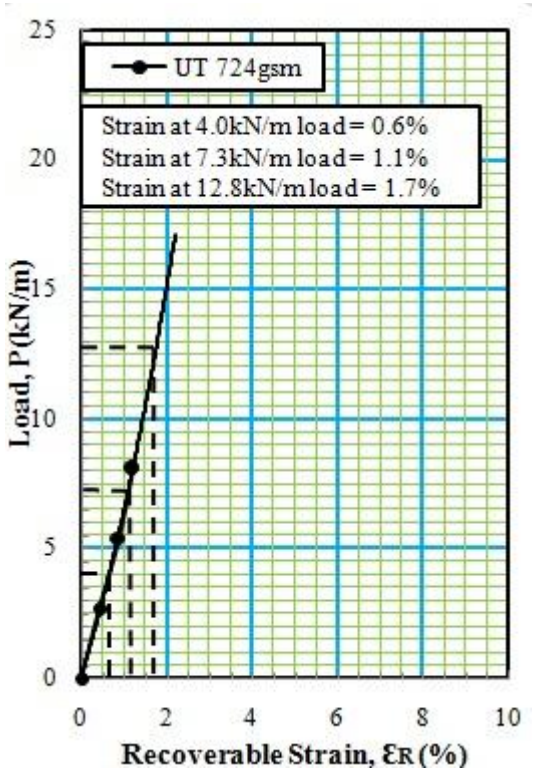
UT 724gsm
Strain at 4.0kN/m load = 0.6%
Strain at 7.3kN/m load = 1.1%
Strain at 12.8kN/m load = 1.7%
Load, P(kN/m)
Recoverable Strain, εR (%)

(j)

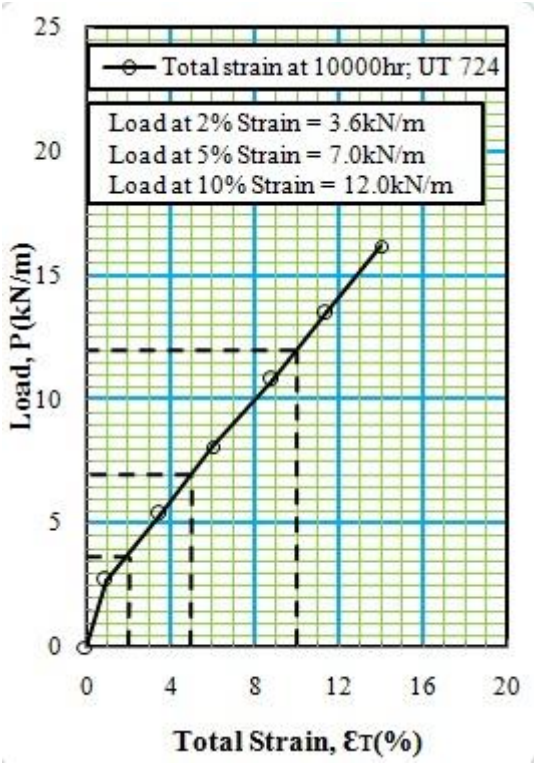

(k)

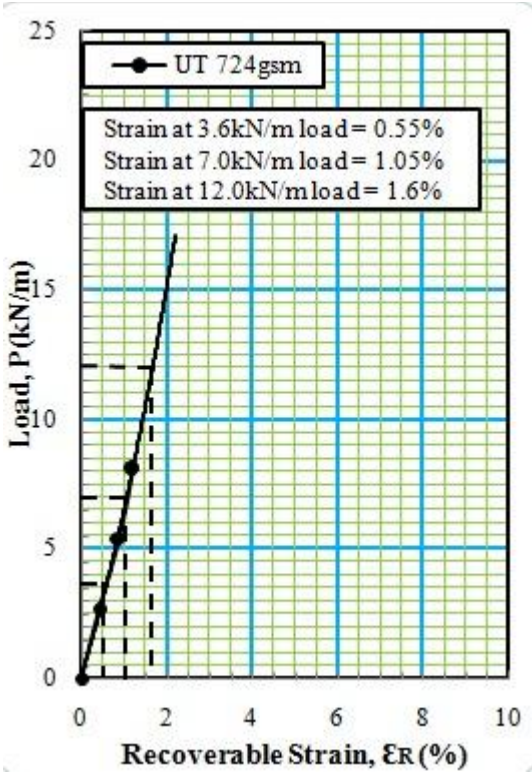

(l)

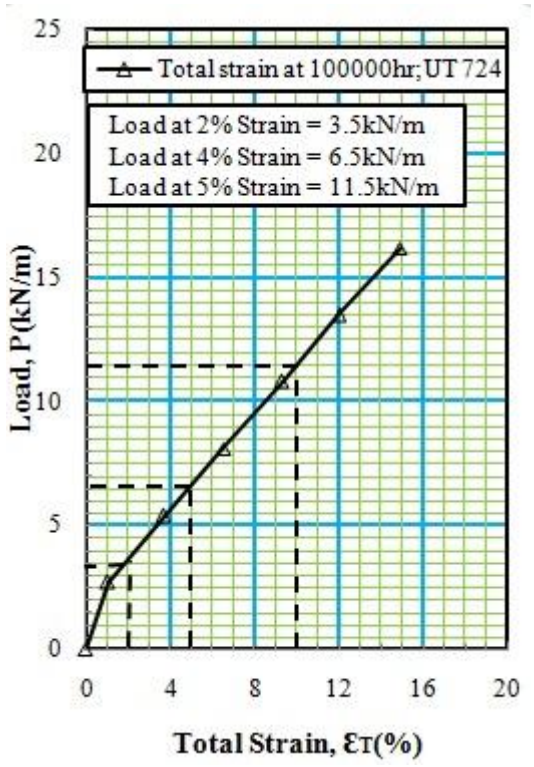

(m)

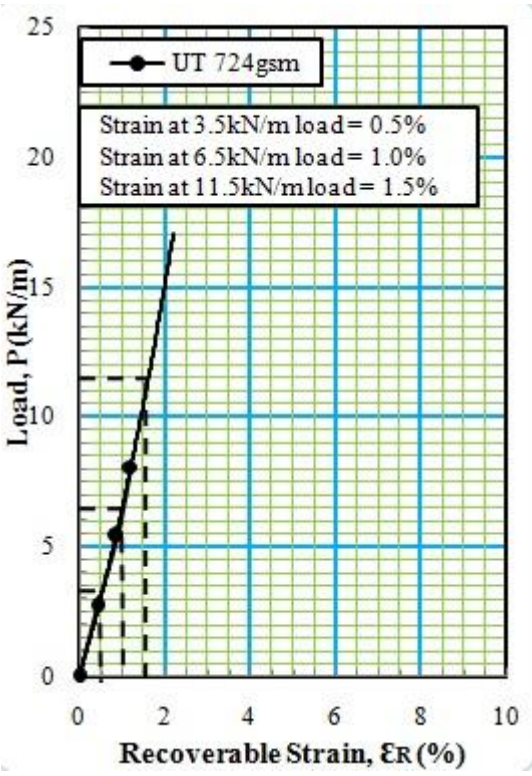

(n)

Fig. 27: Load vs. total strain graph and load vs. recoverable strain graph for untreated 724gsm in machine direction at various time for different limiting strains

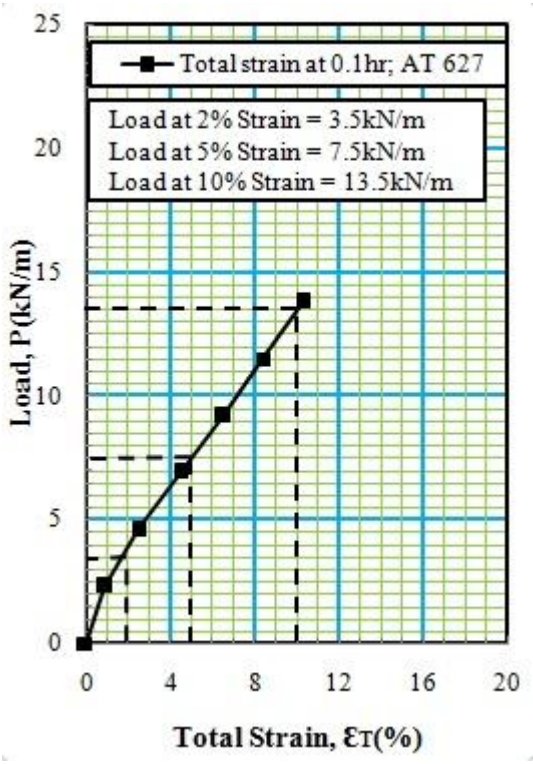
Total strain at 0.1hr; AT 627
Load at 2% Strain = 3.5kN/m
Load at 5% Strain = 7.5kN/m
Load at 10% Strain = 13.5kN/m
Load, P(kN/m)
Total Strain, εT(%)

(a)

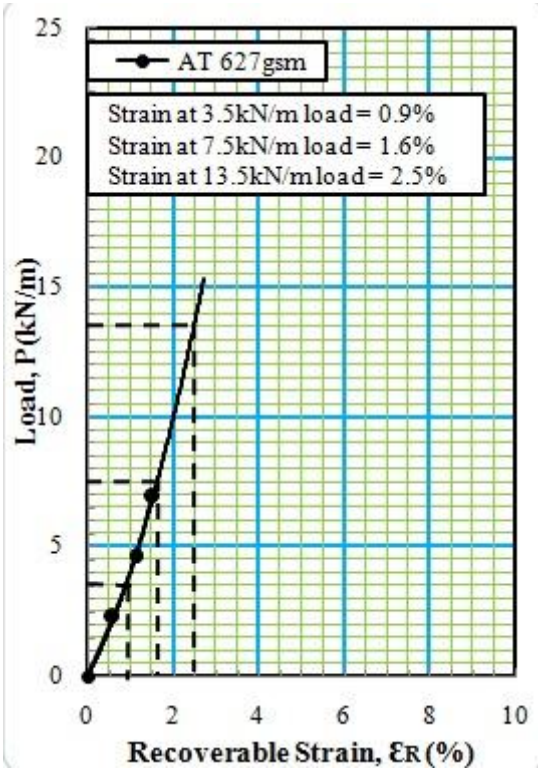
AT 627gsm
Strain at 3.5kN/m load = 0.9%
Strain at 7.5kN/m load = 1.6%
Strain at 13.5kN/m load = 2.5%
Load, P(kN/m)
Recoverable Strain, εR (%)

(b)

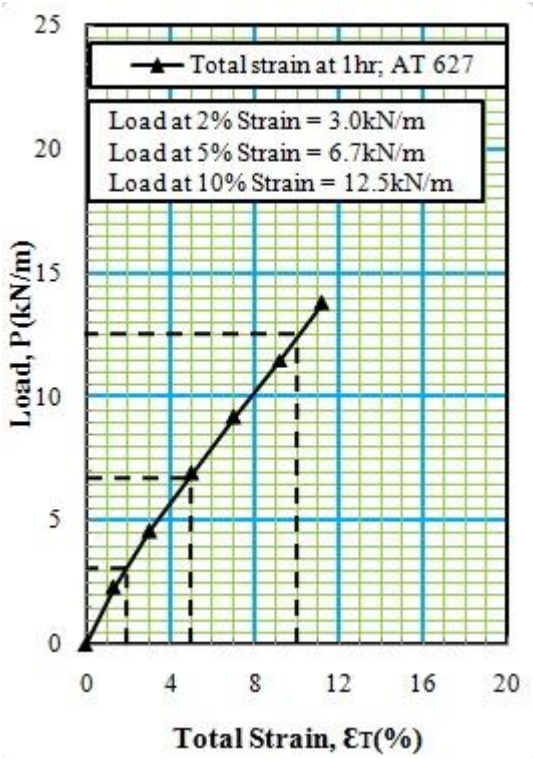
Total strain at 1hr; AT 627
Load at 2% Strain = 3.0kN/m
Load at 5% Strain = 6.7kN/m
Load at 10% Strain = 12.5kN/m
Load, P(kN/m)
Total Strain, εT(%)

(c)

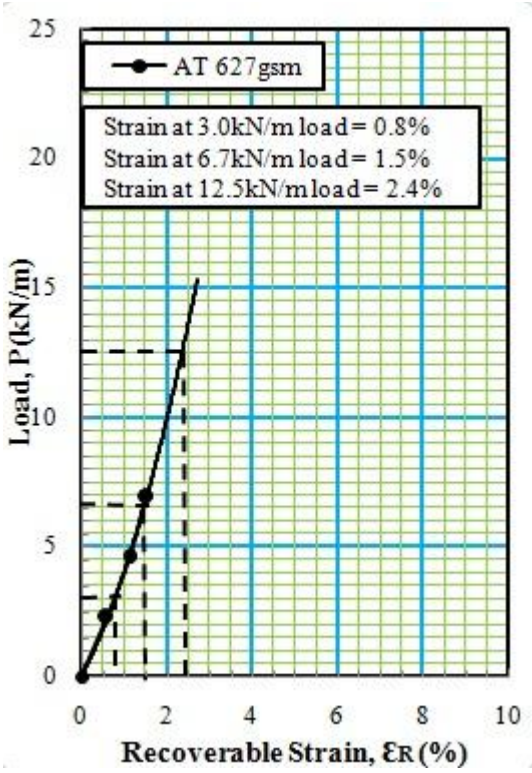
AT 627gsm
Strain at 3.0kN/m load = 0.8%
Strain at 6.7kN/m load = 1.5%
Strain at 12.5kN/m load = 2.4%
Load, P(kN/m)
Recoverable Strain, εR (%)

(d)

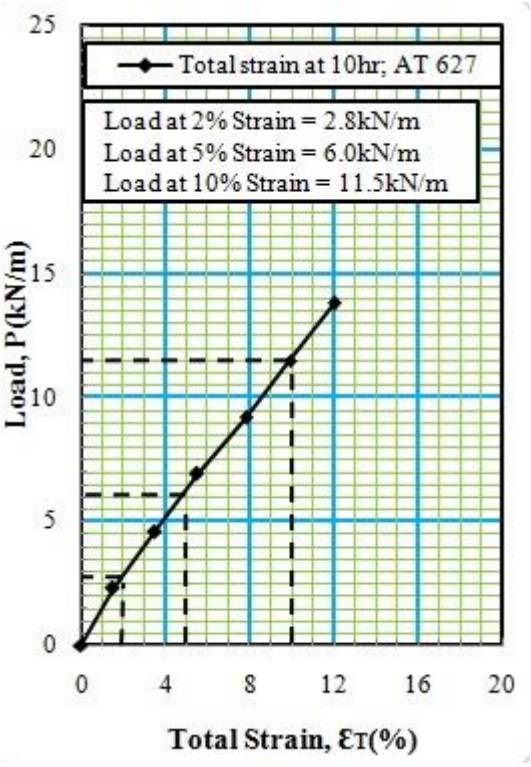
Total strain at 10hr; AT 627
Load at 2% Strain = 2.8kN/m
Load at 5% Strain = 6.0kN/m
Load at 10% Strain = 11.5kN/m
Load, P(kN/m)
Total Strain, εT(%)
0
4
8
12
16
20
5
10
15
20
25

(e)

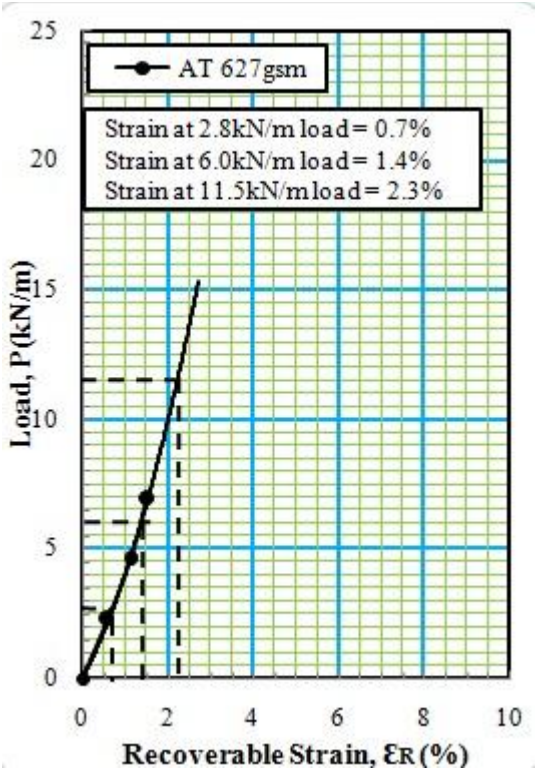
AT 627gsm
Strain at 2.8kN/m load = 0.7%
Strain at 6.0kN/m load = 1.4%
Strain at 11.5kN/m load = 2.3%
Load, P(kN/m)
Recoverable Strain, εR (%)
0
2
4
6
8
10
5
10
15
20
25

(f)

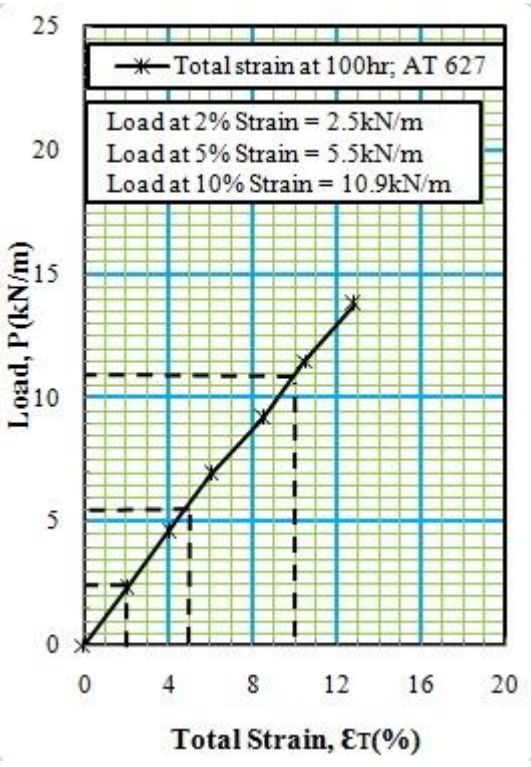
Total strain at 100hr; AT 627
Load at 2% Strain = 2.5kN/m
Load at 5% Strain = 5.5kN/m
Load at 10% Strain = 10.9kN/m
Load, P(kN/m)
Total Strain, εT(%)
0
4
8
12
16
20
5
10
15
20
25

(g)

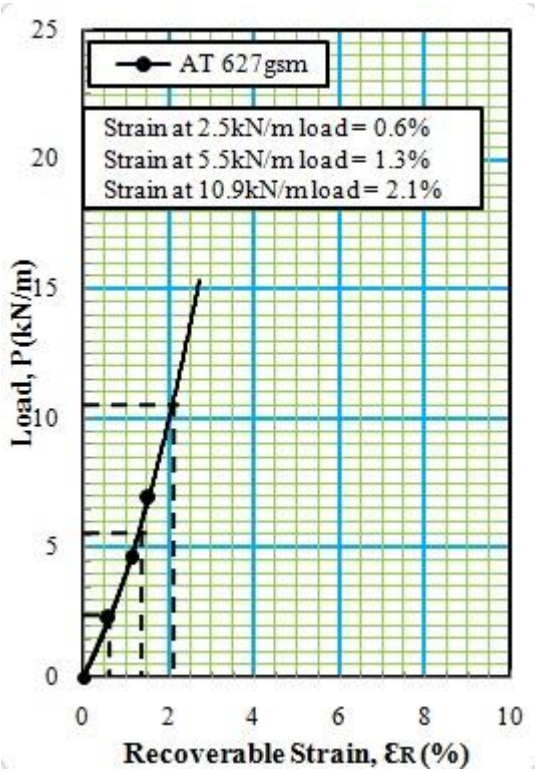
AT 627gsm
Strain at 2.5kN/m load = 0.6%
Strain at 5.5kN/m load = 1.3%
Strain at 10.9kN/m load = 2.1%
Load, P(kN/m)
Recoverable Strain, εR (%)
0
2
4
6
8
10
5
10
15
20
25

(h)

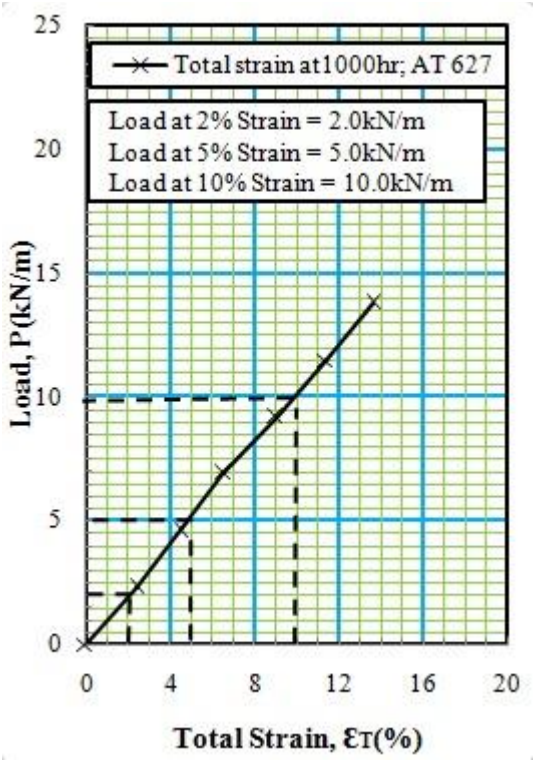
Total strain at1000hr; AT 627
Load at 2% Strain = 2.0kN/m
Load at 5% Strain = 5.0kN/m
Load at 10% Strain = 10.0kN/m
Load, P(kN/m)
Total Strain, εT(%)
0
4
8
12
16
20
0
5
10
15
20
25

(i)

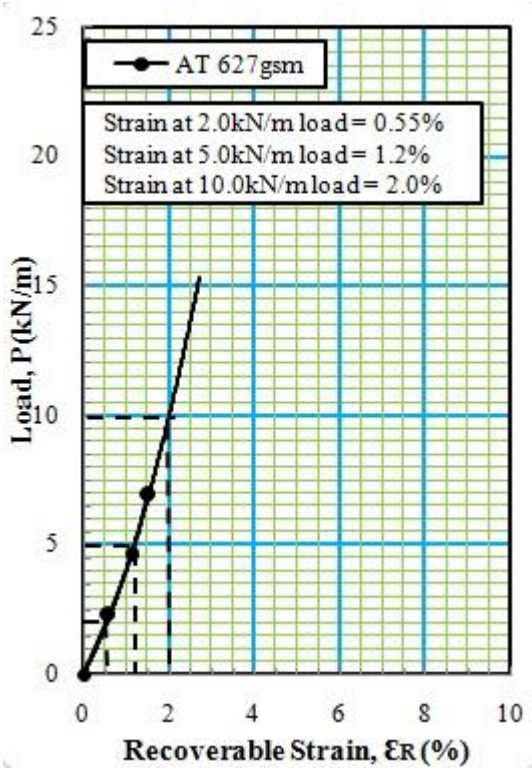
AT 627gsm
Strain at 2.0kN/m load= 0.55%
Strain at 5.0kN/m load= 1.2%
Strain at 10.0kN/m load= 2.0%
Load, P(kN/m)
Recoverable Strain, εR (%)
0
2
4
6
8
10
0
5
10
15
20
25

(j)

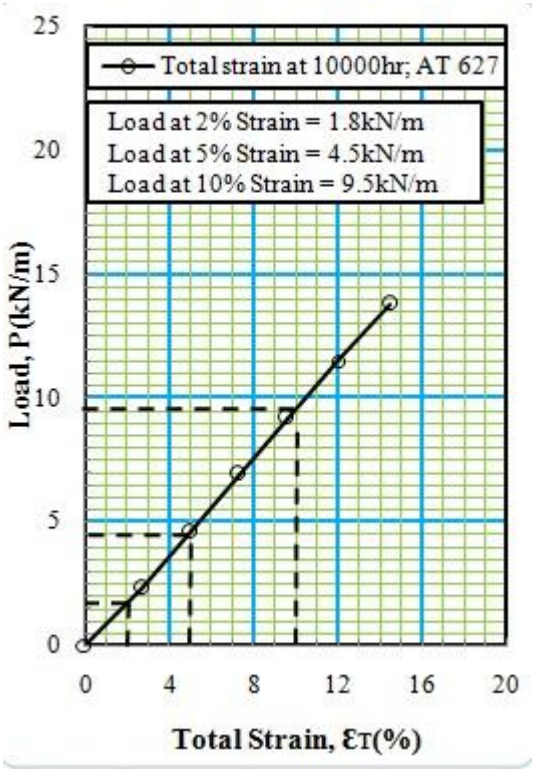
Total strain at 10000hr; AT 627
Load at 2% Strain = 1.8kN/m
Load at 5% Strain = 4.5kN/m
Load at 10% Strain = 9.5kN/m
Load, P(kN/m)
Total Strain, εT(%)
0
4
8
12
16
20
0
5
10
15
20
25

(k)

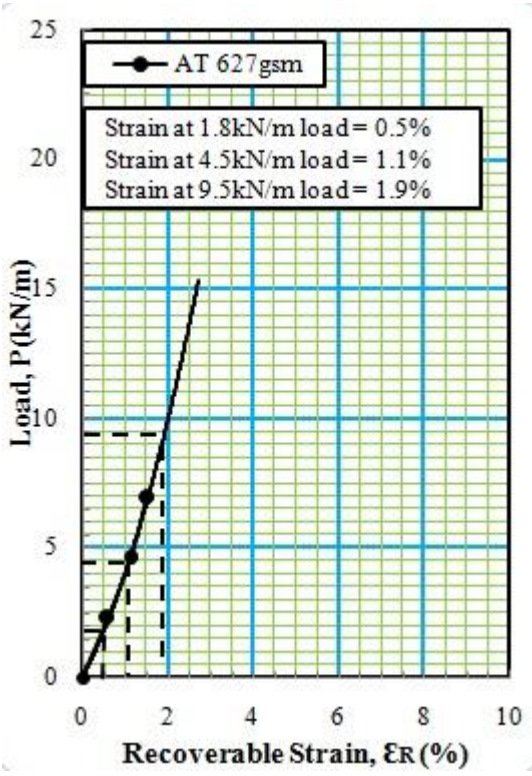
AT 627gsm
Strain at 1.8kN/m load= 0.5%
Strain at 4.5kN/m load= 1.1%
Strain at 9.5kN/m load= 1.9%
Load, P(kN/m)
Recoverable Strain, εR (%)
0
2
4
6
8
10
0
5
10
15
20
25

(l)

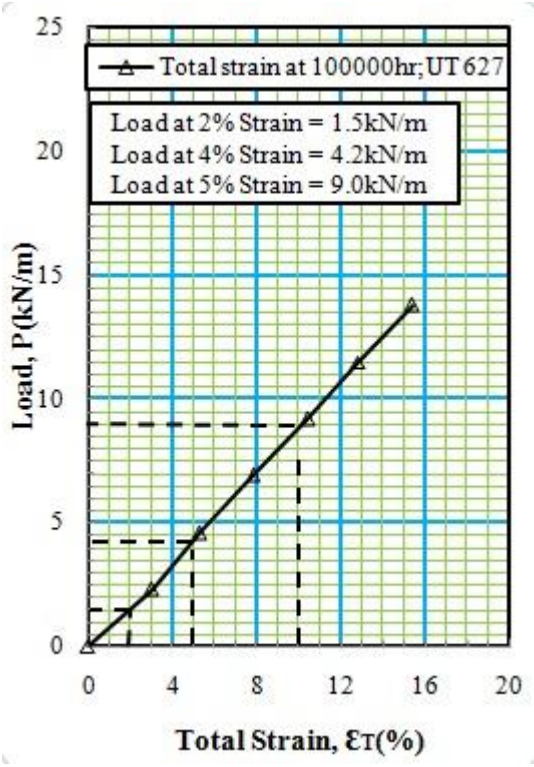

(m)

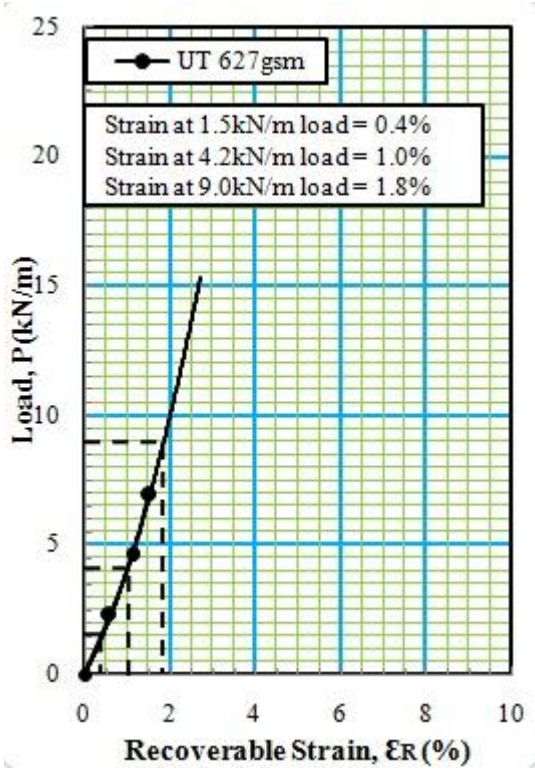

(n)

Fig. 28: Load vs. total strain graph and load vs. recoverable strain graph for additive treated 627gsm in machine direction at various time for different limiting strains

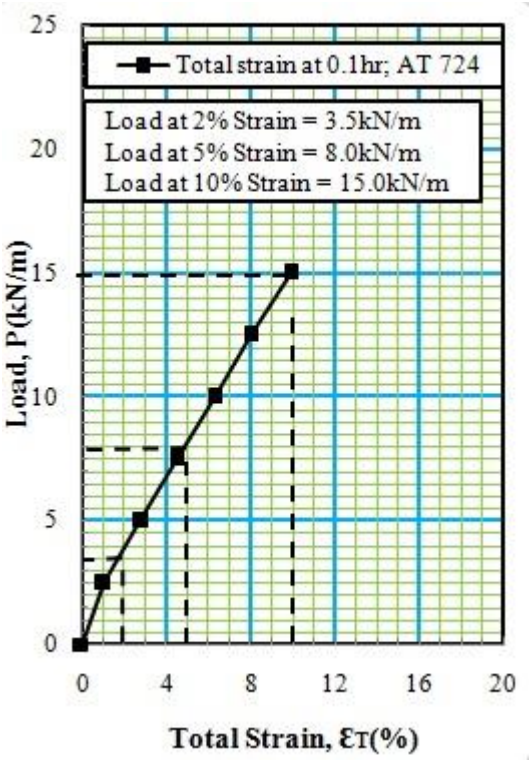

(a)

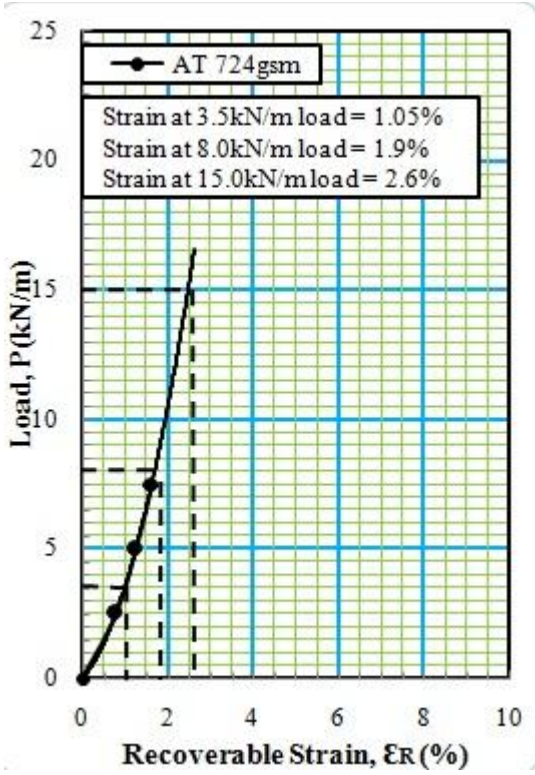

(b)

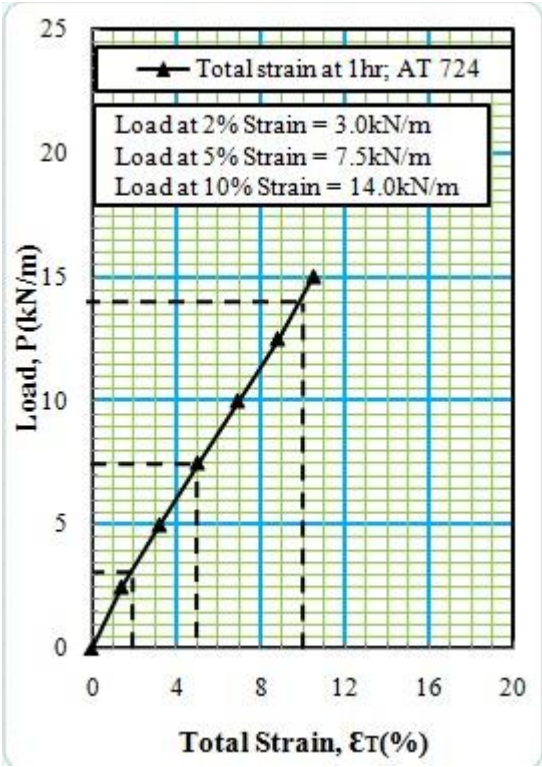
Total strain at 1hr; AT 724
Load at 2% Strain = 3.0kN/m
Load at 5% Strain = 7.5kN/m
Load at 10% Strain = 14.0kN/m
Load, P(kN/m)
Total Strain, εT(%)

(c)

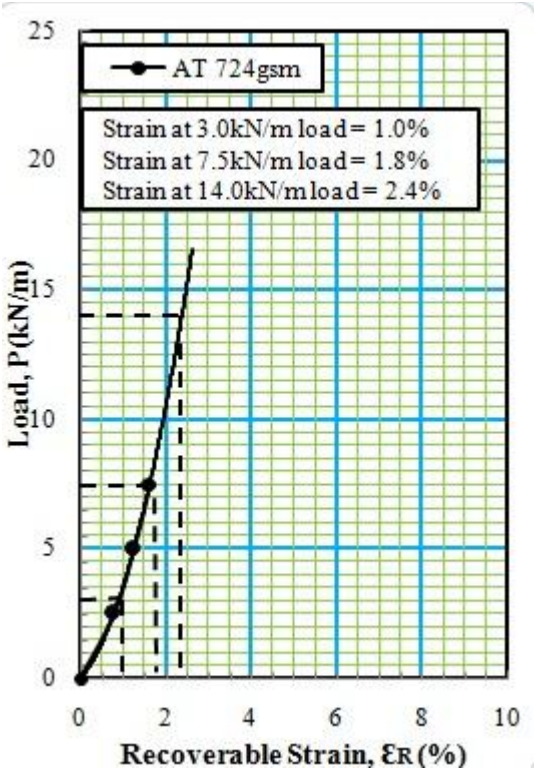
AT 724gsm
Strain at 3.0kN/m load = 1.0%
Strain at 7.5kN/m load = 1.8%
Strain at 14.0kN/m load = 2.4%
Load, P(kN/m)
Recoverable Strain, εR (%)

(d)

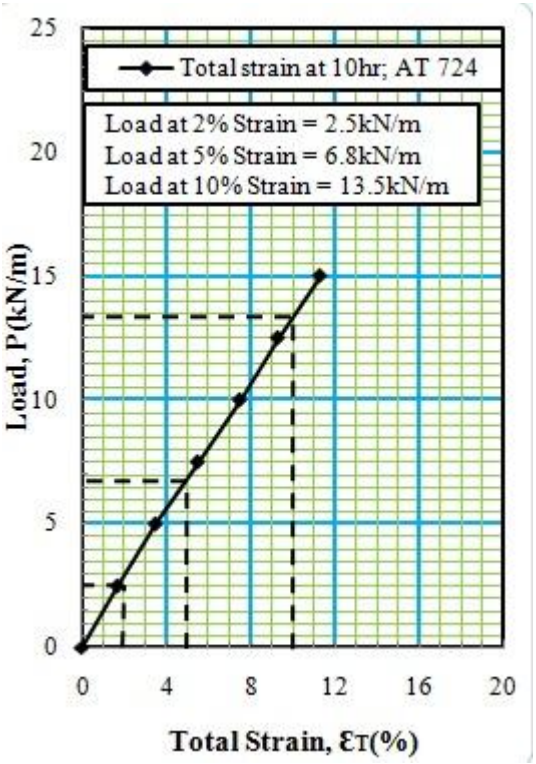
Total strain at 10hr; AT 724
Load at 2% Strain = 2.5kN/m
Load at 5% Strain = 6.8kN/m
Load at 10% Strain = 13.5kN/m
Load, P(kN/m)
Total Strain, εT(%)

(e)

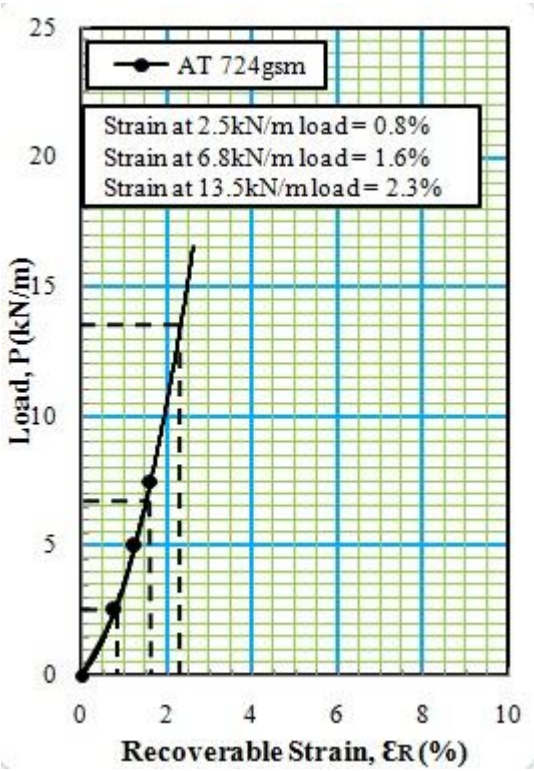
AT 724gsm
Strain at 2.5kN/m load = 0.8%
Strain at 6.8kN/m load = 1.6%
Strain at 13.5kN/m load = 2.3%
Load, P(kN/m)
Recoverable Strain, εR (%)

(f)

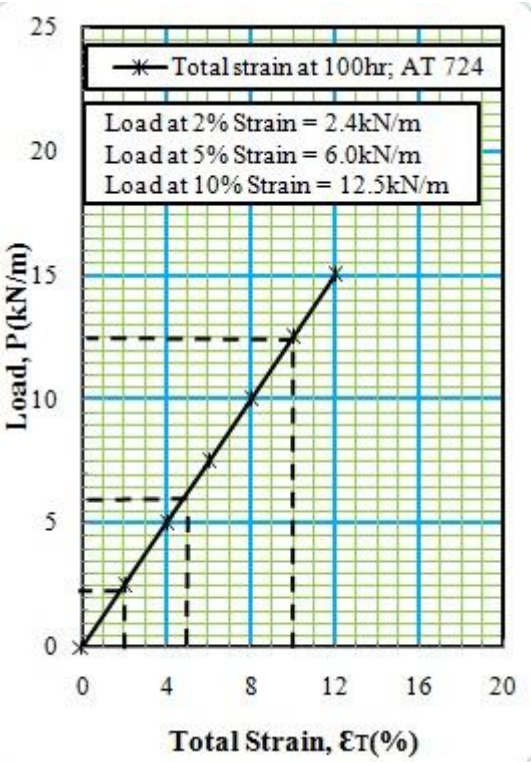
Total strain at 100hr; AT 724
Load at 2% Strain = 2.4kN/m
Load at 5% Strain = 6.0kN/m
Load at 10% Strain = 12.5kN/m
Load, P(kN/m)
Total Strain, εT(%)

(g)

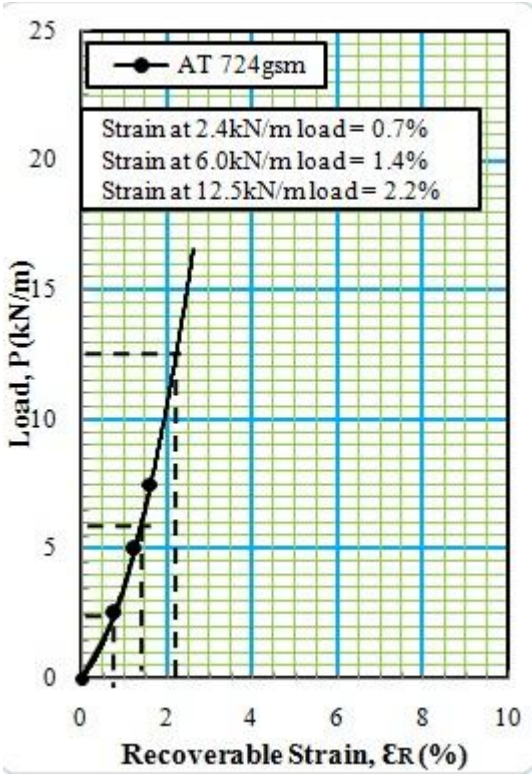
AT 724gsm
Strain at 2.4kN/m load = 0.7%
Strain at 6.0kN/m load = 1.4%
Strain at 12.5kN/m load = 2.2%
Load, P(kN/m)
Recoverable Strain, εR (%)

(h)

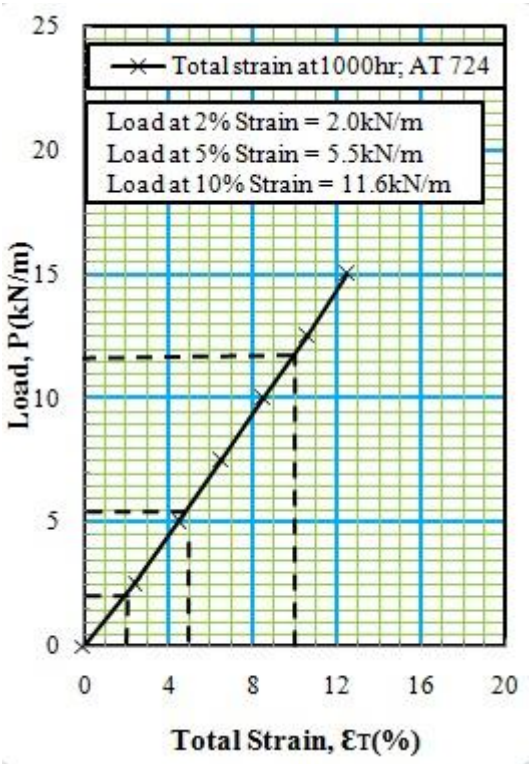
Total strain at 1000hr; AT 724
Load at 2% Strain = 2.0kN/m
Load at 5% Strain = 5.5kN/m
Load at 10% Strain = 11.6kN/m
Load, P(kN/m)
Total Strain, εT(%)

(i)

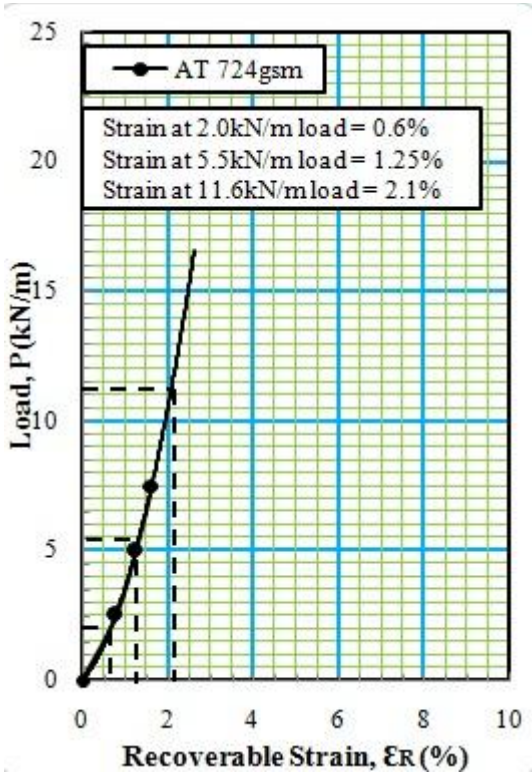
AT 724gsm
Strain at 2.0kN/m load = 0.6%
Strain at 5.5kN/m load = 1.25%
Strain at 11.6kN/m load = 2.1%
Load, P(kN/m)
Recoverable Strain, εR (%)

(j)

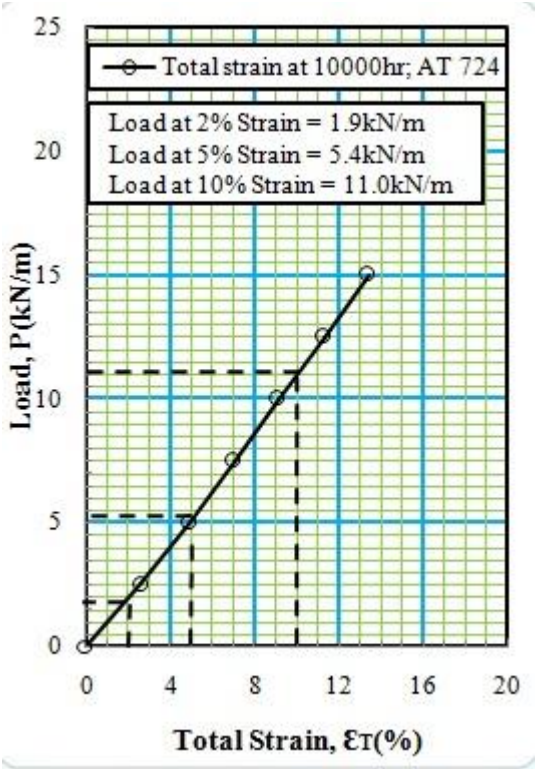

(k)

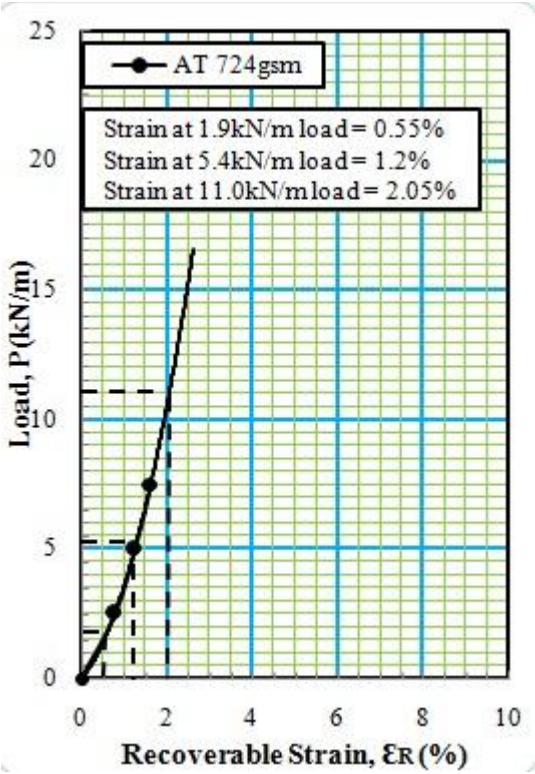

(l)

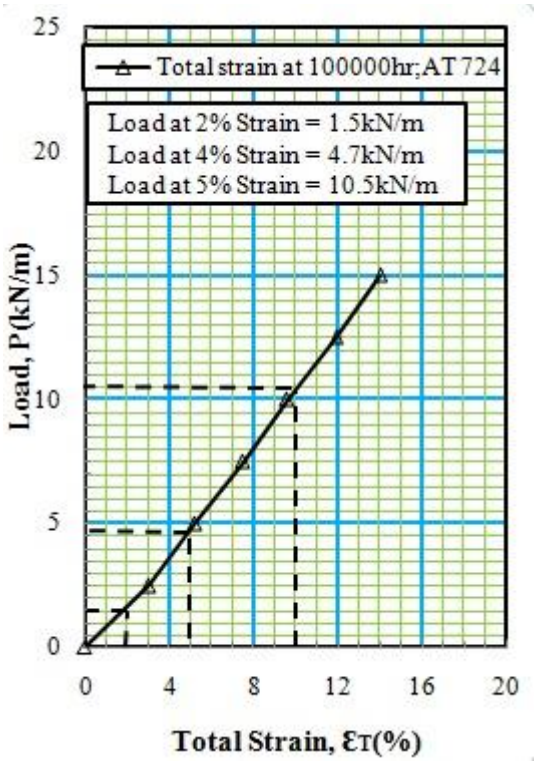

(m)

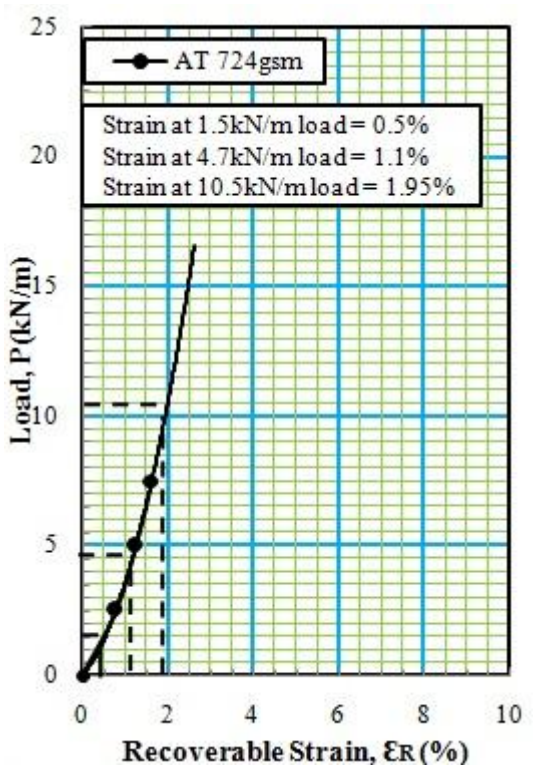

(n)

Fig. 29: Load vs. total strain graph and load vs. recoverable strain graph for additive treated 724gsm in machine direction at various time for different limiting strains

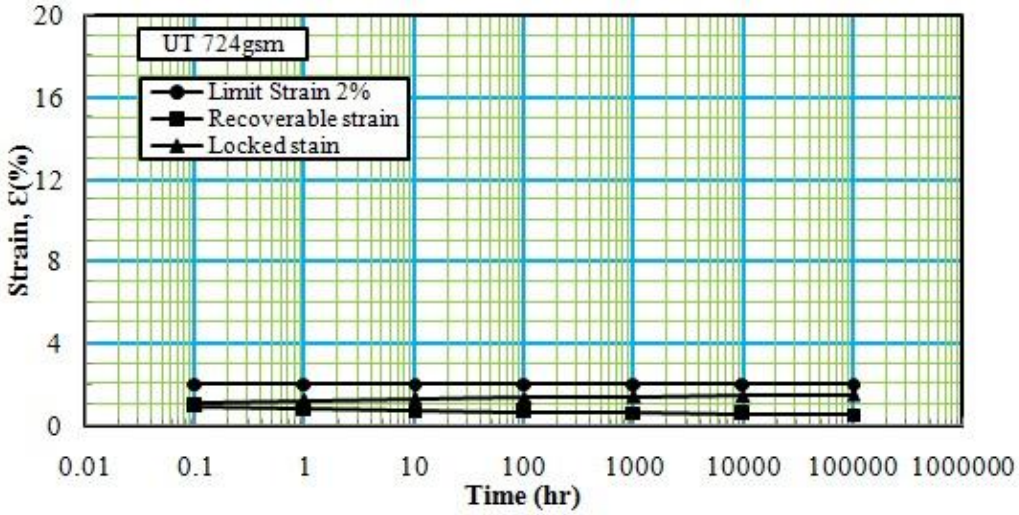

(a)

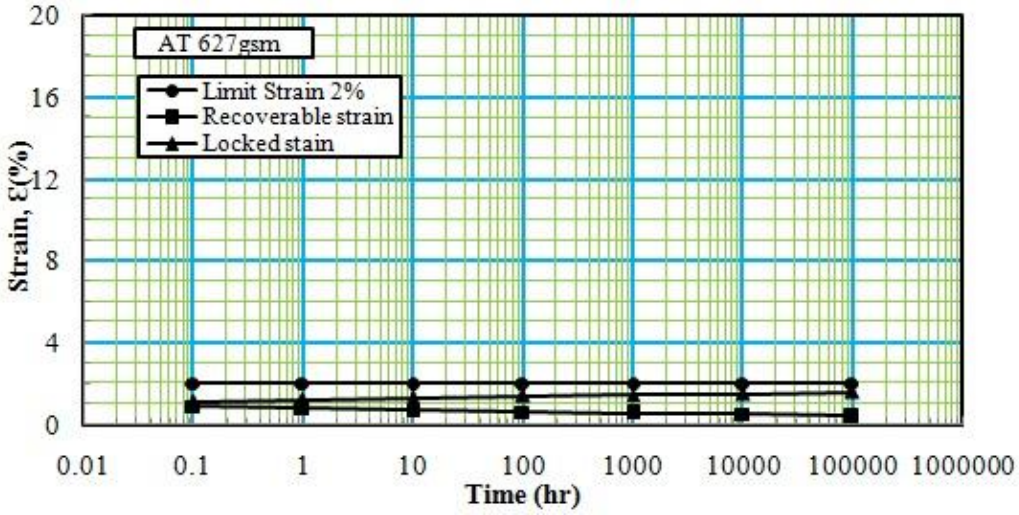

(b)

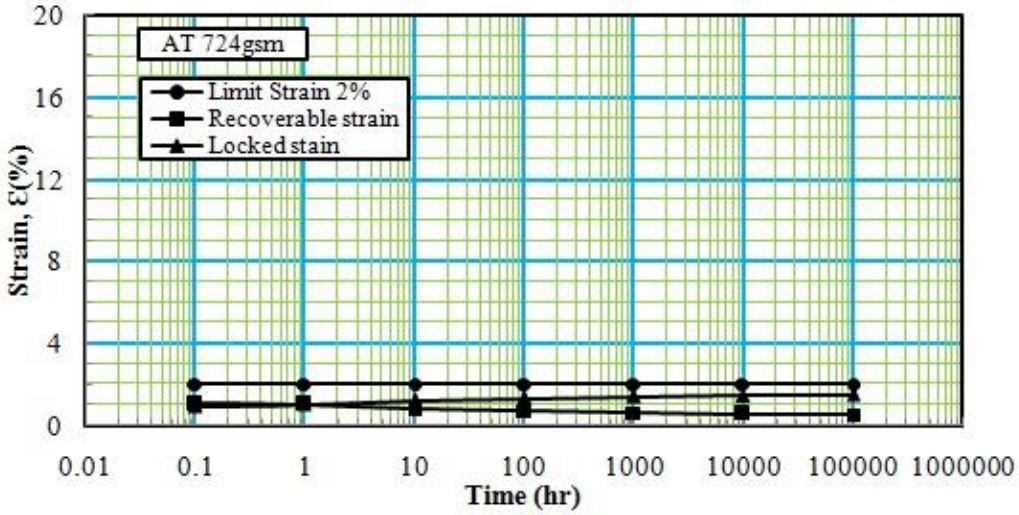

(c)

Fig. 30: 2% limit strain and it's component vs log time obtained from creep test in machine direction: (a) untreated 724gsm, (b) additive treated 627gsm and (c) additive treated 724gsm

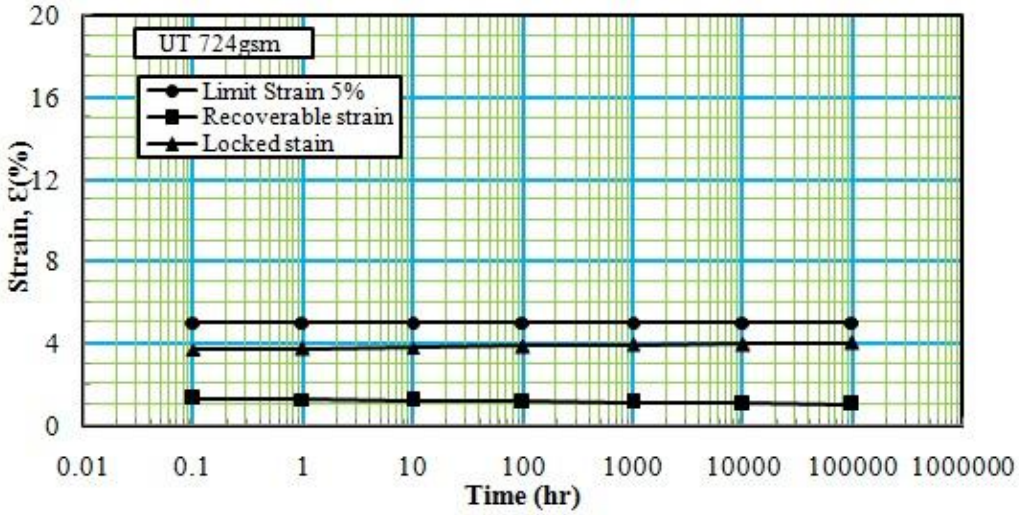

(a)

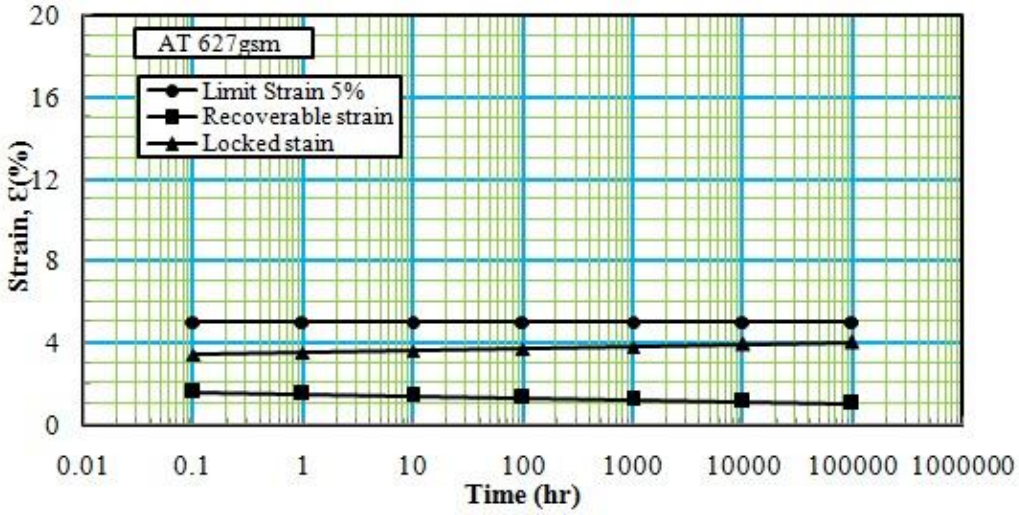

(b)

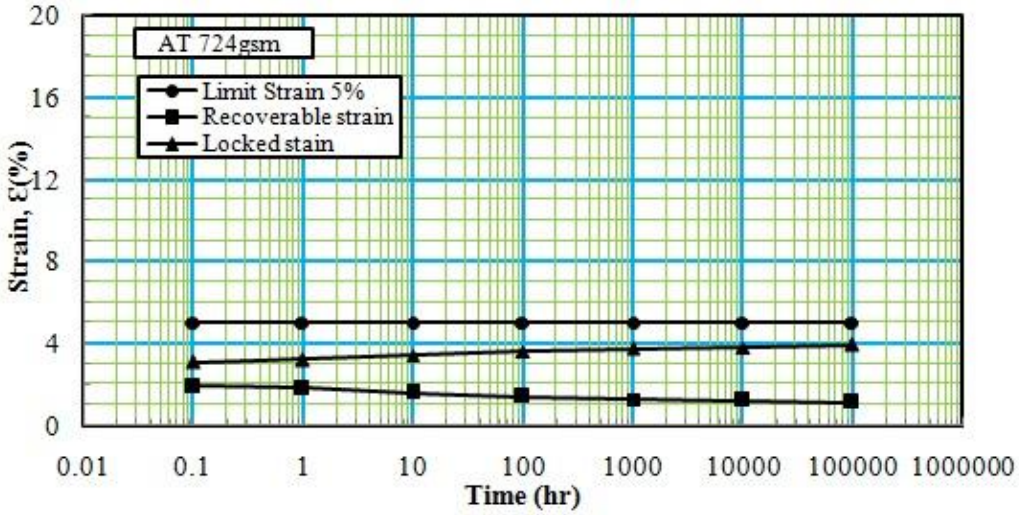

(c)

Fig. 31: 5% limit strain and it's component vs log time obtained from creep test in machine direction: (a) untreated 724gsm, (b) additive treated 627gsm and (c) additive treated 724gsm

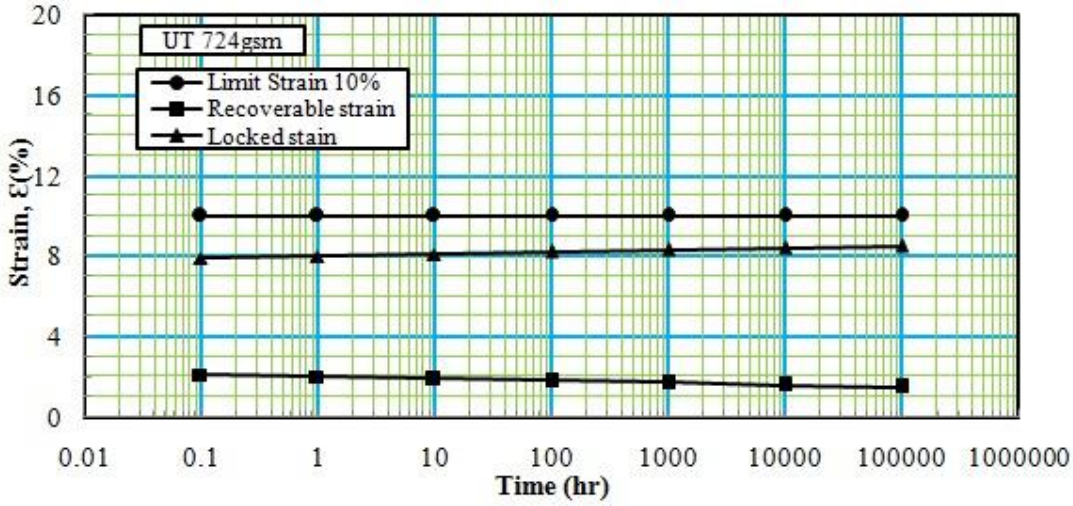

(a)

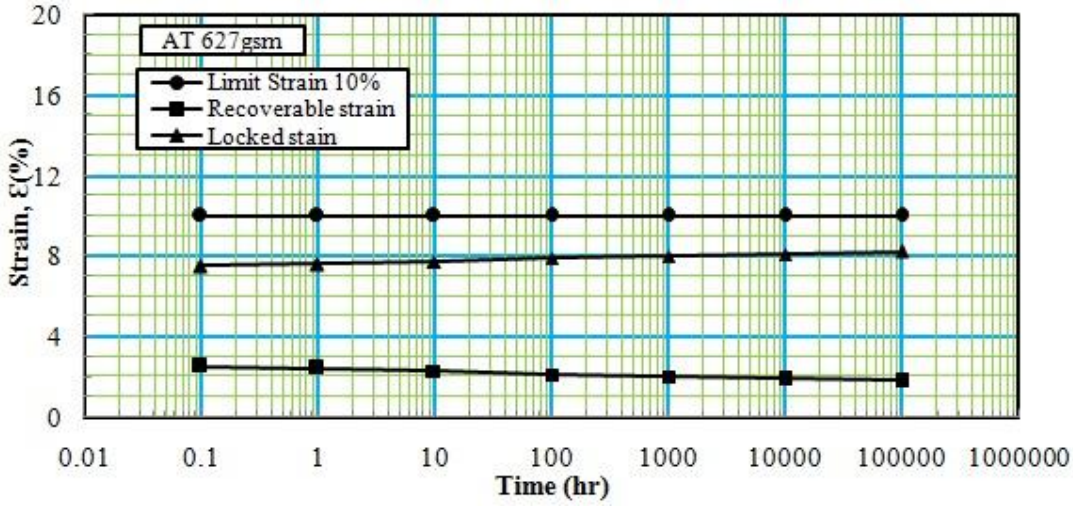

(b)

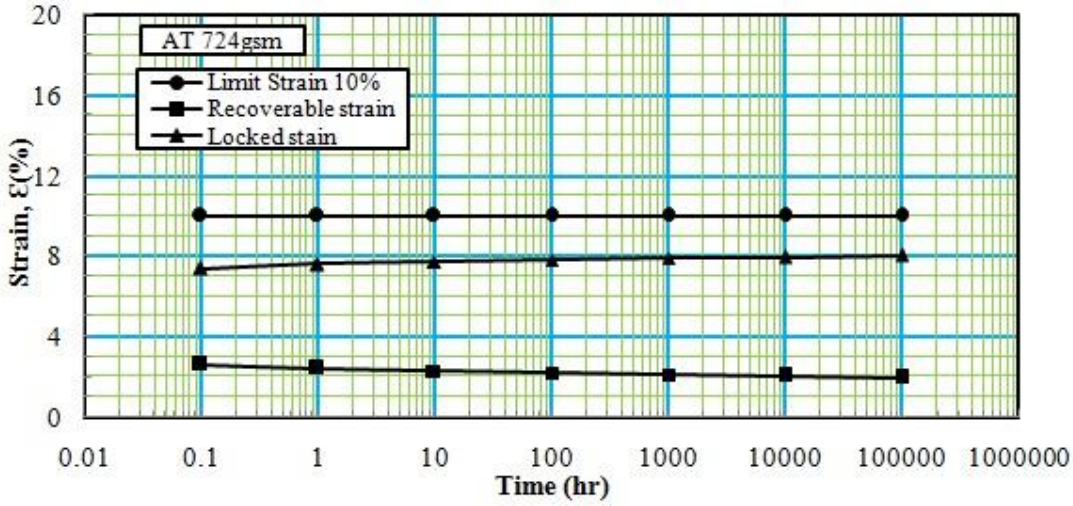

(c)

Fig. 32: 10% limit strain and it's component vs log time obtained from creep test in machine direction: (a) untreated 724gsm, (b) additive treated 627gsm and (c) additive treated 724gsm